

Provenance and evolution of East Asian large rivers recorded in the East and South China Seas: A review

Licheng Cao¹, Lei Shao^{2,†}, Douwe J.J. van Hinsbergen³, Tao Jiang^{1,4,‡}, Di Xu¹, and Yuchi Cui²

¹Hubei Key Laboratory of Marine Geological Resources, China University of Geosciences, Wuhan 430074, China

²State Key Laboratory of Marine Geology, Tongji University, Shanghai 200092, China

³Department of Earth Sciences, Utrecht University, Princetonlaan 8A, 3584 CB, Utrecht, Netherlands

⁴Southern Marine Science and Engineering Guangdong Laboratory (Guangzhou), Guangzhou 511458, China

ABSTRACT

Large rivers are the arteries of continents. Those originating from the Tibetan Plateau and traversing East Asia have a relatively young history due to continuous Cenozoic perturbations. However, it has been a long journey to reconstruct their genesis and dynamic evolution, in which many puzzles and challenges remain. The river history is documented by provenance information in the ultimate sediment sinks in the East and South China Seas, but a regional-scale correlation of provenance data is still developing. Here, we explore the promise of this provenance perspective by reconstructing the evolution of three large rivers in China (the Yangtze, Pearl, and Red Rivers) by compiling and reevaluating a large volume of published provenance data (zircon U-Pb geochronology, K-feldspar Pb isotopes, and whole-rock Nd isotopes) from both Cenozoic strata and modern sediments from the East and South China Seas and the large river basins. Unlike traditional approaches that average provenance signatures, intersample variability was carefully evaluated. The general inheritance of zircon age spectral patterns and small fluctuations of Nd isotopes in the Neogene strata suggest provenance stabilization in the East and South China Seas and the establishment of near-modern drainage configurations. The paleodrainage basins before the Miocene are interpreted to have been smaller than their modern sizes, and drainage expansion likely occurred over the Oligocene. Our analysis suggests that the widely accepted models that link drainage between the ancient Yangtze

and Red Rivers may be unlikely. The compiled provenance signatures and prior paleocurrent measurements of Paleogene strata distributed in the southeastern Tibetan Plateau margin show sediment supplied from local terranes instead of through-flowing river systems.

INTRODUCTION


Large rivers that drain major continents provide a primary link in hydrological and geochemical cycles and in the transport of rock from erosion to deposition, and they play a key role in human habitation (Milliman and Farnsworth, 2011). Large river networks normally change over time through the complex interplay of exogenic and endogenic factors (e.g., plate tectonics, local faulting, and climatic changes), intrinsic river dynamics (e.g., meandering), and, more recently, anthropogenic disturbances (e.g., damming and dredging) (Vandenbergh et al., 2010). Different large rivers thus have different histories, and reconstruction of their genesis and dynamic evolution has been of great interest to scientists (Ashworth and Lewin, 2012; Gibling, 2017; Gupta et al., 2020).

Large river histories and fluvial landscapes are typically investigated based on drainage basin morphometry and thermochronometry and paleoaltimetry of source terranes. Morphometric analysis normally embeds simplifying assumptions on boundary conditions and variables (e.g., precipitation and sediment load) to describe natural landscapes, and the establishment and interpretation of diagnostic morphometric criteria for the same area may be inconsistent (e.g., the low-relief, high-elevation surface formation; Whipple et al., 2017; Yang et al., 2015; Yuan et al., 2022). Low-temperature thermochronometry is widely applied in elevation profiles of river gorges to determine episodes of rapid exhumation and river incision (Reiners and

Brandon, 2006). It does not provide direct information on surface uplift (England and Molnar, 1990), and the interpretation of regional incision may be complicated by issues of intensified monsoon and localized faulting (e.g., Ou et al., 2021; Replumaz et al., 2020). Paleoaltimetry has recently centered on the stable isotopic composition of continental carbonates (Rowley and Garzione, 2007). It makes implicit assumptions about the carbonate growth temperature and source of moisture that could be potentially challenged by the changing paleogeography and atmospheric-hydrological dynamics in the past (Botsyun et al., 2019).

The geologic history of large rivers is also documented in the sediment source-to-sink system, which is an integrated, dynamic system of Earth surface processes governing the fate of particulate sediment from multiple source areas through complex sediment-routing routes to ultimate depositional sinks (Allen, 2017). By establishing the link between potential source terranes and potential lowland depocenters, provenance analysis can be used to reconstruct the configuration of upstream networks over time (Haughton et al., 1991). Unfortunately, recognition of such large, ancient river systems on land is challenging due to difficulties in facies interpretation, poor characterization of catchment size, and low preservation potential of trunk stream deposits (Ashworth and Lewin, 2012; Bhattacharya et al., 2016; Miall, 2006). The siliciclastic sediments transported by large rivers eventually accumulate on continental margins and in ocean basins. The provenance analysis of discharged sediments avoids the complexity of recognizing and correlating sparse, relict records of ancient rivers on land, and it provides insights into the evolution of river basins by disentangling the signal of interest from “noise” (Romans et al., 2016).

Referred to as the “Roof of the World,” the Tibetan Plateau and surrounding mountains are

Lei Shao  <https://orcid.org/0000-0002-6403-4985>

†Corresponding authors: lshao@tongji.edu.cn; taojiang@cug.edu.cn.

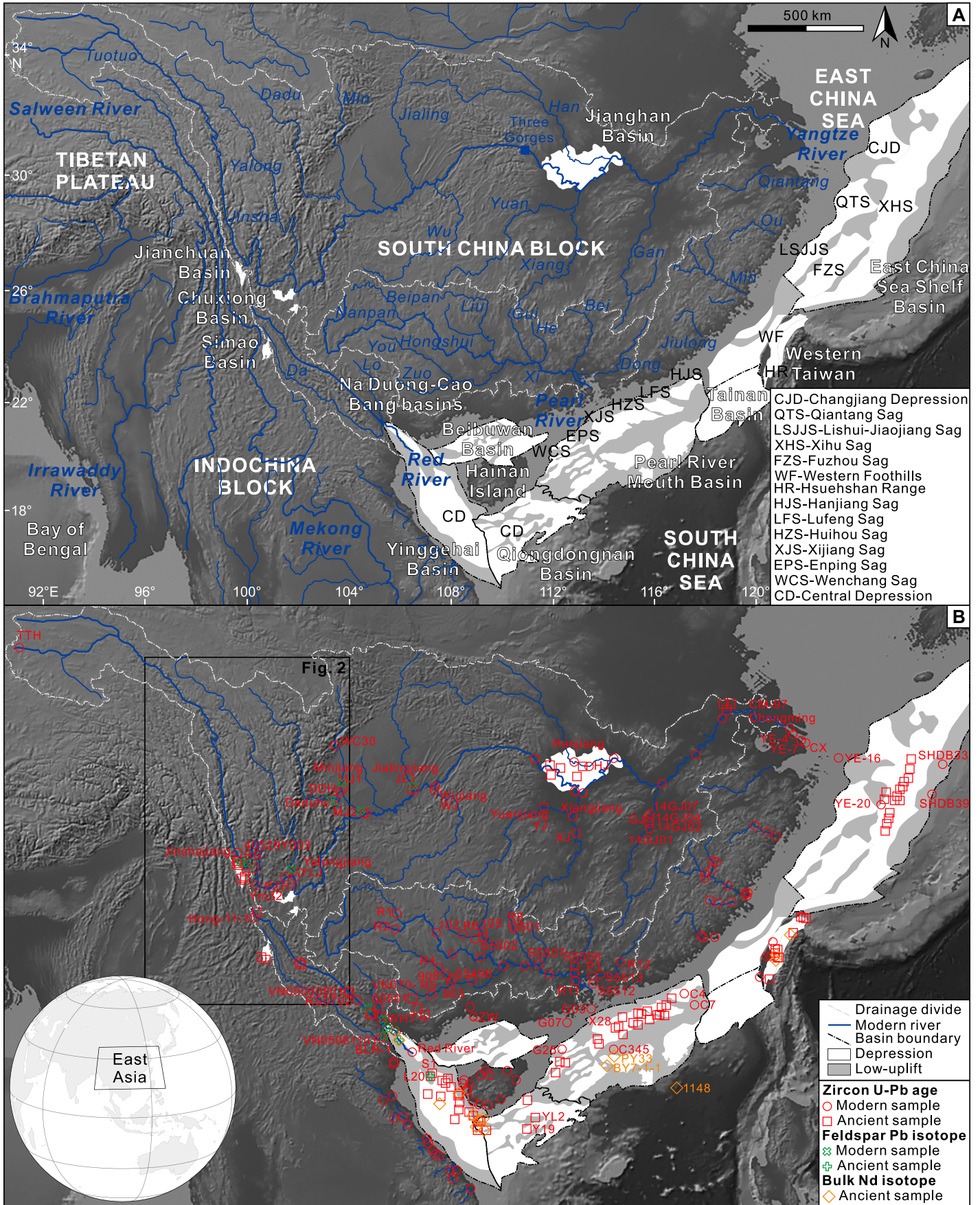


Figure 1. Maps of East Asia showing (A) the drainage networks, inland basins traversed by large rivers, and offshore basins of the East and South China Seas (modified from Cliff et al., 2020; Gourbet et al., 2017; Wang et al., 2014b; Zheng, 2015), as well as (B) compiled samples of sediments and sedimentary rocks. Base map of topography and rivers was made with GeoMapApp (www.geomapapp.org). Drainage divides of the studied three large rivers (i.e., the Yangtze, Pearl, and Red Rivers) and basin boundaries of the East and South China Seas are outlined by gray and black dashed lines, respectively. For basins along the southeast margin of the Tibetan Plateau, areas of Paleogene strata are shown. In offshore basins, areas of depressions and uplifts are shown in light and dark gray, respectively, and only names of key studied depressions are marked. Samples are symbol- and color-coded according to their ages and types of provenance data. For brevity, parts of sample names (e.g., Jianchuan Basin, western Taiwan, and central Vietnam) are not shown; see Tables S1–S3 for a full summary of sample information (see text footnote 1).

traversed by several continent-scale drainage systems (Fig. 1). The landscape of this region has been shaped by the process of the India-Asia collision and the Asian monsoon systems over the Cenozoic (Ding and Chan, 2005; Royden et al., 2008; Yin, 2010), such that the histories of large Asian rivers are relatively younger compared to ancestral rivers originating in the Jurassic and Cretaceous as Pangea broke up (e.g., the paleo-Mississippi and paleo-Congo rivers; Gibling, 2017; Gupta et al., 2020). However, reconstructing their origins and distributions has long been subject to controversy and uncertainty (Brookfield, 1998; Clark et al., 2004). While a range of models has been proposed for the Yangtze, Red, and Yarlung-Brahmaputra Rivers (e.g., Cliff et al., 2006a; Lang and Huntington, 2014; Zheng, 2015), some others like the Mekong River are still poorly understood (e.g., Hennig et al., 2018). The holistic histories of these large rivers have been recorded in the provenance of sediments discharged into ocean sinks along the Asian margin. The continental margin of the seas in East Asia is identified as one of the best-studied passive margins in the world, where Cenozoic depositional records are continuous and well correlated through decades of commercial exploration and scientific drilling programs (e.g., Larsen et al., 2018; Li et al., 2015a; Wang et al., 2014b), and a growing body of provenance data has been obtained (Fig. 1). Previous provenance studies on this margin mostly focused on one basin or selected areas of different basins (e.g., Cao et al., 2021a; Guo et al., 2021; Shao et al., 2019) and have proposed various models of provenance reconstruction to trace the evolution of large rivers, particularly regarding the diagnostic criteria of large river sources and the genesis of near-modern drainage patterns. This dilemma demands a comprehensive correlation of provenance data on regional scales to test the existing models of provenance and river history.

In this study, we aimed to reconstruct the sediment provenance of Cenozoic strata of the East and South China Seas and the evolution of three large rivers in China (the Yangtze, Pearl, and Red Rivers), especially regarding the initiation of their near-modern configurations (Fig. 1). We

therefore synthesized a large volume of different types of published data (including detrital zircon U-Pb geochronology, detrital K-feldspar Pb isotopes, and whole-rock Nd isotopes; Fig. 1) to systematically investigate the source-to-sink evolution. The three river basins together occupy an area of 2,450,000 km² and contribute ~3.5% (~660 Mt) of the global annual discharge of fluvial sediment (Milliman and Farnsworth, 2011). The Yellow River and Mekong River, although they discharge into the East and South China Seas, are not considered due to the young history of river integration in the Quaternary (Craddock et al., 2010; Xiao et al., 2020) and the absence of provenance data in offshore basins, respectively. This article first introduces the geologic settings of ultimate source and sink areas of the studied large rivers and then reviews the existing models of their drainage evolution. Then, we reexamine the provenance signatures of Cenozoic strata from the East and South China Seas and extend the comparison from basin scale to regional scale. The intersample variability is quantitatively investigated, and sample representativeness is carefully evaluated to rigorously interpret the provenance similarity and dissimilarity. Last, we discuss the provenance response to the evolution of the studied large rivers by incorporating previous findings and provide future perspectives.

This article presents a large compilation of ~600 currently available samples and different types of provenance data from the East Asian large rivers and the East and South China Seas, especially regarding detrital zircon U-Pb ages (~36,000 grains), which lays a solid foundation for future provenance research in the region. We highlight the necessity of evaluating sample representativeness and intersample variability in the provenance analysis of river-discharged sediments, and the preferred strategies of data treatment and analysis can be readily applied to drainage reconstruction in regions other than East Asia. We suggest provenance stabilization in the East and South China Seas and the potential genesis of large rivers in East Asia from the Miocene, which provides a new understanding of the geomorphologic and tectonic evolution of East Asia.

GEOLOGIC SETTING

East-Southeast Tibetan Plateau

Surface uplift in hinterland mountains of the east-southeast Tibetan Plateau has created the headwaters of large rivers, and this landscape evolution is critical to the formation of near-modern drainage patterns (Fig. 1; Brookfield, 1998; Clark et al., 2004; Zhang et al., 2019). The rise and growth of the Tibetan Plateau are the results of prolonged plate convergence and continental collision, where the thickened crust and high-relief landscape with valleys and highlands during the Mesozoic were further modified during the Cenozoic collision between India and Asia (Liu et al., 2016; Spicer et al., 2021; Yin and Harrison, 2000). In the southeastern part of the plateau, where several large rivers (e.g., the Yangtze, Red, and Mekong Rivers; Fig. 2) have their sources, surface uplift occurred first during block extrusion and transpression between the Indian block and the rigid lithosphere underlying the Sichuan Basin in the Eocene to middle Miocene (Li et al., 2017; Tapponnier et al., 2001) and subsequently may have been modified by regional-scale, ductile crustal flow from the interior plateau toward its margin (Clark and Royden, 2000; Wang et al., 2008).

Reconstructions of surface uplift in the eastern and southeastern margins of the Tibetan Plateau center on low-temperature thermochronometry, such as (U-Th)/He and fission-track ages, and stable isotope paleoaltimetry (Fig. 2). Cooling ages since the middle Miocene obtained from elevation profiles of river gorges have been considered synchronous with a regional episode of rapid exhumation and river incision (e.g., Clark et al., 2005; Ouimet et al., 2010). However, the increased incision downstream in large rivers occurred as early as the early Miocene (Jiao et al., 2021; Nie et al., 2018; Wang et al., 2016b). Moreover, the growing recognition of exhumation episodes in the Cretaceous to Paleogene in the southeastern plateau margin, yet locally isolated, hints at an earlier onset of surface uplift (Cao et al., 2021; Liu-Zeng et al., 2018; Shen et al., 2016). Recent stratigraphic revisions of Cenozoic strata in several hinterland

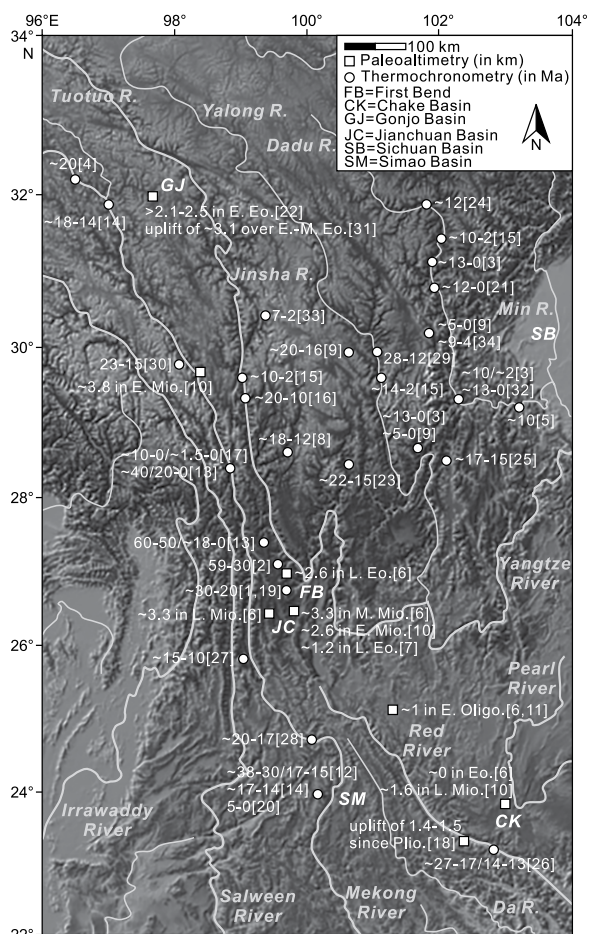


Figure 2. Topographic map of the margin of the east-southeast Tibetan Plateau showing thermochronometric and paleoaltimetric histories recorded in valleys of large rivers and nearby mountains. For thermochronometric data, ages (in Ma) stand for the episodes of moderate to rapid exhumation. Reference numbers are shown in brackets, and see Table S4 for a summary of references (see text footnote 1).

basins of the southeastern plateau margin (e.g., Gourbet et al., 2017; Li et al., 2020) and their paleoaltimetric estimates based on pedogenic carbonate oxygen isotopes (Hoke et al., 2014; Li et al., 2015b; Xiong et al., 2020) together confirmed that the elevated topography had already expanded southeastward to the eastern Qiangtang terrane and Lanping-Simao terrane in the late Eocene (Fig. 3). A similar conclusion was also reached by evaluating evidence of floral modernization in the late Paleogene (Linnemann et al., 2018; Su et al., 2019).

Continental Margin of the East and South China Seas

The curved continental margin of China was located above a prolonged subduction zone during the Mesozoic, consuming oceanic lithosphere of the Panthalassa Ocean and building wide magmatic arc belts between South China and offshore China seas (Fig. 3; Cui et al., 2021; Li and Li, 2007; Suo et al., 2019). This convergent setting was diachronously and episodically replaced by continental rifting from the Late Cretaceous (Morley, 2016; Zhang et al., 2016; Zhu et al., 2019), laying the foundation for today's paleogeographic framework of the West Pacific marginal seas. In the Paleogene, extension intensified, and series of rift basins developed along the outer margin, including, from northeast to southwest, the East China Sea Shelf

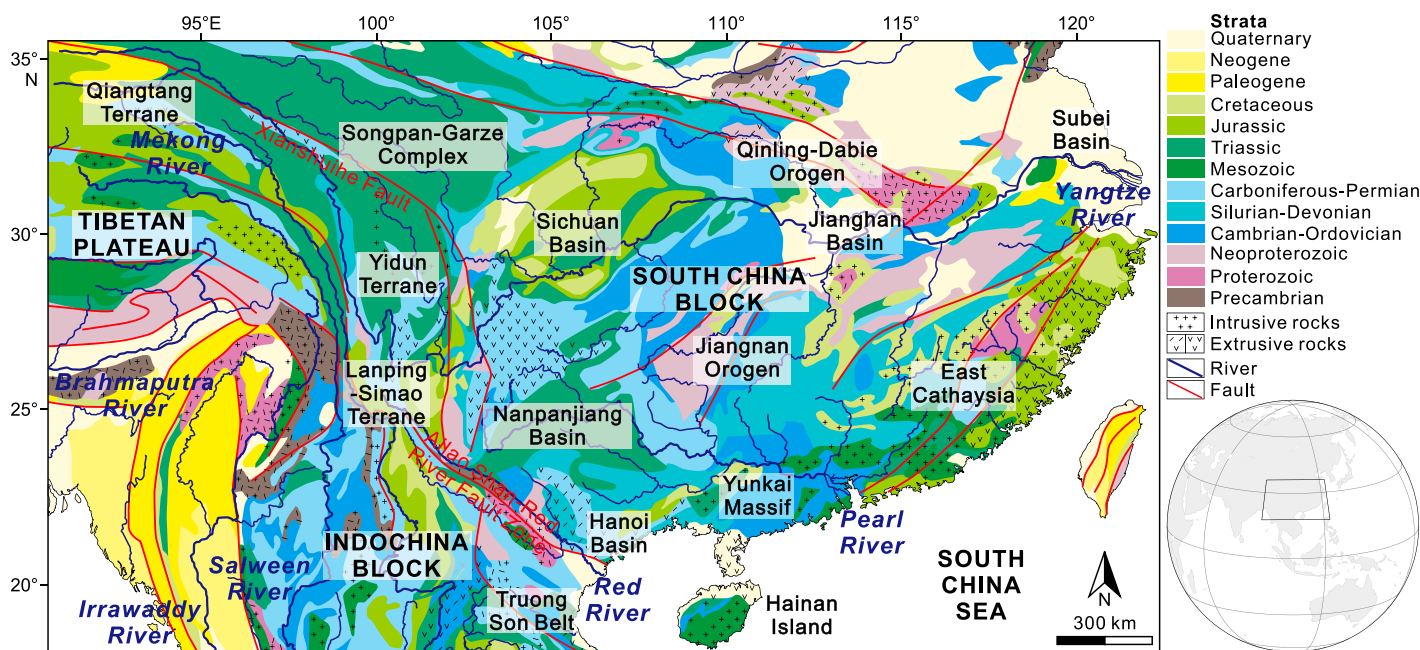


Figure 3. Simplified geologic map of East Asia (modified from Geological Survey of Canada, 1995) showing the distribution of lithologic and tectonic units along large river courses.

Basin, Tainan Basin, Pearl River Mouth Basin, Qiongdongnan Basin, Yinggehai Basin (Song Hong Basin), and Beibuwan Basin (Fig. 1). Final breakup and seafloor spreading occurred in the Oligocene–early Miocene South China Sea (Briais et al., 1993; Larsen et al., 2018; Li et al., 2015a).

Extension and subsidence on the continental margin of the East and South China Seas have created accumulation space for river-discharged sediment, and the margin shows little bathymetric expression of the attenuated crust due to burial by thick sedimentary successions (Fig. 1; Wang et al., 2014b; Zhu et al., 2019). With decades of commercial exploration and scientific drilling, the Cenozoic stratigraphy of the region has been well established and correlated (Wang et al., 2014b; Wang and Li, 2009). Locally, in west Taiwan, the stratigraphy of the southeast China margin was folded and uplifted from the Pliocene (Fig. 3; Chen, 2016; Huang et al., 2012). In general, sedimentary successions of the region are subdivided according to synrifting and postrifting stages (Fig. 4). Due to the diachronous nature of rifting and transgression and the possible connectivity with preexisting oceans (e.g., proto–South China Sea), marine deposition started first in the East China Sea and today’s Taiwan Island during the Paleocene and then expanded southwestward into the northern South China Sea during the middle Eocene and finally into the Qiongdongnan Basin during the early

Oligocene (Li et al., 2016b; Zhu et al., 2019). In contrast, the remaining areas (e.g., Yinggehai and Beibuwan Basins) mainly accumulated non-marine deposits during the rifting that were composed of alluvial, fluvial, lacustrine, and deltaic facies with occasional volcanoclastic intercalations (Zhang et al., 2020a, 2020b).

Marine deposition in the East China Sea Shelf Basin occurred as early as the Paleocene and mainly developed in deep depressions in the southeast (Fig. 4). In contrast, lacustrine, deltaic, and littoral facies prevailed in the northwestern part of the basin. After the Oligocene, the basin was characterized by deformation and basin inversion with accumulation of lacustrine to deltaic deposition. In the northern South China Sea, postrift lithofacies with a mixture of terrigenous and shallow-marine origins were highly variable across different basins. Meanwhile, along with the overall sea-level rise since the Miocene (Fig. 4), carbonate and hemipelagic components became widespread with a seaward increase in the proportion of marine biotic particles (Zhang et al., 2020b).

EXISTING MODELS OF STUDIED LARGE RIVERS

Models of the Yangtze and Red Rivers

In the southeastern margin of the Tibetan Plateau, prominent strike-slip movements may have

caused river valleys to form close to each other along tectonic structures (Fig. 2; Zheng, 2015). This evolving geometry demonstrates a tendency for drainage networks to change by continuous divide migration or discrete events of river capture (Hallet and Molnar, 2001). In this regard, the contemporaneous evolution of the Yangtze and Red Rivers has long been considered (Barbour, 1936; Brookfield, 1998). Because of the similar southeast-trending courses of the upper Yangtze and Red Rivers (Fig. 2; Clark et al., 2004) and the very thick successions (up to 16 km) of the Yinggehai Basin that cannot be accounted by the estimated volume of rocks eroded from the modern Red River catchment (Fig. 1; Clift et al., 2006a; Métivier et al., 1999), a Red River predecessor has been hypothesized to have drained much larger areas than today, flowing southeastward from the southeast Tibetan Plateau into the Yinggehai Basin. Following this hypothesis, sparse Paleogene deposits, characterized by fluvial facies with occasional intercalations of shallow lacustrine facies, in several basins between the Yangtze and Red Rivers (Fig. 1; Chen et al., 2017b; Deng et al., 2018; Zhang et al., 2010) are possible remnant records of the paleo–Red River. It was recently envisaged to flow southeastward through the Jianchuan and Simao Basins until the final outlet in the Hanoi Basin and Na Duong–Cao Bang Basins, based on the interpreted provenance similarity of Paleogene deposits therein (Fig. 1; Chen et al., 2017b; Clift

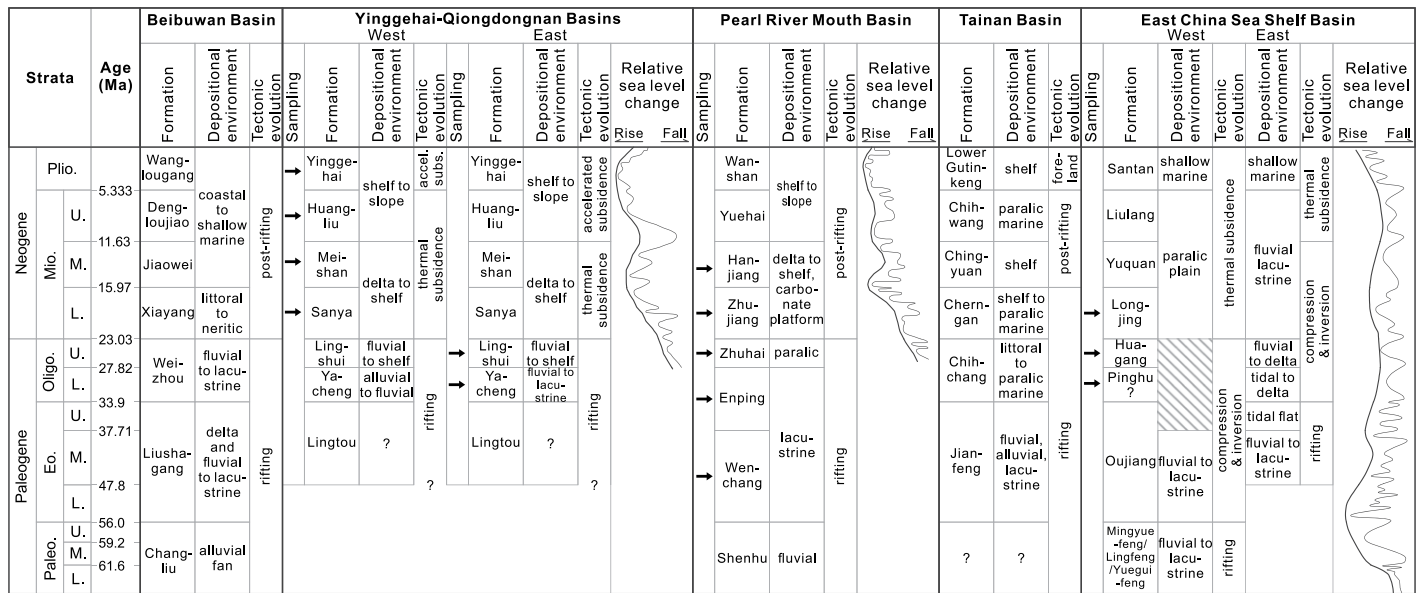


Figure 4. Simplified stratigraphic framework and relative sea-level curves of main offshore basins in the East and South China Seas (modified from Wang et al., 2014b; Wang and Li, 2009). In each basin, Cenozoic formations and corresponding depositional environments and tectonic stages are given. Note that a slight change in depositional ages is made for the Upper Eocene–Oligocene strata of the East China Sea Shelf Basin, based on the results of zircon U–Pb ages therein (Yuan et al., 2014; Zhang et al., 2020c). See Wang et al. (2014b) and Zhu et al. (2019) for detailed descriptions of lithostratigraphic columns of individual basins. Arrows indicate the key formations where published detrital zircon geochronology data were compiled. Paleo.—Paleocene; Eo.—Eocene; Oligo.—Oligocene; Mio.—Miocene; Plio.—Pliocene; U.—Upper; M.—Middle; L.—Lower.

et al., 2020; He et al., 2021). Possible drivers for drainage reorganization of the paleo-Red River and the loss of its upper reaches to the Yangtze River include the strike-slip movement of the Ailao Shan-Red River shear zone, the clockwise rotation of the Lanping-Simaó terrane, and the inversion of the Jianchuan Basin (Fig. 3; e.g., Chen et al., 2017b; Gourbet et al., 2017; Zheng et al., 2021).

Regarding the genesis of the Yangtze and Red Rivers, different models have been proposed based on different lines of evidence obtained from the two river basins, and we used flow charts to schematize different combination scenarios of potential source terranes linked by drainage networks (Figs. 5A and 5C). Within the Red River Basin, zircon U-Pb-Hf analyses of Miocene clastic rocks suggest initiation of near-modern sources in the late Miocene (van Hoang et al., 2009; Wysocka and Świerczewska, 2010). In contrast, Nd isotopes obtained from the Hanoi Basin exhibit a positive excursion over the Paleogene, indicating termination of drainage reorganization from that time forward (Clift et al., 2006a). Clift et al. (2006a) interpreted the distal source of Paleogene strata as the upper Yangtze River, but potential supply from the middle Yangtze or a combination thereof has also been proposed based on detrital K-feldspar Pb isotopes from the river mouth and offshore boreholes (Fig. 5C; Clift et al., 2008; Wang et al., 2019a; Zhang et al., 2014). In the Yangtze River Basin, the near-synchronous, rapid exhumation over the middle-late Eocene found in the Three Gorges and upstream Sichuan Basin was earlier attributed to the capture of the middle Yangtze reaches by the lower reaches (Figs. 1 and 3; Richardson et al., 2010). However, the continuous lacustrine and evaporitic deposition in the Paleogene Jiangnan Basin to the east was considered to be strong evidence against a through-flowing river before the Oligocene (Fig. 5A; Wang et al., 2014c; Yang et al., 2021; Zheng et al., 2013). Downstream from the Three Gorges (Fig. 1), widespread coarse-grained sediment, termed “Yangtze Gravel,” has been assigned a distal fluvial origin and dated as early as the early Miocene (e.g., Sun et al., 2021; Zheng et al., 2013). While the comparable zircon age signatures between Neogene gravel and modern river sediments were proposed to indicate a pre-Miocene initiation of the Yangtze River (Zheng et al., 2013), recent muscovite and feldspar $^{40}\text{Ar}/^{39}\text{Ar}$ geochronology on the gravel revealed no representative signatures of the upper reaches at least until the late Miocene (Sun et al., 2021).

There are also some arguments against a drainage linkage between the ancient Yangtze and Red Rivers. Zhang et al. (2021c) found no

unradiogenic feldspar grains in the Eocene-Miocene strata of the Hanoi and Yinggehai Basins, which characterize the upper and middle reaches of the Yangtze River, and Wissink et al. (2016) favored a predominantly local source for zircons in alluvial and lacustrine deposits of the southeastern plateau margin. A similar conclusion was also reached by analyzing paleocurrent measurements of Eocene strata in the Jianchuan Basin (Wei et al., 2016; Wissink et al., 2016), which mainly recorded northward and eastward flows in the southern basin.

Models of the Pearl River

The modern Pearl River does not extend into the interior of the Tibetan Plateau, and its evolution has been traditionally considered to have been independent of other Asian large rivers (Fig. 5B; Clark et al., 2004). Although the headwater area of the Pearl River is sometimes invoked as a potential source feeding the northeastern catchment of the paleo-Red River (van Hoang et al., 2009; Jiang et al., 2015), the northeastward paleocurrent directions obtained from the Eocene Jianshui Basin in between the upper Pearl River and Red River provide the evidence for their long-lived drainage divide (Fig. 2; Wissink et al., 2016). Instead, the geologic history of the Pearl River has been mainly constrained by sediment provenance in the northern South China Sea. Years of investigations on the Pearl River Mouth Basin revealed significant shifts in different provenance proxies around the Oligocene-Miocene boundary and in the late Miocene, which was previously interpreted to reflect drainage reorganization of the Pearl River (e.g., Cao et al., 2018; Clift et al., 2002; He et al., 2020a; Yan et al., 2018). Although the timing of provenance shifts and the distribution of Pearl River-derived sediments in the basin are still debated, the process of drainage reorganization can be simply portrayed as a progressive drainage expansion from the southeast China margin westward to the plateau margin (Fig. 5B; e.g., Cao et al., 2018; Fu et al., 2021a; Wang et al., 2019b; Yan et al., 2018).

STRATEGIES, SAMPLES, AND DATA

Selection of Provenance Proxies

A range of analytical approaches (e.g., elemental analysis, heavy mineral analysis, Nd isotope analysis, and zircon U-Pb dating) has been used for provenance analyses of whole rock, grain-size fractions, or single grains of detrital minerals in the East and South China Seas and the Yangtze, Pearl, and Red River basins. Each type of provenance analysis has its advantages

and disadvantages. In general, traditional proxies of whole-rock geochemistry and mineralogy provide the richest sources of information regarding the compositional nature and tectonic setting of dominant source terranes, and they have proven to be useful in discriminating different sources of modern sediments within individual river basins (e.g., Clift et al., 2008; Shao et al., 2016a; Vezzoli et al., 2016). The current sample coverage of whole-rock geochemistry and mineralogy in the Cenozoic strata of the East and South China Seas is limited to certain boreholes (e.g., Cao et al., 2017; Li et al., 2016a; Sun et al., 2014; Yan et al., 2011). These provenance proxies are generally sensitive to the effects of hydrodynamic sorting during deposition and chemical dissolution by diagenesis and weathering (Vermeesch and Garzanti, 2015), rendering a poor correlation between modern river sources and ancient basin sediments. This is reflected in case studies of the Yinggehai and Qiongdongnan Basins, where the observed variations in mineral assemblages of Neogene strata could be an artifact of diagenesis-induced compositional maturity (Fyhn et al., 2019) rather than changing provenance signals (Jiang et al., 2015; Wang et al., 2016a). Compared to whole-rock geochemistry, Sm-Nd isotope systematics are generally unaltered during sedimentary processes, which makes Nd isotopes a robust tracer of source composition by revealing the relative input of juvenile materials derived from the mantle compared to evolved materials recycled from the crust (Garçon et al., 2014; McCulloch and Wasserburg, 1978; McLennan et al., 1993). The current sample coverage of whole-rock Nd isotopes in the East and South China Seas is also limited (Fig. 1), but its continuous record is effective in detecting a change in provenance signals and is a valuable complement to the sparsely sampled single-grain data.

Single-grain approaches, although prone to the biases likely introduced by differential mineral fertility of source terranes, sedimentary recycling, and fractionation of grains during the sediment-forming process (e.g., Andersen et al., 2022; Chew et al., 2020; Moecher and Samson, 2006), are superior at discriminating and unmixing the provenance signatures of multiple sources (von Eynatten and Dunkl, 2012; Vermeesch and Garzanti, 2015). Zircon is among the most physiochemically resilient detrital minerals, and it is able to survive multiple sedimentary cycles. It is an excellent U-Pb geochronometer and commonly dated by the laser ablation-(multicollector)-inductively coupled plasma-mass spectroscopy (LA-[MC]-ICP-MS) method with high efficiency and low cost (von Eynatten and Dunkl, 2012; Fedo et al., 2003; Gehrels, 2014). These features have made zircon

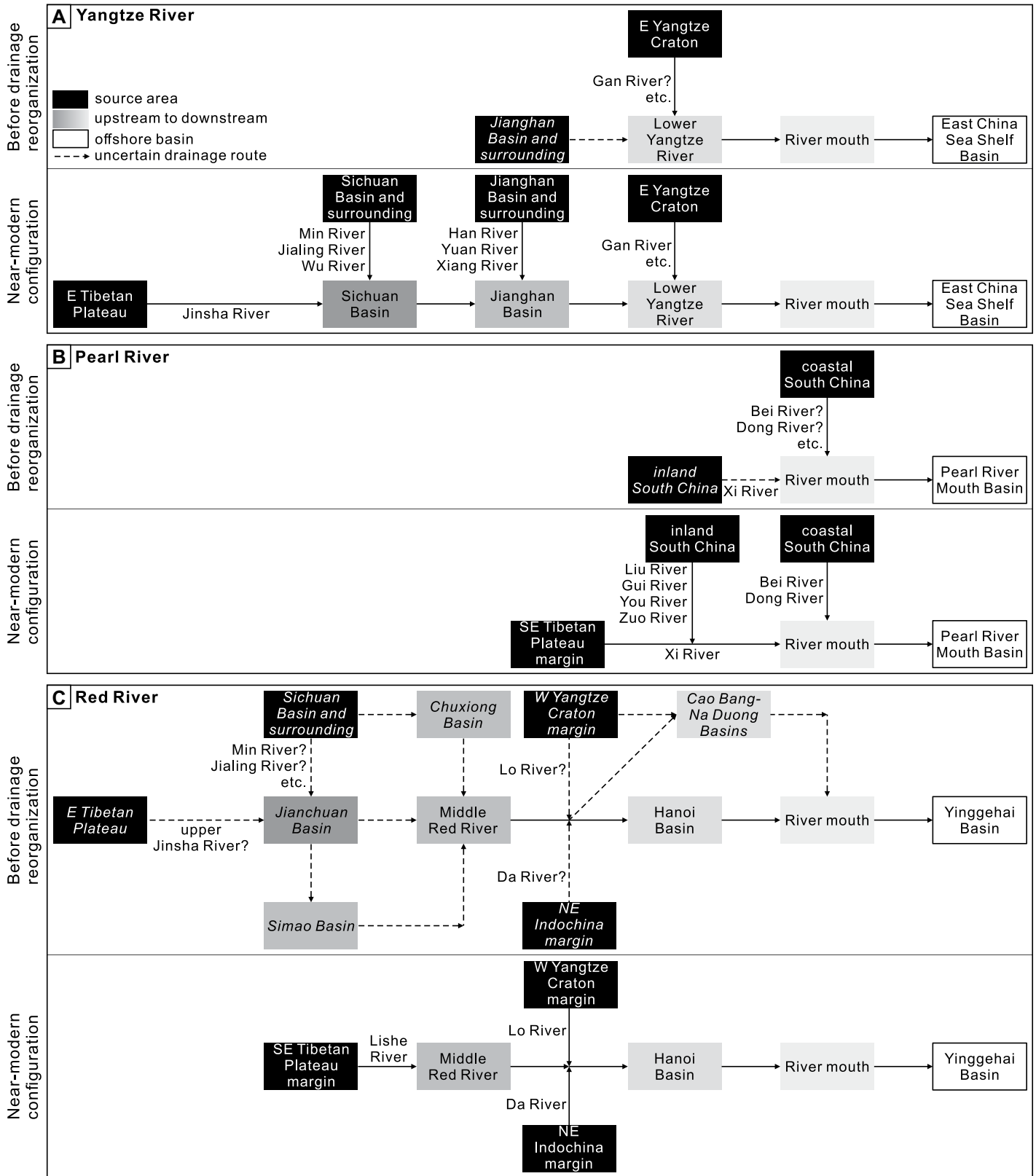


Figure 5. Schematic models proposed for Cenozoic drainage reorganizations of (A) the Yangtze River, (B) the Pearl River, and (C) the Red River. The assumed coevolution of the Yangtze and Red Rivers is shown as today's upper and middle reaches of the former feeding the latter before drainage reorganization, whereas the evolution of the Pearl River is depicted to be independent of the others. See the text for detailed explanations and references.

U-Pb geochronology one of the most prominent approaches in the realm of provenance analysis, and in the case of the East and South China Seas and large Asian rivers, the large volume of published zircon age data allows researchers to unveil the complexity of provenance signatures and establish the sediment source-to-sink relationship on regional scales (Fig. 1). Another commonly used single-grain approach in the region is detrital K-feldspar Pb isotopes, especially in sediments from the northwestern South China Sea and the Yangtze and Red Rivers (e.g., Clift et al., 2008; Wang et al., 2019a; Zhang et al., 2021c, 2021d). Feldspar, as a framework mineral, is representative of the main proportion of sediment, and, because of its relatively labile behavior, it mainly records the first-cycle provenance (Barham et al., 2021; Tyrrell et al., 2006). The primary Pb isotopic composition of K-feldspar does not change significantly over time and has been shown to be distinct among various crustal domains, which makes this approach favorable for sediment provenance analysis (Clift et al., 2008; Tyrrell et al., 2006, 2007). In addition to the above zircon and feldspar proxies, detrital muscovite-feldspar $^{40}\text{Ar}/^{39}\text{Ar}$ geochronology (van Hoang et al., 2010a; Sun et al., 2021), detrital monazite electron microprobe geochronology (Fan and Li, 2008; Yang et al., 2006a), and detrital garnet chemistry (Garzanti et al., 2021) have also been reported from the studied large river basins.

For the deep-time record of river-discharged sediments, an integration of different proxies is beneficial to overcome methodological limitations and minimize uncertainties in provenance interpretation. Given the advantages and disadvantages of different proxies and their data availability in both source and sink areas, here we mainly focused on detrital single-grain zircon U-Pb ages and K-feldspar Pb isotopes and whole-rock Nd isotope data to investigate the evolution of the Yangtze, Pearl, and Red Rivers.

Samples and Data Compilation

To investigate the provenance evolution of river-discharged sediments in the East and South China Seas, we compiled published samples from surface sediments and Cenozoic strata in several continental margin basins therein (Fig. 1). Modern river sediments and relict fluvial sediments on land were also included in the compilation because, as described in later sections, they provided valuable information for characterizing the provenance signatures of source areas and constraining the ancient sediment-routing systems, respectively. The former included sediment samples from both large and small rivers of East Asia (Fig. 1) to recognize

and discriminate their different source contributions to the East and South China Seas. The latter included sediment samples from Cenozoic strata in inland basins (Fig. 1; e.g., the Jiangnan and Jianchuan Basins) that could have once been traversed by the studied three large rivers.

Sediment samples of the East and South China Seas were mainly collected from commercial boreholes drilled by the China National Offshore Oil Corporation (CNOOC). The extensive well-log data, seismic profiles, and paleontological data obtained through commercial exploration by CNOOC and several scientific drilling programs provided a reliable basis for establishing the regional stratigraphy of the East and South China Seas (Larsen et al., 2018; Li et al., 2015a; Wang et al., 2014b; Wang and Li, 2009). Here, we started with the widely used stratigraphic framework of the region (Chen, 2016; Wang et al., 2014b; Zhu et al., 2019) and then incorporated recent revisions on some Paleogene strata (Fig. 4). We tentatively assigned an early Oligocene age to the Pinghu Formation of the East China Sea Shelf Basin because of the discovery of young zircons in clastic sediments and tuffs (Yuan et al., 2014; Zhang et al., 2018a). Following Chung et al. (2018), the Hsitsun and Szeleng Formations of west Taiwan were tentatively assigned to the Upper Eocene. The ages of stratigraphic boundaries followed the International Chronostratigraphic Chart v2021/07 (Cohen et al., 2013). In contrast to the well-correlated stratigraphy of the East and South China Seas, those of inland basins of concern within larger river basins are loosely defined in places. This is especially the case for the Paleogene stratigraphy of the Jianchuan Basin (Yan et al., 2012; Gourbet et al., 2017), and we tentatively adopted the recent scheme of Zheng et al. (2021), in which the Eocene strata comprise the Baoxiangsi, Jinsichang, and Shuanghe Formations. For samples compiled from the East and South China Seas and inland basins, we followed their stratigraphic positions assigned in previous studies.

The large volume of zircon U-Pb age data from sediment samples from the East and South China Seas and river basins are compiled in Table S1.¹ These ages were mostly obtained by LA-ICP-MS with ablation spots located on oscillatory zones, and thus dated the magmatic crystallization of zircon grains. Detailed analytical procedures of zircon U-Pb dating typically

¹Supplemental Material. Description of the studied large river basins, Figures S1–S11, and Tables S1–S4. Please visit <https://doi.org/10.1130/GSAB.S.21598371> to access the supplemental material and contact editing@geosociety.org with any questions.

followed those described by, e.g., van Hoang et al. (2009), He et al. (2014), and Cao et al. (2015). It should be noted that samples from the East and South China Seas are not indiscriminately associated with large river sources, and other potential sources may include small rivers and basinal highs. Compared to rivers, a basinal high could be “invisible” in the present topography yet a primary local source during sea-level lowstands and the phases of basin rifting and inversion (e.g., Cao et al., 2021b; Gawthorpe and Leeder, 2000; Hou et al., 2022; Voigt et al., 2008). To reduce the first-order bias of these spurious sources, we selected zircon samples closer to the large river mouth than further out seaward in the basin depocenter (Fig. 1). In particular, zircon samples from northeast-striking sags of the northern Pearl River Mouth Basin were selected to determine the sink area that has potentially recorded the Pearl River source. Those from the southern Pearl River Mouth Basin and adjacent continent-ocean transition zone were excluded where local intrabasinal and basin-bounding highs have been revealed to prevail during the Paleogene rifting period (Cao et al., 2021b; Han et al., 2017; Shao et al., 2016b). Zircon samples from the Yinggehai Basin were preferred to trace the Red River source. However, because these samples are mostly limited to the Neogene strata, we also integrated zircon samples from the Paleogene strata of the neighboring Qiongdongnan Basin. Tracing the zircon supply of the Yangtze River in the East China Sea Shelf Basin was challenging, and only samples from the Xihu Sag were available to use.

To build an internally consistent database of detrital zircon geochronology, modern and ancient samples with unclear sampling information (e.g., borehole name) and no data accessibility were excluded. The strategies used to filter discordant U-Pb analyses and determine the best ages of individual zircon grains often vary in different studies (Nemchin and Cawood, 2005; Puetz et al., 2021). In accordance with the age treatment adopted by most of the compiled studies and to facilitate cross-study comparisons, the accepted zircon ages were selected from a subset of ages with $\leq 10\%$ discordance and 10% uncertainty (1σ), wherein the $^{206}\text{Pb}/^{238}\text{U}$ age and $^{207}\text{Pb}/^{206}\text{Pb}$ age were adopted for grains younger and older than 1000 Ma, respectively. As shown from the compiled results in later sections, using 1000 Ma as a boundary to divide ages is favored by the natural break in zircon age distributions of the study area. In some samples, the number of accepted analyses was so low that the visualization of their age-frequency distributions and intersample comparison tended to be biased (Saylor and Sundell, 2016). Thus, samples with less than 40 zircon grains were tentatively

omitted. In total, 36,034 zircon grains from 390 samples finally met the criteria. The geographic localities and stratigraphic positions of zircon samples are displayed in Figure 1 and Figure 4, respectively. Detailed sampling information and references are summarized in Table S1.

Following the strategy of sample selection for the zircon age database, we compiled detrital K-feldspar Pb isotope data from Cenozoic strata of the northern part of the Yinggehai Basin and the Hanoi Basin (Clift et al., 2008; Wang et al., 2019a; Zhang et al., 2021c) as well as modern sediments of the upper Yangtze and Red Rivers (e.g., Bodet and Schärer, 2001; Clift et al., 2008; Zhang et al., 2014, 2017, 2020d) to trace the evolution of the Red River (Fig. 1). We restricted data compilation to this source-to-sink system because the counterparts in offshore sinks of the Yangtze and Pearl Rivers have not been reported. The Pb isotope data from 842 feldspar grains from 28 samples, along with sampling information and references, are summarized in Table S2. These data were mostly obtained by LA-MC-ICP-MS and ion microprobe techniques, and the detailed analytical procedures have been described by Tyrrell et al. (2007) and Clift et al. (2008).

We compiled whole-rock Nd isotopes of Cenozoic strata from both borehole and outcrop samples in the continental margin of the East and South China Seas (Fig. 1), including the Western Foothills and Hsuehshan Range of west Taiwan (Lan et al., 2014), the continent-ocean transition zone of the northern South China Sea (Ocean Drilling Program Site 1148; Li et al., 2003), the southern Pearl River Mouth Basin (boreholes PY33 and BY7-1-1; Shao et al., 2004; Yan et al., 2018), the joint area of the Yinggehai–Qiongdongnan Basins (Yan et al., 2007), and the Hanoi Basin (Clift et al., 2006a). The Nd isotope data set contained a total of 205 sediment samples of Eocene to Pliocene ages (Table S3), and those obtained from the clay fraction samples (<2 μm) of Site 1148 (Clift et al., 2002) were not included for data consistency. These data were obtained by MC-ICP-MS, with detailed analytical procedures described by Li et al. (2003) and Clift et al. (2006a).

Data Visualization and Comparison

The zircon age data are shown as probability distributions, and age estimates are marked for peaks with more than five analyses. The kernel density estimation (KDE) spectrum with a bandwidth of 30 m.y. was selected instead of the probability density plot (PDP) to properly smooth scattered age measurements (Vermeesch, 2012). For a large data set of zircon ages, it is common practice to group samples

with the same geographic locations and stratigraphic positions as a synthetic sample (e.g., Chen et al., 2022; Zhang et al., 2021b; Zhao et al., 2021). Such an averaging scheme, however, ignores the potential variability within each group and may yield biased provenance signatures (Ibañez-Mejía et al., 2018; Zimmermann et al., 2015). Instead, a careful examination of intersample variability provides a more solid basis for subdividing sample groups, which allows different source areas within river basins to be identified, as well as to determine if a single source or multiple sources were involved in feeding sink areas (Cao et al., 2018, 2021b). In this study, the intersample quantitative comparison was assessed using the cross-correlation coefficient (R^2) of age spectra (Saylor and Sundell, 2016) instead of the Kolmogorov-Smirnov (K-S) test of cumulative frequency distributions (Vermeesch, 2013). The former is directly linked to the visualization of KDEs and sensitive to the presence, absence, and relative magnitude of age peaks, whereas the latter inherently requires large sample sizes to accurately represent the zircon age signature (Saylor and Sundell, 2016; Vermeesch, 2018). A higher R^2 value toward 1 indicates a more similar sample pair that can be used for sample grouping. Still, this technique cannot fully convey the complexity of entire probability distributions, especially in samples with a low number of accepted age analyses (Saylor and Sundell, 2016). Therefore, the final determination of the grouping scheme was verified by the careful inspection of KDE spectra of individual samples. For brevity, we show the KDE plots of grouped samples by stratigraphic intervals and geographic areas as well as the multidimensional scaling (MDS) plots for individual samples. MDS is an iterative ordination technique to visualize the relative dissimilarities among samples and has been widely applied to detrital geochronology in recent years (e.g., Jiang et al., 2015; Vermeesch, 2013, 2018; Wissink et al., 2016, 2018). For the compiled zircon U-Pb age data sets, MDS transforms the matrix of pairwise dissimilarities, calculated as the cross-correlation coefficient of KDE spectra, in two-dimensional and three-dimensional space, where sample points with relatively dissimilar age signatures normally separate from each other (Vermeesch, 2013). The nonmetric MDS, which uses relative ranks of ordinal dissimilarities to determine the iterative ordination, is preferred to the metric one, which uses absolute values of dissimilarities, because the former usually yields better fits (Vermeesch, 2013; Wissink et al., 2018). The degree of distortion in the MDS transformation is monitored by the stress value, and the obtained values in different comparison scenarios of this study were mostly

around 0.1, indicating a fair goodness-of-fit (Vermeesch, 2013).

Detrital K-feldspar Pb isotope data are shown as diagrams of $^{206}\text{Pb}/^{204}\text{Pb}$ ratios versus $^{207}\text{Pb}/^{204}\text{Pb}$ ratios, where the distribution of sample points is used to diagnose the similarity or dissimilarity of isotopic signatures. Whole-rock Nd isotope data were calculated as $\epsilon_{\text{Nd}}(0)$ values relative to the chondritic uniform reservoir, with higher values indicating a relatively juvenile nature of source areas (Hamilton et al., 1983). Due to the poor age model and low sampling interval for some studied sites of the East and South China Seas, samples of Nd isotopes were grouped into stratigraphic intervals.

PROVENANCE EVOLUTION OF THE EAST AND SOUTH CHINA SEAS

In this section, we reinterpret the provenance of compiled samples from the continental margin basins of the East and South China Seas. By further recognizing and excluding the potential influences from local sources (e.g., small rivers or basinal highs), the contributions from large rivers were determined and potential provenance shifts were thus assigned to drainage reorganization events.

Provenance Signatures within Large River Basins

Characterization of potential source areas at an appropriate scale is a prerequisite for accurate provenance discrimination. Traditional provenance investigations on continental margins normally use samples from either the river mouth, the catchment-scale tectonic plates, or even the whole river basin to represent a source end member; such a loose characterization hinders the extraction of more in-depth information on provenance evolution and sediment dispersal routes. Indeed, the MDS plot for zircon age data sets of large and small rivers discharging into the East and South China Seas shows large variability within and across each group (Fig. S1), which confirms that their provenance signatures are too dissimilar to be averaged. Alternatively, the source end members within large river basins can be subdivided according to the modern configuration of drainage networks and the discriminative signatures of major tributaries, which has been applied in recent provenance investigations on detrital single grains from East Asian large rivers (e.g., Cao et al., 2018; He et al., 2014; Sun et al., 2021; Wang et al., 2019a; Zhang et al., 2021c). Here, the provenance signatures within the studied large river basins were characterized by detrital single-grain zircon U-Pb ages and K-feldspar Pb isotopes from modern sediments

of the uppermost reaches and major tributaries. This strategy centers on the direct source-to-sink relationship between bedrock and river sediment at a tributary scale and, compared to bedrock data, is less biased by sampling strategy, preservation potential, and exposure (Cao et al., 2018; Condie et al., 2017).

In the Yangtze River Basin, the zircon U-Pb age signatures of modern sediments were recently deemed to be too similar to discriminate (Sun et al., 2021; Zhang et al., 2021d). However, the MDS plot of the newly compiled data set shows that zircon samples from the upper reaches and most of the tributaries are well distinguished (Fig. 6A). Sample TTH of the Yangtze River headwater (Tuotuo River; Fig. 6B) is distinct from those of the other tributaries in very abundant Paleogene zircons. A reduced percentage of these young ages is inherited in the upper Jinsha River, which also shows multiple clusters peaking at ca. 2480 Ma, 1855 Ma, 920 Ma, 800 Ma, 440 Ma, and 240 Ma (Fig. 6C). In contrast, three tributaries (i.e., Yalong, Dadu, and Min) joining the Jinsha River feature two dominant peaks at ca. 810–770 Ma and 240–210 Ma, and their different magnitude causes a small intersample variability (Fig. 6D). In the middle and lower reaches, tributaries like the Jialing, Yuan, Han, and Gan Rivers are well distinguished by different age signatures, whereas further sample coverage is still required to explain the large intersample variability of the Wu River and Xiang River. In the estuary, two sample groups are comparable in major age peaks (Fig. 6E), and the group (samples Chongming, CM-97, and CX) with a stronger Paleoproterozoic peak at ca. 1850 Ma is comparable to the Jinsha River samples. For K-feldspar Pb isotopes of the Yangtze River Basin, a narrow range of $^{206}\text{Pb}/^{204}\text{Pb}$ ratios characterizes the Jinsha River (Fig. 7A). In contrast, data from main tributaries from the upper and middle reaches roughly plot along the average crust growth curve (Stacey and Kramers, 1975), with a few unradiogenic grains found in the Jialing River and overlap of isotopic signatures between the Dadu River and Min River.

In the Pearl River Basin, the MDS plot shows distinct zircon age signatures among upper reaches and tributaries (Fig. 8A). The Hongshui River and its headwater rivers (Nanpan and Beipan) show a strong age peak at ca. 280 Ma and two subordinate peaks at ca. 835 Ma and 445 Ma (Fig. 8B). In the middle reaches, Liu River and Gui River to the north are dominated by different Neoproterozoic peaks, whereas You River and Zuo River to the southwest show a dominant Permian cluster and a different percentage of Ordovician–Silurian ages (Fig. 8C). In contrast, samples from the lower reaches (He, Bei, and Dong) are discriminated by the presence of

abundant Jurassic–Cretaceous ages, and their variability is caused by a varying percentage of Ordovician–Silurian and Precambrian ages. Samples R11 and S5512 from the periphery of the delta have been used to represent the Pearl River estuary (Fig. 1B; He et al., 2020a; Zhao et al., 2015a), but the representativeness is challenged by their relatively limited range of zircon ages (Fig. 8D).

In the Red River Basin, the poor sample coverage of zircon age data hinders reliable characterization of provenance signatures (Fig. 9). This is especially the case for the two tributaries (Da and Lo), where a high intersample variability is observed, and samples VN07060501 and BLR-1 are likely influenced by local sources due to their unimodal spectra (Fig. 9D). A single headwater sample Hong-11-01 contrasts with the other samples, which has a strong late Eocene peak (Fig. 9B). The midstream (RS0701 and VN05060801) and estuary samples, albeit with different percentages of Ordovician–Silurian and Precambrian ages, are loosely comparable in the presence of two strong peaks at ca. 750 Ma and 250 Ma (Figs. 9C and 9E). The unique contribution from Lo River to the estuary is identified by a common ca. 1860 Ma peak. For K-feldspar Pb isotopes of the Red River Basin (Fig. 7B), the available data from river sediments demonstrate relatively poor performance of provenance discrimination. In total, 30 feldspar grains from the Da and Lo tributaries show an overlap of Pb isotopic signatures, and the fewer analyses ($n = 9$) from upstream differ from them in slightly lower $^{207}\text{Pb}/^{204}\text{Pb}$ ratios. In contrast, the downstream data show a much wider range of both $^{206}\text{Pb}/^{204}\text{Pb}$ ratios (17.3–20.4) and $^{207}\text{Pb}/^{204}\text{Pb}$ ratios (15.2–15.9).

East China Sea and West Taiwan

A Yangtze source of sediment delivered to the East China Sea was recently proposed to have initiated as early as the early Oligocene based on the similarity of zircon age distributions between Oligocene strata of the Xihu Sag and modern sediments of the Yangtze River (Huang et al., 2018; Zhang et al., 2021b). However, the zircon age distributions were averaged too much in these previous studies due to the implementation of relatively loose KDE bandwidth (50 m.y.) and sample grouping of stratigraphic intervals (Zhang et al., 2021b). Alternatively, the dominant sediment supply to the Oligocene Xihu Sag could have been from nearby basement uplifts or preexisting deposits on structural highs. The Oligocene samples show large variability in the MDS plot, represented by different spectral patterns in both cluster ages and peak magnitudes (Figs. 10A and 10D–10F), which makes a single

source model unlikely. On the other hand, the sags to the west (e.g., Changjiang, Lishui, and Jiaojiang) did not receive the Yangtze-derived sediments over the Oligocene but experienced erosion and a hiatus in accumulation (Figs. 1 and 4; Zhu et al., 2019).

Samples from the Lower Miocene strata and modern sediments of the East China Sea show a first-order similarity of age spectra, with strong Triassic peaks and subordinate peaks at ca. 1890–1825 Ma, 790–770 Ma, and 435–420 Ma (Fig. 10C), probably indicating stabilization of provenance signatures from the early Miocene. Based on sites located close to the southwestern basin boundary, Fu et al. (2021b) emphasized the change in the percentage of Neoproterozoic populations over the Eocene–late Miocene interval and favored younger provenance stabilization from then on. However, this interpretation was rooted in the averaged data sets of both source and sink areas, and their samples from individual sites did not show a consistent change pattern: The strong Neoproterozoic peak can be observed in the Eocene sample from site Z1, but it is absent in the Upper Miocene sample from site L1 (Fu et al., 2021b). These sites, compared to the Xihu Sag, were more vulnerable to the dilution of sediment supply from small rivers of coastal southeast China (e.g., Ou and Jiulong Rivers; Fig. 1), as witnessed by the presence of abundant Cretaceous zircons in the former (Fig. S2).

To the south of the East China Sea, the Oligocene–Lower Miocene strata of west Taiwan record a negative excursion in Nd isotopes (Fig. 11A; Lan et al., 2014) and an addition of Precambrian zircons (Figs. 12B and 12C; e.g., Hou et al., 2021; Lan et al., 2016). Lan et al. (2016) initially interpreted the provenance shift as driven by drainage expansion of small rivers of coastal southeast China (e.g., Min River) northwestward into inland areas that are now drained by lower reaches of the Yangtze River (e.g., Gan River; Fig. 1; Fig. S4B). In contrast, Xu (2017) highlighted the role of headwater areas (Wuyi Mountains) of today's Min River in contributing Precambrian zircons, without the necessity of introducing a drainage expansion model. Our examination of zircon age signatures of the Gan and Min Rivers (Fig. 6D; Fig. S2E), however, revealed that neither of them could have generated enough Paleoproterozoic zircons (ca. 2500–2400 Ma) to have supplied those observed in the Lower Miocene samples of west Taiwan (Fig. 12B). Thus, a contribution from the Yangtze River source is likely necessary to explain the Oligocene–Miocene provenance shift. The Yangtze-derived sediments could have first been transported in the East China Sea Shelf Basin before being further transported or reworked into

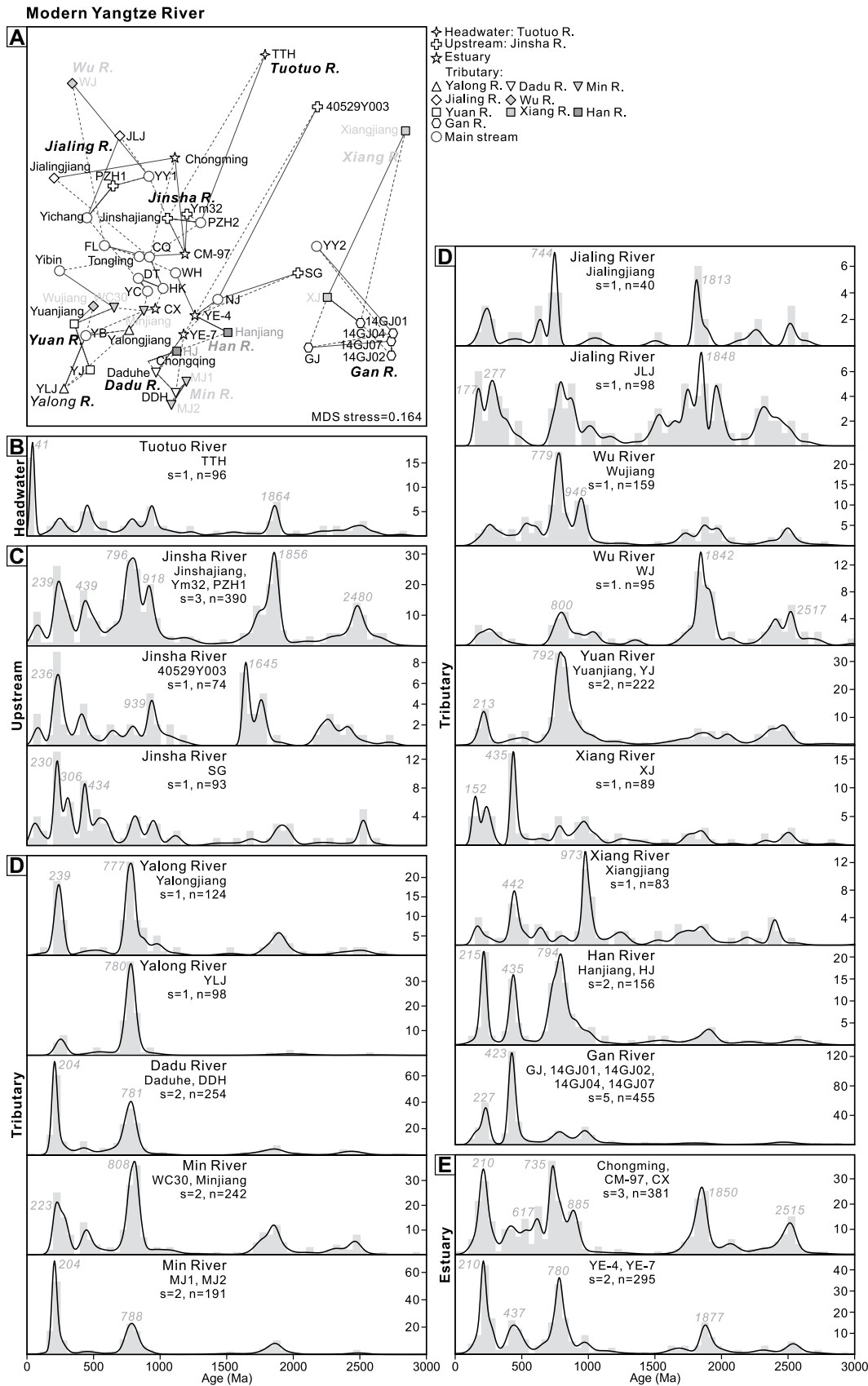


Figure 6. Detrital zircon U-Pb age distributions of modern sediments from the Yangtze River (He et al., 2013, 2014; van Hoang et al., 2009; Huang et al., 2020; Kong et al., 2009, 2011; Wang et al., 2020a; Yang et al., 2012), shown as (A) a nonmetric multidimensional scaling (MDS) plot and (B–E) plots of kernel density estimation (KDE) spectra. In the MDS plot, solid and dashed lines mark the closest and the second closest neighbors, respectively. In the KDE plots, samples are grouped as a function of geographic localities and relative similarities of age signatures revealed by the MDS statistics. The KDE spectra of samples from the lower reaches of the main stream are not shown due to the downstream mixture of detrital grains. *s*—number of compiled samples; *n*—number of concordant analyses. See Figure 1B for sample localities and Table S1 for sampling information and references (text footnote 1).

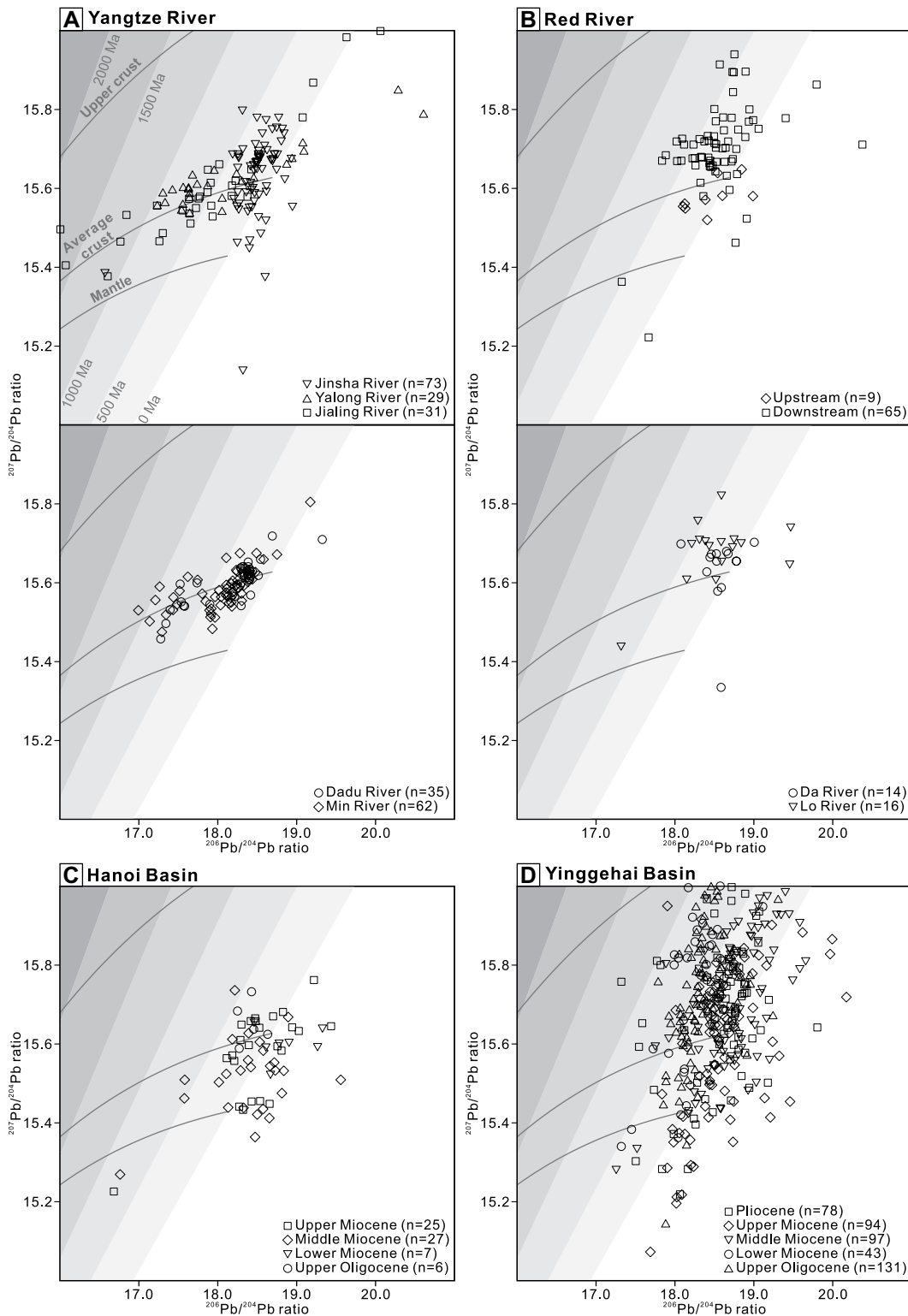


Figure 7. Detrital K-feldspar Pb isotopic compositions of modern sediments from (A) the Yangtze River (Clift et al., 2008; Zhang et al., 2014, 2017, 2020d) and (B) the Red River (Bodet and Schärer, 2001; Clift et al., 2008) as well as of Cenozoic sediments from (C) the Hanoi Basin (Clift et al., 2008) and (D) the northern Yinggehai Basin (Wang et al., 2019a; Zhang et al., 2021c). Error bars are generally small and not shown for brevity. The terrestrial Pb growth curve (Stacey and Kramers, 1975) along with the model age in 500 Ma intervals are marked for reference. For the Yangtze River samples, only those from the upstream and main tributaries were compiled. Ages of stratigraphic boundaries follow the International Chronostratigraphic Chart v2021/07 (Cohen et al., 2013). Many analyses of the Yinggehai Basin samples are outliers with $^{207}\text{Pb}/^{204}\text{Pb}$ ratios above 16.0 (Fig. S3 [see text footnote 1]). n—number of analyses. See Figure 1B for sample localities and Table S2 for sampling information and references (see text footnote 1).

marine sinks in today's western Taiwan (Figs. S4C and S4D; Deng et al., 2017; Garzanti et al., 2021; Wang et al., 2018d). However, due to the lack of sample coverage in the southern part of the basin (Fig. 1), the exact sediment-routing system remains to be investigated.

Northern South China Sea

In the northern Pearl River Mouth Basin, the large intersample variability of the Upper Oligocene–Lower Miocene strata across different sags indicates multiple sediment sources (Fig. 13).

The Eocene Wenchang Formation mainly shows a limited range of zircon ages with strong Jurassic–Early Cretaceous and middle Eocene peaks (Fig. 13G). We interpret sediment supply to have come from local uplifts because the Early Cretaceous (ca. 129 Ma) peak is not observed in the

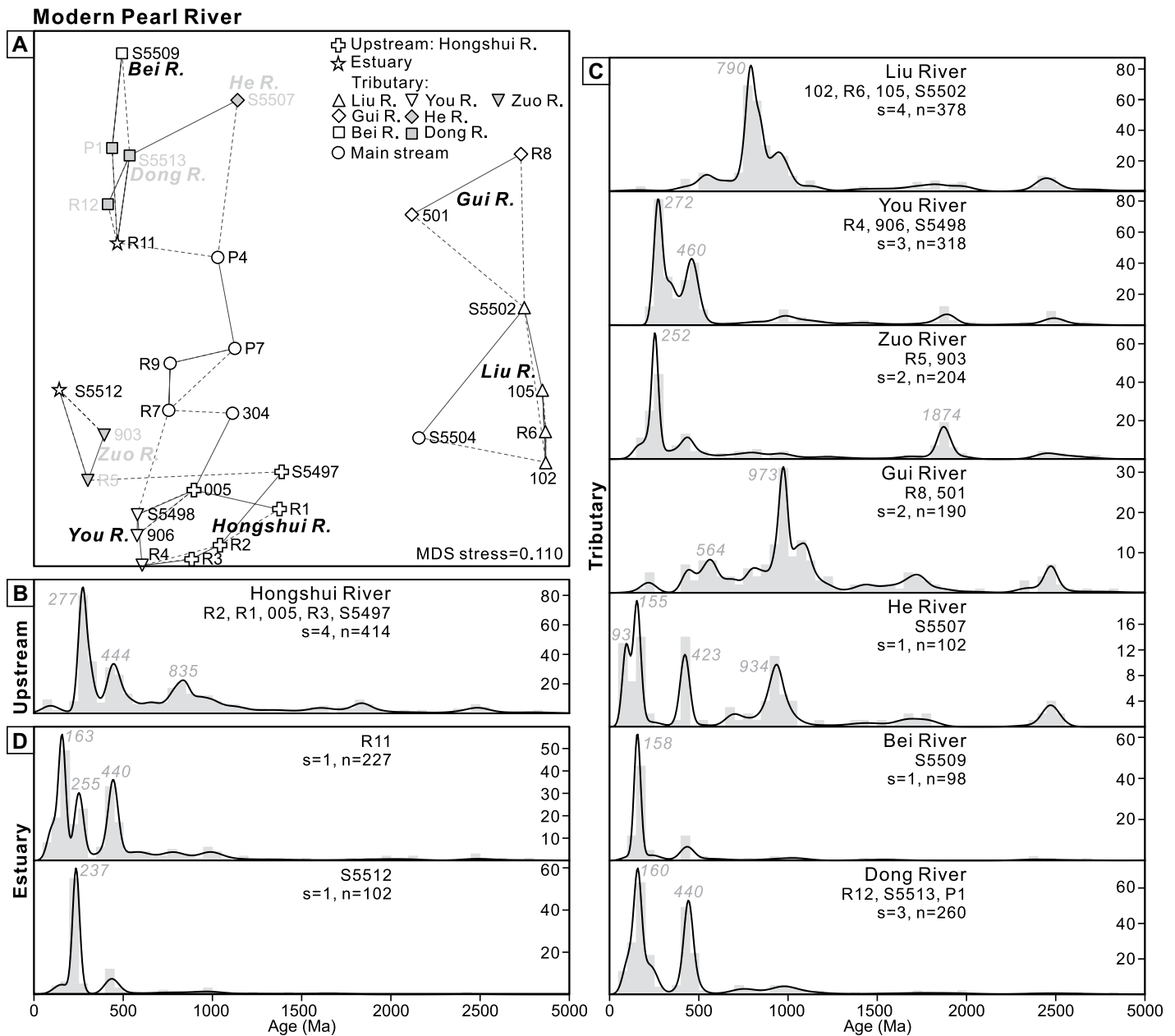


Figure 8. Detrital zircon U-Pb age distributions of modern sediments from the Pearl River (He et al., 2020a; Liu et al., 2017; Zhao et al., 2015a), shown as (A) a nonmetric multidimensional scaling (MDS) plot and (B–D) plots of kernel density estimation (KDE) spectra. See Figure 6 for legend description.

age signatures of the Pearl River (Fig. 8). While the seeming similarity of age signatures between the Bei and Dong Rivers and the Eocene samples (ZI-3-EO, H33-1, and ZI-2-EO) of the Lufeng Sag was proposed to indicate a Pearl River source (Wang et al., 2017), this source-to-sink relationship is considered unlikely because the Xijiang Sag (samples U-1-EO and P5-3920), located closer to the estuary, did not record the corresponding age signatures (Figs. 1 and 13G).

The unimodal age distribution patterns continued in the Oligocene samples (e.g., H28-1

and L2-1) and modern samples (C4 and C7) of the Hanjiang and Lufeng Sags (Figs. 13B and 13E). Thus, the northeastern part of the basin is unlikely to represent the sink of the Pearl River. To the west, both unimodal (e.g., samples H10-5, H1-1, and H10-3) and multimodal (e.g., samples F 3917.5, X1-1, and H9-1) spectra are observed throughout the Upper Eocene–Miocene strata of the Huizhou Sag (Figs. 13C–13F), indicating sediment supply from at least two sources. This multiple-source system makes the Huizhou Sag another undesirable place to study the Pearl

River. Farther westward in the Wenchang and Enping Sags, the Upper Eocene–Lower Oligocene Enping Formation consistently shows a single peak at ca. 150 Ma (Fig. 13F). However, the age signatures become different in the Upper Oligocene Zhuhai Formation (Fig. 13E): Whereas sample W9 of the Wenchang Sag shows a dominant age peak at ca. 430 Ma, samples E1-1 and E7-1 of the Enping Sag show a strong Jurassic peak and a varying percentage of Mesoproterozoic ages. Neither of their spectral patterns is explicitly observed in the modern

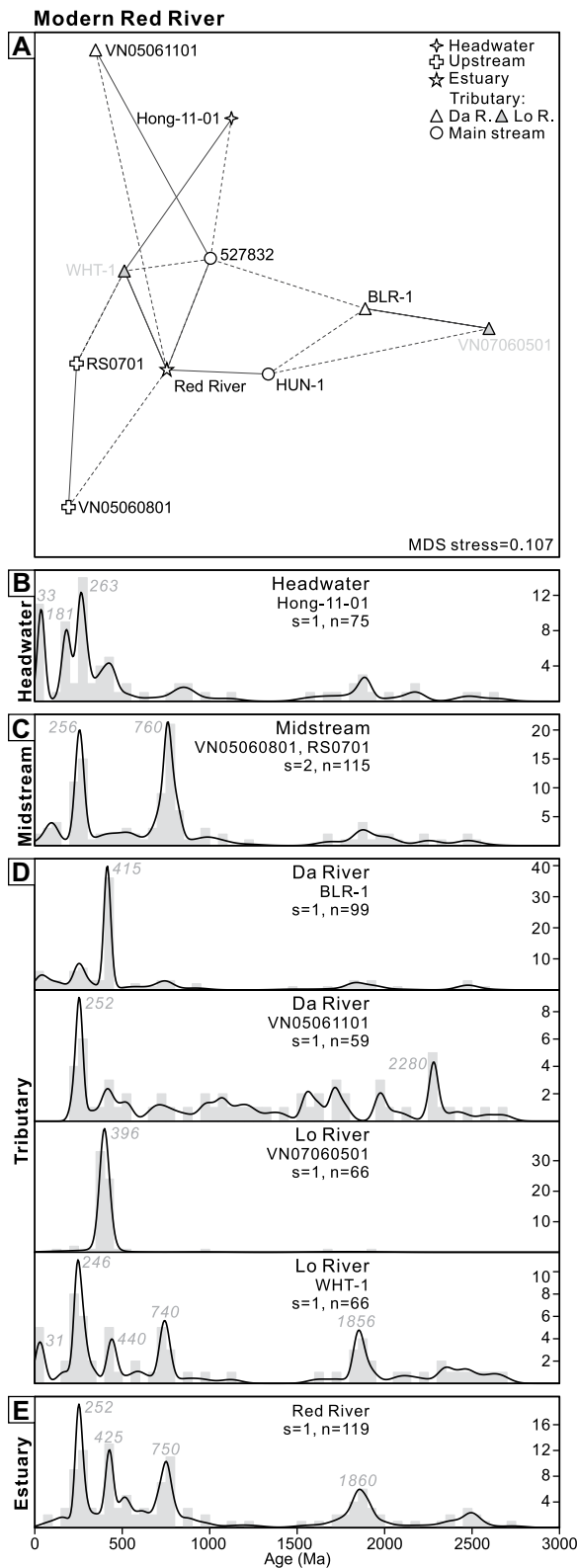


Figure 9. Detrital zircon U-Pb age distributions of modern sediments from the Red River (Clift et al., 2006b; Fyhn et al., 2019; van Hoang et al., 2009; Wang et al., 2018a; Wissink et al., 2016), shown as (A) a nonmetric multidimensional scaling (MDS) plot and (B–E) plots of kernel density estimation (KDE) spectra. See Figure 6 for legend description.

Pearl River (Fig. 8). Moreover, their peak magnitudes of Permian–Triassic ages are smaller than those of samples from the western Pearl River Basin (e.g., the Hongshui, You, and Zuo Rivers).

Based on the above observations, the source-to-sink signals of the Oligocene strata vary among different sags of the northern Pearl River Mouth Basin, and the Xijiang Sag is interpreted

to be the most likely candidate for an ocean sink directly receiving Pearl River–derived sediments. Following prior provenance interpretations of borehole X28 in the Xijiang Sag (Cao et al., 2018), the Lower Oligocene sample X28-2 was likely sourced from the southeast China margin. A large set of southward-prograding deltaic sequences offshore the river mouth recorded this sediment-dispersal route (Pang et al., 2009). Subsequently, a significant provenance shift occurred over the late Oligocene, manifested by a negative excursion of ϵ_{Nd} values from about -11 to -12 in sites 1148 and PY33 (Figs. 11B and 11C; Li et al., 2003; Shao et al., 2004) and an increased percentage of Triassic zircons in borehole X28 (Figs. 13E and 13F). The ϵ_{Nd} values derived from Paleogene strata of borehole BY7-1-1 (Yan et al., 2018) are systematically higher than those from sites 1148 and PY33 (Figs. 11B and 11C), which again verifies our consideration that sediment infilling of the southern Pearl River Mouth Basin was complicated by multiple sources during rifting and should not be simply associated with a Pearl River source. In contrast, the Neogene source-to-sink system likely became stable because the ϵ_{Nd} values obtained from sites 1148 and PY33 are comparable and do not vary much over this period. The near-modern provenance pattern since the early Miocene is also supported by zircon age distributions (Figs. 13B and 13D): The Lower Miocene samples X28-5 and X28-6 and modern sample G25 are similar in the appearance of Neoproterozoic and Permian–Triassic peaks, and the Lower Miocene samples X28-4 and X28-7 and modern samples G03 and G07 are similar in the common ca. 150 Ma peak and low percentage of Precambrian ages. Their intersample variability is interpreted to have been caused by differential contributions from Jurassic–Cretaceous intrusions of the southeast China margin (Fig. 3). A younger age of provenance stabilization was advocated by Yan et al. (2018) based on the changing Nd isotopic compositions in the Lower–Middle Miocene samples of borehole BY7-1-1 (Fig. 11B). However, these samples could likely have been sourced from areas other than the Pearl River, because their ranges of ϵ_{Nd} values are larger than those of borehole PY33 to the north, and the sample coverage of detrital zircon geochronology in the Neogene strata remains to be improved to provide additional constraints on provenance evolution.

Northwestern South China Sea

In the northwestern South China Sea, large numbers of published samples with late Oligocene to Pliocene ages were collected close to the margin of Hainan Island (Fig. 1). They

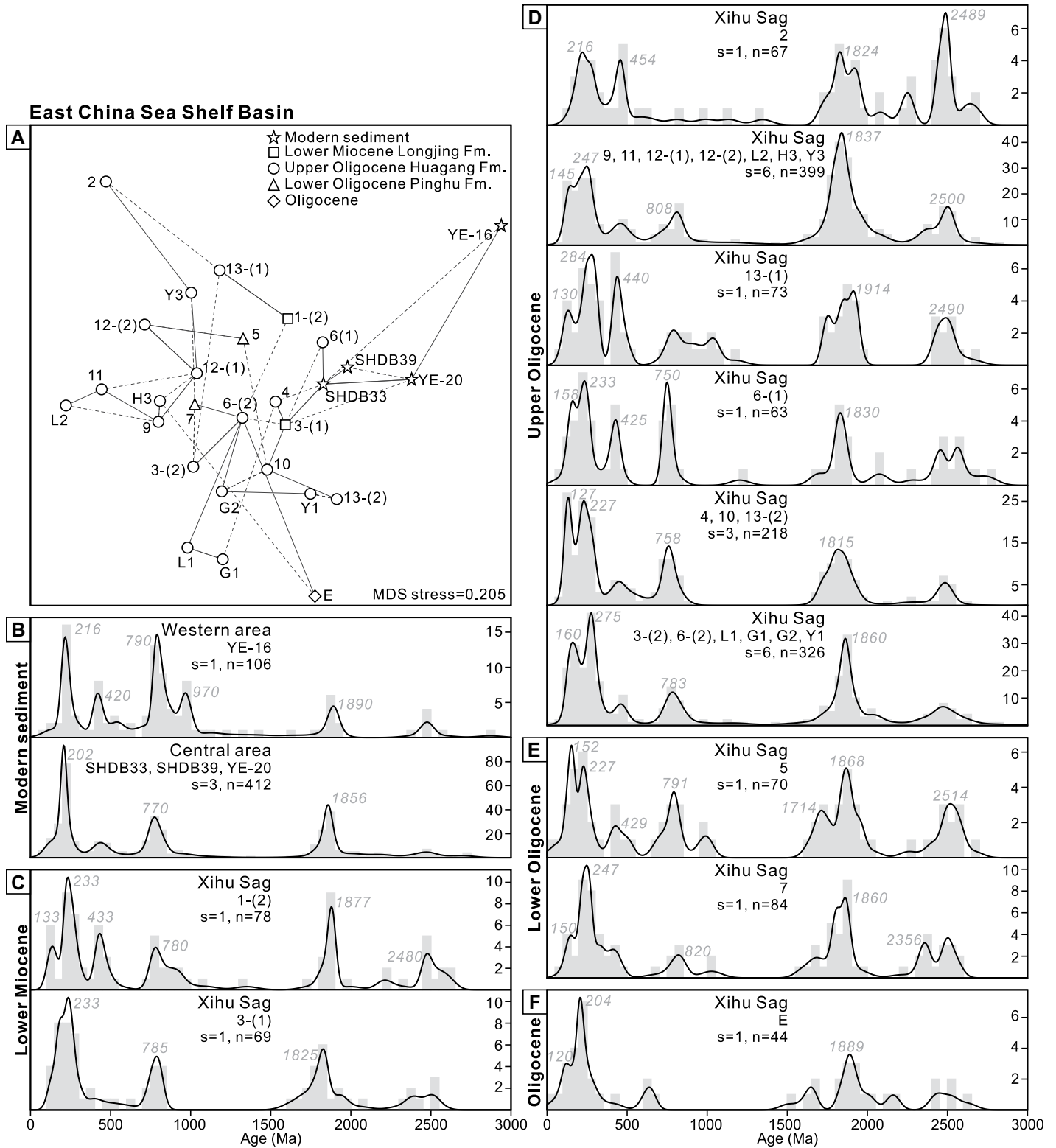


Figure 10. Detrital zircon U-Pb age distributions of Oligocene–Lower Miocene strata and modern sediments from the East China Sea Shelf Basin (Wang et al., 2018d; Yang et al., 2006b; Zhang et al., 2018a), shown as (A) a nonmetric multidimensional scaling (MDS) plot and (B–F) plots of kernel density estimation (KDE) spectra. In the MDS plot, solid and dashed lines mark the closest and the second closest neighbors, respectively. In the KDE plot, samples are grouped as a function of geographic localities and relative similarities of age signatures revealed by the MDS statistics. s—number of compiled samples; n—number of concordant analyses. See Figure 1B for sample localities and Table S1 for sampling information and references (see text footnote 1).

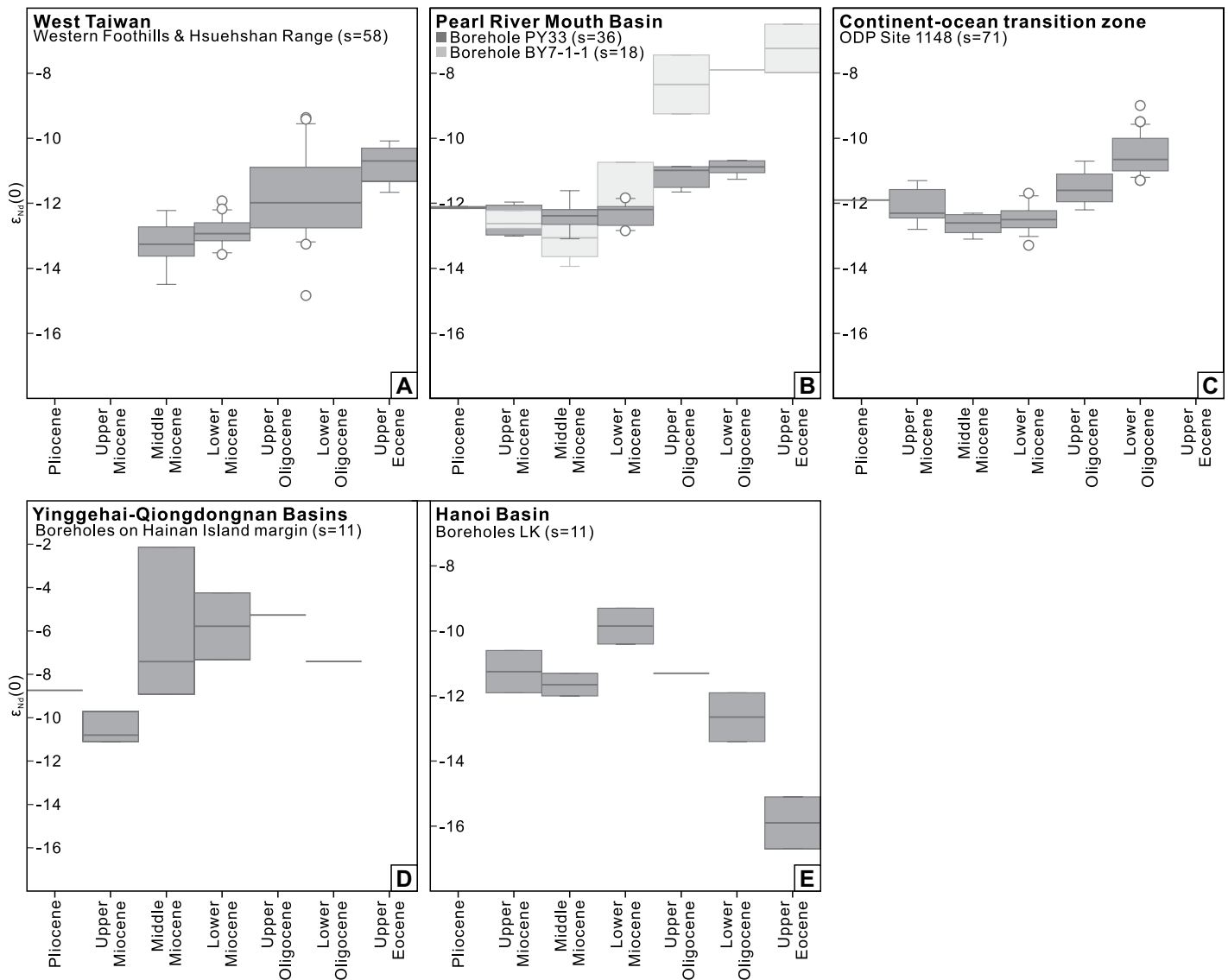


Figure 11. Cenozoic variation of whole-rock Nd isotopes, expressed as $\epsilon_{Nd}(0)$ values relative to the chondritic uniform reservoir (Hamilton et al., 1983), in (A) west Taiwan (Lan et al., 2014), (B) the southern Pearl River Mouth Basin (Shao et al., 2016a; Yan et al., 2018), (C) the adjacent continental-ocean transition zone (Li et al., 2003), (D) the joint area of the Yinggehai–Qiongdongnan Basins (Yan et al., 2007), and (E) the Hanoi Basin (Clift et al., 2006a). Samples from the same stratigraphic intervals are grouped and visualized as box plots showing median values and 10th, 25th, 75th, and 90th percentiles in thick lines, with error bars in thin lines, as well as outliers in circles. Ages of stratigraphic boundaries follow the International Chronostratigraphic Chart v2021/07 (Cohen et al., 2013). The depositional ages of a few samples from west Taiwan were reassigned based on recent stratigraphic revisions (Chen, 2016; Chung et al., 2018). *s*—number of compiled samples; ODP—Ocean Drilling Program.

were first identified to have been fed by proximal sources (Jiang et al., 2015; Wang et al., 2016a; Yan et al., 2011) because most of them are similar to the modern sediments of Hainan rivers in their very limited range of zircon ages (Figs. S5 and S6C). A Hainan source also applies to the joint area of the Yinggehai–Qiongdongnan Basins, where ϵ_{Nd} values of different strata are systematically higher than those from the Hanoi Basin (Figs. 11D and 11E; Clift et al., 2006a; Yan et al., 2007).

In the interior Qiongdongnan Basin, zircons from the Lower Oligocene samples Y211-2 and Y19-2 are dated around 250 Ma (Fig. 14G) and were likely sourced from intrabasinal highs because of the fluvial to lacustrine environment and early stage of rifting at that time (Fig. 4). A similar pattern continued into the Upper Oligocene sample Y19-1 (Fig. 14F). In contrast, the contemporary samples QE-UO and Y211-1 from borehole Y211 show a wider age range, and the latter was recently suggested to be sourced

from the Red River (Lei et al., 2019; Shao et al., 2019). A careful comparison of age signatures of modern rivers surrounding the northwestern South China Sea revealed that the Red River and small Vietnamese rivers may potentially be discriminated by the presence of late Eocene ages and a ca. 750 Ma peak, and the presence of a ca. 900 Ma peak, respectively (Fig. 9; Fig. S6D). Following this criterion of provenance discrimination, sample Y211-1 would better be interpreted as sourced from central Vietnam. The

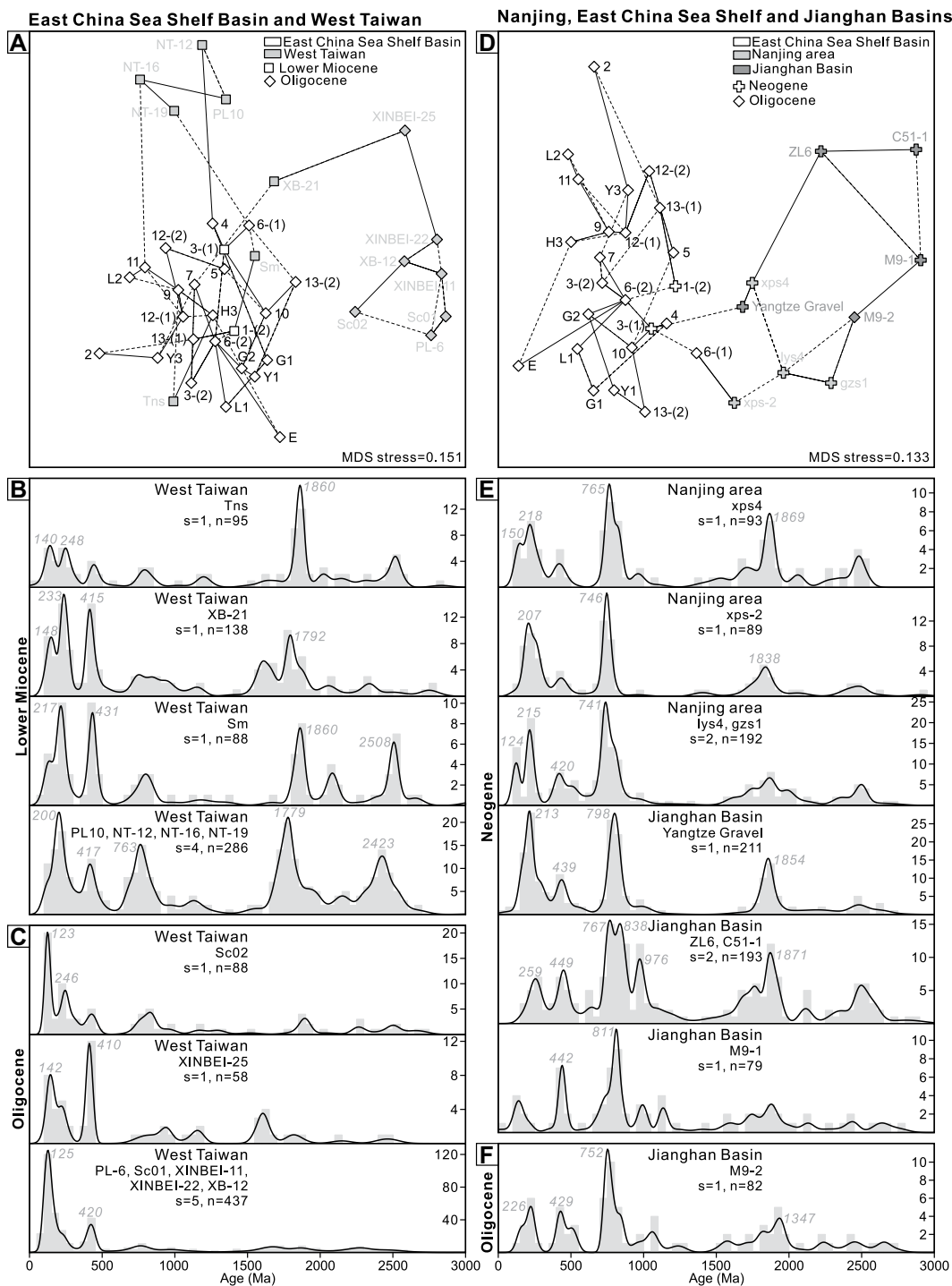


Figure 12. Comparisons of detrital zircon age signatures of Oligocene–Neogene strata from the East China Sea Shelf Basin with those from west Taiwan (Chen et al., 2017a; Lan et al., 2016; Yan et al., 2018) and Nanjing area of the lower Yangtze River Basin (Zheng et al., 2013) and the Jiangnan Basin (Sun et al., 2018; Wang et al., 2014c; Yang et al., 2019), shown as (A, D) nonmetric multidimensional scaling (MDS) plots and (B–C, E–F) plots of kernel density estimation (KDE) spectra. See Figure 10 for legend description and the East China Sea Shelf Basin data set.

small age peak at ca. 730 Ma of sample QE-UO is conspicuous but cannot be definitively associated with a Red River source due to the absence of a ca. 1860 Ma peak and small sample size (Figs. 9 and 14F).

Stratigraphically upward in the Yinggehai Basin, the bimodal Neoproterozoic peaks, albeit with a varying degree of magnitude, continued over the Neogene, and the Late Jurassic–Early

Cretaceous peaks are especially observed in Upper Miocene–Pliocene strata (Figs. 14B–14E). These features prove that the thick sediment successions of the basin had been supplied from multiple sources, including the Red River, central Vietnam, and Hainan Island (e.g., Jiang et al., 2015; Shao et al., 2019; Wang et al., 2018a; Zhao et al., 2015b). The variation in their relative contributions could be the main cause

for the intersample variability observed within the Neogene strata. Nonetheless, we interpret an establishment of provenance stabilization of the Red River in the early Miocene based on the following observations. First, the Nd isotopic compositions of the Hanoi Basin did not change much (average ϵ_{Nd} value of -10.9) after the positive excursion in the Paleogene (Fig. 11E; Clift et al., 2008). Second, the pattern of multiple age

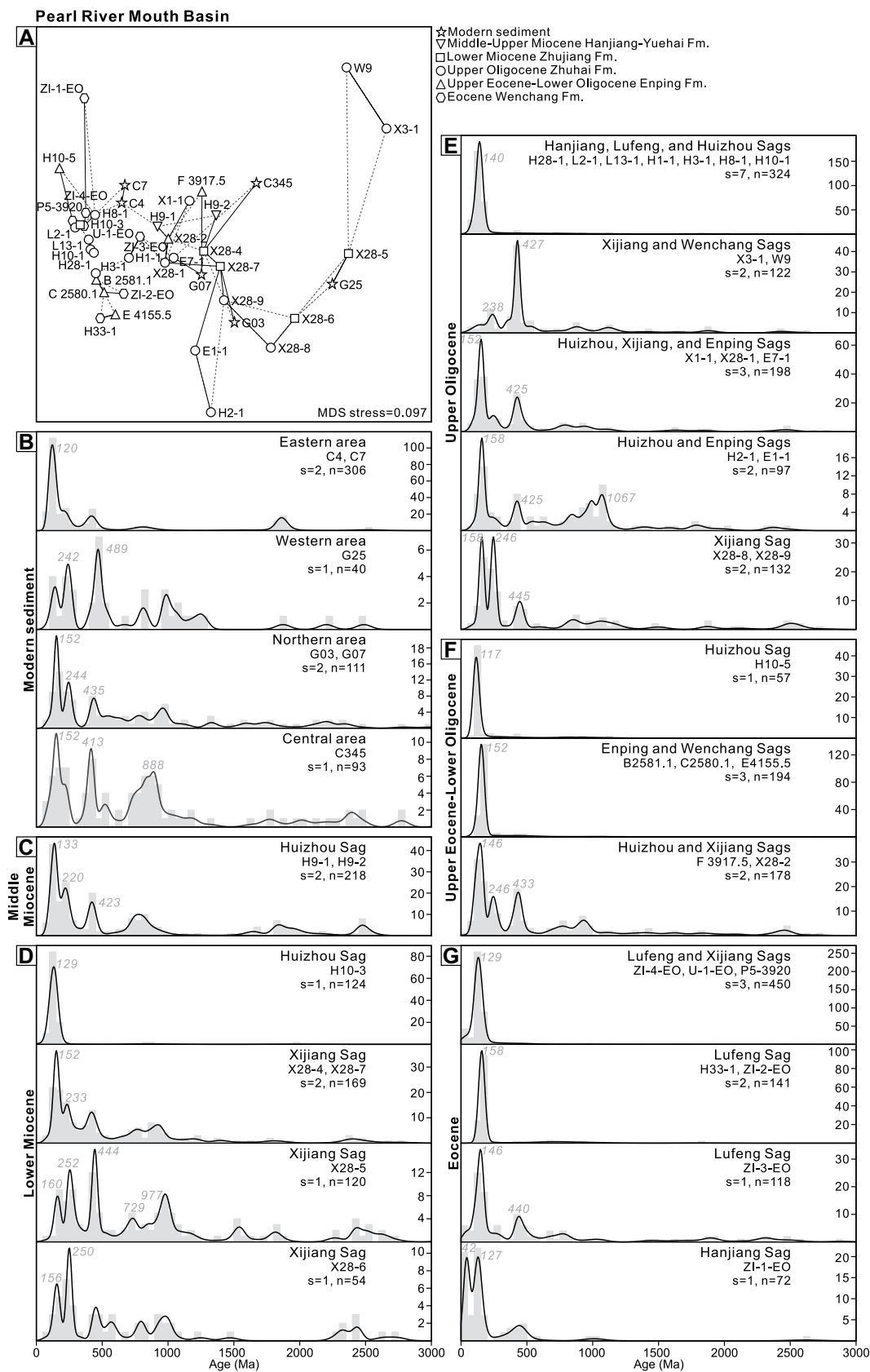


Figure 13. Detrital zircon U-Pb age distributions of Eocene–Miocene strata and modern sediments from the Pearl River Mouth Basin (Cao et al., 2018; Fu et al., 2021a; He et al., 2020a; Shao et al., 2016b, 2019; Wang et al., 2018b, 2017; Zhao, 2015), shown as (A) a nonmetric multidimensional scaling (MDS) plot and (B–G) plots of kernel density estimation (KDE) spectra. See Figure 10 for legend description.

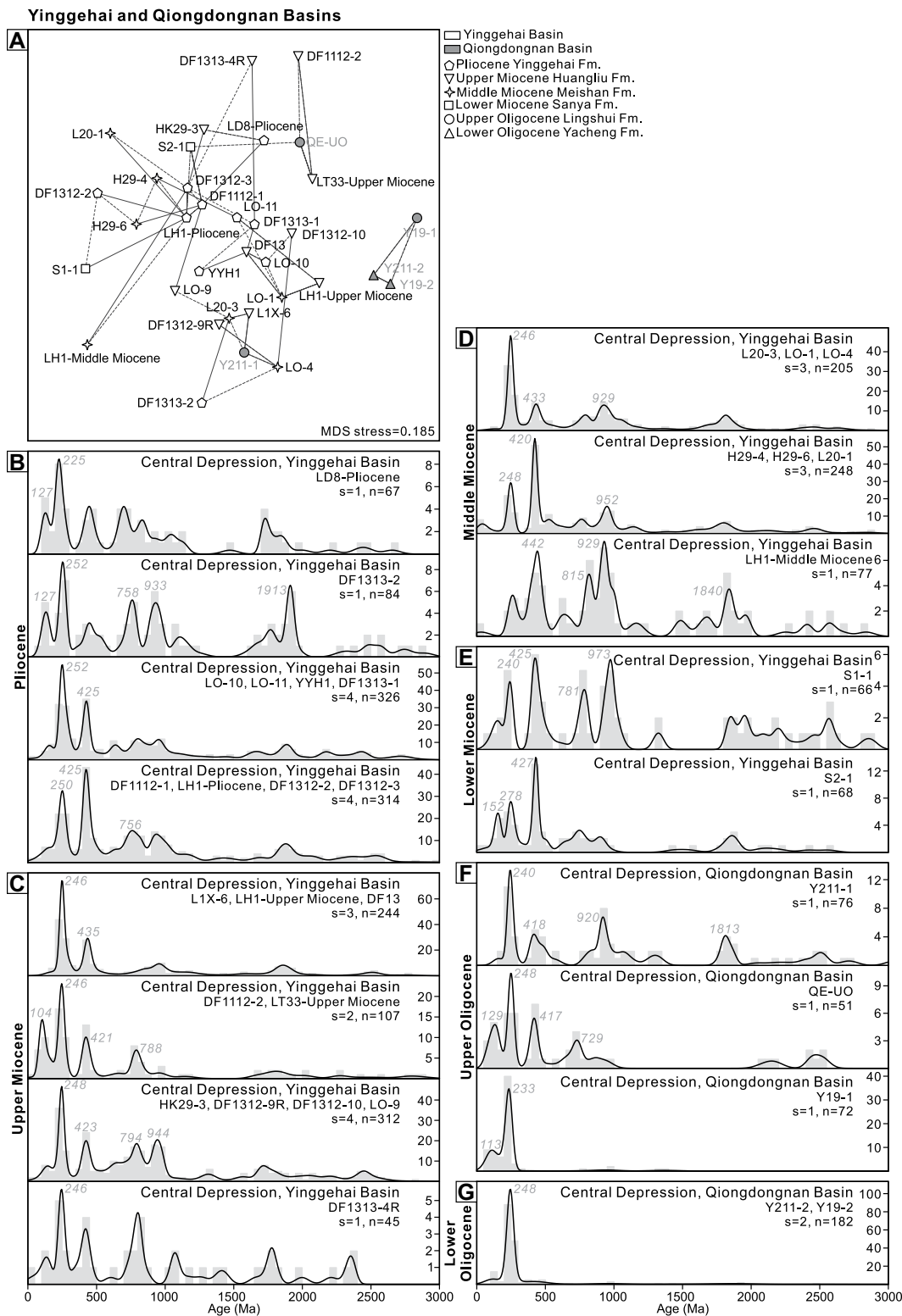


Figure 14. Detrital zircon U-Pb age distributions of Oligocene strata from the Qiongdongnan Basin (Lei et al., 2019; Shao et al., 2016b, 2019) and Neogene strata from the Yinggehai Basin (Cao et al., 2015; Jiang et al., 2015; Wang et al., 2014a, 2016a, 2018a, 2020b; Xie et al., 2016; Yan et al., 2011), shown as (A) a nonmetric multidimensional scaling (MDS) plot and (B–G) plots of kernel density estimation (KDE) spectra. See Figure 10 for legend description.

peaks in Lower Miocene sample S1-1 from the northern Yinggehai Basin was inherited in many younger samples (Figs. 14B–14E). Third, only a single zircon grain with a late Eocene age was found in Lower Miocene sample S2-1, and such

a young age peak is well observed in the Red River Basin (Figs. 9 and 14E).

Detrital K-feldspar Pb isotope data from the Upper Oligocene–Neogene strata from the Hanoi and Yinggehai Basins (Clift et al., 2008;

Wang et al., 2019a; Zhang et al., 2021c) were compared to provide additional provenance constraints. The Pb signatures of different strata from the Hanoi Basin cannot be explicitly distinguished, albeit with slightly lower

$^{207}\text{Pb}/^{204}\text{Pb}$ ratios compared to the modern Red River sediment (Figs. 7B and 7C; Clift et al., 2008). In contrast, the Yinggehai Basin data set displays a great range of both $^{206}\text{Pb}/^{204}\text{Pb}$ and $^{207}\text{Pb}/^{204}\text{Pb}$ ratios within each stratigraphic interval (Fig. 7D). Based on the conspicuous presence of very high $^{207}\text{Pb}/^{204}\text{Pb}$ (up to 16.6) grains in the Oligocene–Middle Miocene strata, Wang et al. (2019a) interpreted an earlier distal source from the areas of today's middle Yangtze River and upper Mekong River. However, such high $^{207}\text{Pb}/^{204}\text{Pb}$ grains, along with those as low as 15.1, are not observed in both modern samples of the Yangtze River and Red River and ancient samples of the Hanoi Basin (Fig. 7; Zhang et al., 2021c), and the Pb isotope data used for defining the Mekong River source is only representative of its middle reaches (Bodet and Schärer, 2001). Thus, the source-to-sink system of detrital feldspar in the northwestern South China Sea remains to be investigated, and a larger sample coverage is required to capture the complexity of source end members.

IMPLICATIONS FOR DRAINAGE AND LANDSCAPE EVOLUTION

A great challenge in analyzing the dynamic evolution of large rivers is to approximate the genesis of near-modern drainage configurations. The specific drainage networks are hard to reconstruct because large rivers divide and rejoin into multiple channels, and the sample coverage of residual, sparse fluvial records on land is usually insufficient to characterize the whole ancient river basin. Instead, it is reasonable to characterize the near-modern drainage configuration from the perspective of the geomorphological framework and sediment provenance (Zheng, 2015), and at least the main stream of a large river should achieve its near-modern distribution to meet the definition of river genesis. Sediment provenance functions as a critical link among ultimate source areas, inland temporary storage areas, as well as ultimate sink areas. In this regard, it is straightforward to estimate the timing of river genesis from the latest major shift in provenance proxies of river-discharged sediments from continental margins.

Our reevaluation of the provenance evolution of ocean sinks of the Yangtze, Pearl, and Red Rivers suggests that their source-to-sink systems could have consistently stabilized since the early Miocene (Fig. 15). To further constrain ancient sediment-routing systems and test previous models of drainage and landscape evolution, we compared the provenance data between the margin of the East and South China Seas and the key inland basins that were likely traversed by the studied large rivers. Admittedly,

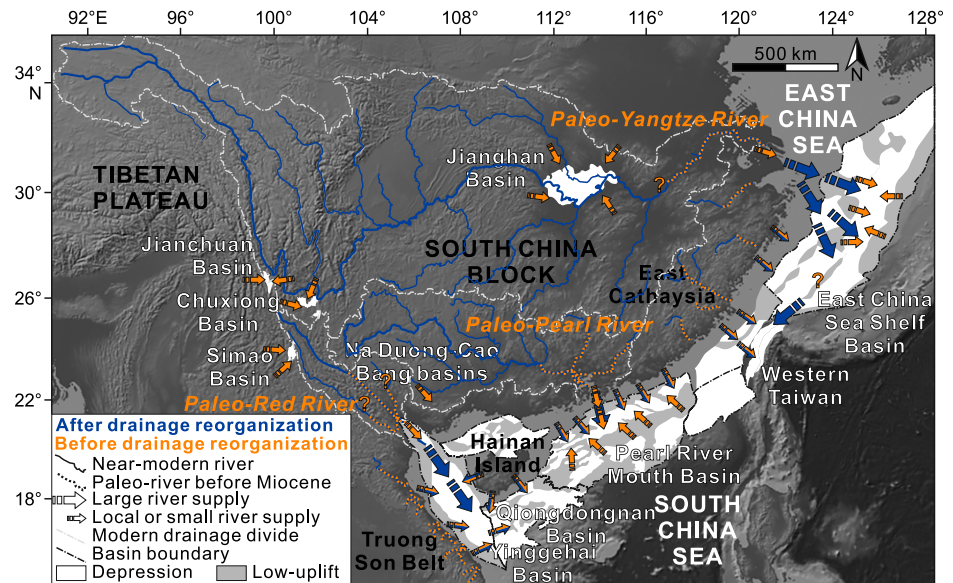


Figure 15. Schematic reconstruction of the Cenozoic drainage evolution of East Asia superimposed on the topographic map with modern drainage networks (in blue). Arrows stand for potential sediment-dispersal routes with their sizes indicative of large river supply and small river/local supply. Large rivers, including the Yangtze, Pearl, and Red Rivers, are interpreted to have established their near-modern drainage configurations since the Miocene, and the corresponding provenance signals were recorded in the Xihu Sag of the East China Sea Shelf Basin and western Taiwan, the Xijiang Sag of the Pearl River Mouth Basin, and the Central Depression of the Yinggehai Basin, respectively. Before the Miocene, these three rivers (in orange) are interpreted to have been dispersed within their modern catchments and, most likely, initiated first as small rivers before subsequent drainage expansion. During the Paleogene, local or small river supply likely prevailed in both inland basins (e.g., Jianchuan Basin and Jiangnan Basin) and offshore basins.

the Cenozoic history of Asian large rivers is such a complicated process that it cannot be fully reconstructed from the perspective of sediment provenance alone. Therefore, we also incorporated provenance information with other lines of evidence, for example, thermochronometry and paleoaltimetry of source terranes.

Pearl River

Previous provenance work on the Oligocene–Miocene strata of the Pearl River Mouth Basin, including the discrimination and sediment unmixing of detrital zircon geochronology (Cao et al., 2018; He et al., 2020a) and the change of whole-rock Nd isotopes (Li et al., 2003; Shao et al., 2004), suggested a progressive drainage expansion of the Pearl River. It could have evolved from small rivers confined within the southeast China margin in the early Oligocene to a large river system possibly incising the Tibetan Plateau margin in the late Oligocene, and finally to a near-modern drainage configuration in the early Miocene with the joining of rivers originating from the Jiangnan orogen (Fig. 15). Given the present drainage configuration of the Pearl

River delta (Fig. 1), the Bei and Dong tributaries could have evolved independently of the mainstream Pearl River in transporting sediment to the northern South China Sea. He et al. (2020a) proposed the initiation of these two tributaries as early as Early Cretaceous time, when the South China margin was above the subduction zone of the Panthalassa Ocean (Cui et al., 2021; Li and Li, 2007; Suo et al., 2019). However, during this tectonically active period, the sediment-dispersal routes could have significantly differed from the present distribution of river courses, making the definition of river genesis before the Cenozoic very loose. Although the coastal mountains underwent rapid exhumation, diachronous along strike, before the Oligocene (Yan et al., 2009), the Eocene synrift strata of the Pearl River Mouth Basin should not be simply associated with a paleo-Pearl River source as previously thought (e.g., Chen et al., 2021; Wang et al., 2017). The apparent similarity of zircon age signatures may be caused by the wide distribution of late Mesozoic igneous rocks in the southeast China margin (Fig. 3).

The occurrence of a provenance shift and drainage expansion hints at a change in the

headwater location that was likely driven by the late Oligocene surface uplift of the Tibetan Plateau margin. The landscape of southwest China prior to the late Paleogene development of the upper Pearl River remains poorly understood. The isotope-based paleoaltimetry of the Chake Basin along today's Nanpan River revealed an Eocene elevation near sea level (Fig. 2; Hoke et al., 2014). This area was once interpreted as a potential source of the northwestern South China Sea sediment to explain the conspicuous occurrence of Neoproterozoic zircons, particularly of ca. 900 Ma ages, in some samples of the Yinggehai and Na Duong–Cao Bang Basins (van Hoang et al., 2009; Jiang et al., 2015). However, this age signature, based on our reevaluation, was likely contributed by sources from small rivers in the eastern Vietnamese margin instead. The northeastward paleocurrent direction obtained from the Eocene Jianshui Basin also confirms a long-lived drainage divide between the Pearl River and the Red River (Wissink et al., 2016).

Yangtze River

Within the Yangtze River Basin, Cenozoic strata are thicker and more widespread downstream in the Jiangnan and Subei Basins than in the Sichuan Basin (Fig. 3). Published zircon age data from the Oligocene–Neogene strata of the Jiangnan Basin, Nanjing area of the Subei Basin, and East China Sea Shelf Basin are compared in Figures 12D–12F. The distinct age signatures of the Oligocene samples between the East China Sea Shelf Basin and Jiangnan Basin confirm their different sediment sources. This difference continued into the Neogene strata (e.g., samples ZL6, C51-1, and M9-1). However, the Yangtze Gravel samples of the Jiangnan Basin and Nanjing area and the Lower Miocene samples of the East China Sea Shelf Basin plot with closer proximity in the MDS plot (Fig. 12D). The comparison of KDE spectra shows that their intersample variability is mainly reflected by different percentages of Paleoproterozoic and Ordovician–Silurian peaks (Figs. 10C and 12E). These observations favor a common origin of the Yangtze Gravel, representing a through-flowing river discharging into the East China Sea during the Neogene (Fig. 15). Therefore, the records of detrital geochronology and Nd isotopes (Lan et al., 2014) consistently indicate an early Miocene genesis of the near-modern Yangtze River, which confirms the previous interpretation of Zheng et al. (2013).

In contrast, some studies favored a younger history of the Yangtze River. Recent muscovite and K-feldspar $^{40}\text{Ar}/^{39}\text{Ar}$ geochronology of Yangtze Gravel suggested the genesis of the Yangtze River before the late Miocene, based

on the observation that Cenozoic grains of muscovite and feldspar, typical of an upper Yangtze River source, are absent in relatively old gravel samples (Sun et al., 2021). The downstream mixture effect, although excluded by Sun et al. (2021), still holds potential for explaining the observation. This effect is evident in the modern zircon age data set, in which Paleogene grains are abundant in the Jinsha River but are hardly seen downstream to the estuary (Fig. 6). On the other hand, the sources of Cenozoic muscovite and feldspar grains remain to be carefully investigated because these grains from the Jinsha River are older than those from the Nanjing and Wuhan areas (Sun et al., 2021). In addition to the Yangtze Gravel, the provenance changes observed in the Pliocene–Quaternary strata of the Yangtze River Basin in places have been interpreted to indicate the relatively late formation of near-modern drainage configurations (e.g., Fan and Li, 2008; Jia et al., 2010; Sun et al., 2018; Yang et al., 2006a). However, these changes could be biased by the geometric disequilibrium of the Yangtze River Basin in response to the high-frequency climate oscillation in the late Cenozoic when river networks dynamically adjusted their drainage areas (Clift, 2006; Willett et al., 2014). Moreover, the Pliocene to Quaternary pulses of accelerated incision found in the headwater area could have been caused by local tectonism and strong monsoons rather than the final integration of the Yangtze River (Fig. 2; e.g., Ou et al., 2021; Ouimet et al., 2010; Yang et al., 2016).

Models assuming an earlier initiation of the Yangtze River also exist. Based on the near-synchronous, enhanced cooling ca. 45–40 Ma in the Three Gorges and Sichuan Basin (Fig. 3), Richardson et al. (2010) proposed a river incision model related to progressive expansion of lower Yangtze reaches into the Sichuan Basin. However, the Eocene paleo–Yangtze River system in hinterland areas, if it existed, was unlikely to be exorheic to transport erosional detritus from the Sichuan Basin eastward to the East China Sea. The strongest evidence is the presence of prolonged lacustrine facies and salt diapirism in the Eocene Jiangnan Basin (Wu et al., 2017; Zheng et al., 2013), refuting the existence of a large river traversing the basin. Recent inverse modeling of river profiles in the Three Gorges also advocated for onset of river incision as early as the early Miocene (Jiao et al., 2021). Before the Oligocene, the Yangtze River Basin should have been much smaller in size than the present configuration (Fig. 15). The drainage expansion from the Oligocene to early Miocene was a dynamic process but is very difficult to reconstruct, especially in the upper reaches, where the Oligocene fluvial records are rarely

preserved, and not much provenance data are available. An added difficulty is that the zircon age distributions of current sediment samples from a few areas of the river basin (e.g., the Wu and Xiang tributaries; Fig. 6D) are too different to exclusively characterize individual source end members.

Red River and Lost Drainage Systems

Among various models of the paleo–Red River, the Jianchuan, Simao, and Chuxiong Basins (Fig. 1) have often been proposed to be the key candidates for inland sinks archiving now-vanished sediment-dispersal routes. Here, we briefly reevaluated the provenance data of the latest models to determine if the source-to-sink systems of these basins were interconnected within a large river system.

In recent reconstructions by Deng et al. (2018) and Zhao et al. (2021), a preexisting large river was depicted over the Late Cretaceous–early Paleogene, originating from the eastern Tibetan Plateau margin (near Sichuan Basin), flowing southwestward via the Simao and Chuxiong Basins, and possibly discharging into the Neotethyan Ocean. Their claim for the drainage connectivity of different basins was mainly based on the similarity of averaged provenance signals. We revisualized the zircon age data set of Zhao et al. (2021) into KDE spectra as a function of individual basins and strata (Fig. S7) and found that large dissimilarities in age signals exist, not only across different basins, but also between the Upper Cretaceous and Lower Paleogene strata within individual basins. Thus, a regional correlation of these provenance signals from different localities and strata should be made with due caution.

A contrasting hypothesis is that a southeast-flowing large river was distributed along the modern courses of the upper Yangtze and Red Rivers during the Paleogene, traversing the Jianchuan and Simao Basins, and possibly the Na Duong–Cao Bang Basins (Fig. 5C; e.g., Chen et al., 2017b; Clift et al., 2020; He et al., 2021). In the Jianchuan Basin, the Eocene strata (including the Baoxiangsi, Jinsichang, and Shuanghe Formations) were recently proposed to be sourced from the upper Yangtze River (He et al., 2021; Zheng et al., 2021). A quick comparison of their detrital zircon geochronology, however, shows that the Shuanghe Formation and volcanoclastic Jianchuan Formation differ from the underlying Baoxiangsi and Jinsichang Formations in having abundant zircon grains of latest Eocene–early Oligocene ages (Fig. S8A). Such young magmatism is widely distributed in the Jianchuan Basin (Cao et al., 2021; Feng et al., 2021; Gourbet et al., 2017) and argues

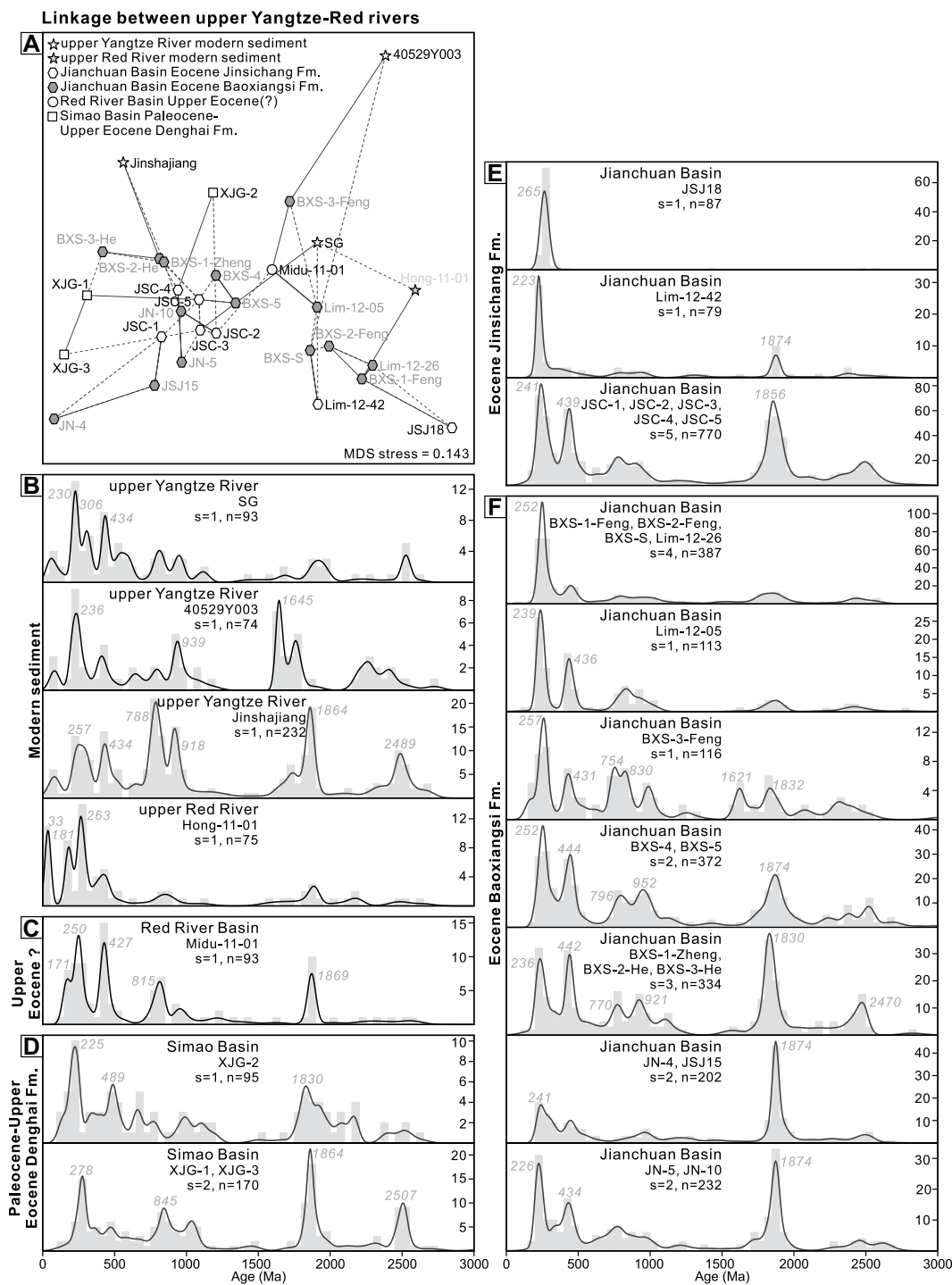


Figure 16. Comparisons of detrital zircon age signatures among the modern sediments of the upper Yangtze River and Red River and the Eocene formations of the Jianchuan Basin (Clift et al., 2020; Feng et al., 2021; He et al., 2021; Wissink et al., 2016; Yan et al., 2012; Zheng et al., 2021) and Simao Basin (Chen et al., 2017b), shown as (A) a nonmetric multidimensional scaling (MDS) plot and (B–F) plots of kernel density estimation (KDE) spectra. See Figure 10 for legend description and Figure S9 (text footnote 1) for comparison with the data set of the Na Duong-Cao Bang Basins.

against a stable tectonic period during the late Eocene to sustain a larger river system running through the basin. For this reason, only the data from the Baoxiangsi and Jinsichang Formations were used for regional comparison (Fig. 16; Fig. S9). In the Simao Basin, the Paleocene–Upper Eocene Denghai Formation instead of the overlying Upper Eocene–Oligocene Mengla Formation was compared because Chen et al. (2017b)

related them to a distal fluvial supply and a local supply source, respectively.

According to the MDS plot (Fig. 16; Fig. S9), the separation of samples of the Na Duong-Cao Bang Basins from the other samples challenges the broad provenance similarity as previously interpreted (Clift et al., 2020). A further examination of the remaining data set revealed additional intersample variability (Fig. 16),

especially in the Jianchuan Basin, which cannot be simply attributed to a single river source. Although some samples from the Jianchuan Basin are comparable in displaying multiple age peaks, much simpler spectral patterns are also observed (e.g., samples JSJ18, Lim-12-42, and BXS-S; Figs. 16E and 16F). This contrasting age signature, combined with field observations (Cao et al., 2021; Wei et al., 2016), hints at the

perturbation in local supplies likely derived from peripheral terranes of the basin. The range of facies observed in the Eocene strata (including alluvial-fan, lacustrine, fan-delta, and braided-stream facies) was probably developed in an intermontane rift setting (Wei et al., 2016) during the time largely coeval with the activation of the adjacent Ludian-Zhonghejiang fold-and-thrust belt (Cao et al., 2021). A local source interpretation was also reached by analysis of paleocurrent measurements of pebble imbrications and cross-stratifications in the Baoxiangsi Formation, which revealed predominantly eastward to northward directions (Wei et al., 2016; Wissink et al., 2016). Even if a northerly source is assumed for the Eocene Jianchuan and Simao Basins, its link with a distal river system is not supported by the absence of early Paleogene zircons therein (Figs. 16D–16F), which are typical of the upper Yangtze River source (Fig. 6C). In addition, the Simao Basin data set reveals that the Mengla Formation does not significantly differ from the underlying Denghei Formation in the KDE spectral pattern (Fig. S8B), probably challenging the provenance shift interpreted by Chen et al. (2017b).

We also argue that the hypothesis of lost drainage systems does not apply to Oligocene time as previously illustrated (e.g., Clift et al., 2020; Guo et al., 2021; Wang et al., 2019a). First, late Eocene–early Oligocene time represents an episode of magmatic flare-up in areas along the Jinshajiang fault and Ailao Shan–Red River fault zone (Fig. 3; Deng et al., 2014), which was also recorded in detrital zircons from the headwater sample Hong-11-01 of the Red River (Fig. 16B) and the Upper Eocene sample Midu-11-02 (Wissink et al., 2016). Such young magmatism and associated crustal doming and surface uplift should have dynamically shaped the landscape on regional scales unfavorable for any possible large rivers (Feng et al., 2022; Gourbet et al., 2017). Second, active tectonism continued in the Ailao Shan–Red River fault zone, where large-scale sinistral movement in the upper ranges could have already begun in the early Eocene (Li et al., 2017) and propagated toward the southeast as early as ca. 34 Ma (Leloup et al., 2001; Schärer et al., 1994). Third, the rapid exhumation and inversion of the Jianchuan Basin during the Oligocene (Fig. 2; Cao et al., 2019; Shen et al., 2016; Zheng et al., 2021) made it a topographic barrier to any south-directed flows. Fourth, the Upper Oligocene strata of the Hanoi and Yinggehai Basins do not contain enough feldspar grains with unradiogenic Pb signals, which is typical of sources from the upper and middle reaches (e.g., Dadu and Jialing Rivers) of the Yangtze River (Fig. 7; Zhang et al., 2021c).

We advocate the idea that much of the fluvial and lacustrine facies in Paleogene strata distributed in the southeastern Tibetan Plateau margin were syntectonic in response to crustal shortening (Royden et al., 2008; Zhang et al., 2010). Their depositional process was likely to be strongly influenced by proximal source terranes (Fig. 15), a view consistent with the prior provenance investigation by Wissink et al. (2016). In this scenario, the Paleogene paleo-Red River, if it existed, likely developed as relatively small rivers confined within the modern river basin (Fig. 15). The positive Nd excursion in the Paleogene Hanoi Basin (Fig. 11E) is here interpreted as reflecting a decreasing contribution from nearby terranes with an evolved isotopic composition, rather than from more distal terranes within the Yangtze River Basin as previously assumed (Clift et al., 2006a). Potential candidates of such sources are found in the Red River fault zone (i.e., Day Nui Con Voi Massif), where the reported $\epsilon_{Nd}(0)$ values of gneisses and granitic rocks of Proterozoic and Paleogene ages are as low as -18 (Anczkiewicz et al., 2012; He et al., 2020b; Lan et al., 2000). In addition to sediment provenance, the much lower estimate of sediment budget deposited in the Hanoi and Yinggehai Basins than that eroded from the modern-scale Red River was also considered to be evidence for the existence of a larger paleo-Red River (Clift et al., 2006a; Métivier et al., 1999). This gap, given its large uncertainty, could be an artifact. The eroded rock volume was previously underestimated due to failure to incorporate early episodes of rapid exhumation (Fig. 2; e.g., Wang et al., 2016b). More importantly, sediment mass in offshore sinks was not unmixed to extract the sole contribution of the Red River (Wissink et al., 2016). Based on the provenance reevaluation of the Yinggehai and Qiongdongnan Basins, we consider that the Cenozoic sediment budget from Hainan Island and central Vietnam should be much higher than commonly appreciated.

To constrain the drainage configuration of the paleo-Red River, we integrated the few published zircon age data from Oligocene–Neogene strata within the Red River Basin (Fig. S10; Clift et al., 2020; van Hoang et al., 2009). The Upper Oligocene samples from the upstream and the middle Miocene sample from the midstream show dominant age peaks at ca. 750 Ma and 250 Ma that are also seen in modern sediments (Fig. 9; Fig. S10D). In contrast, the Upper Miocene samples show a multimodal spectral pattern, and, notably, the abundant late Eocene–early Oligocene (ca. 39–29 Ma) zircons in samples RS0701 and 4V-316 could have been sourced from the headwater area (Fig. 9; Fig. S10C). Unfortunately, the poor coverage

of these samples in both geography and stratigraphy as well as the potential bias of local source supply render a poor comparison with contemporary records from the Yinggehai and Qiongdongnan Basins (Fig. S10A). For detrital feldspar Pb isotopes, the striking difference between the Hanoi and Yinggehai Basins and the large intrastratal variability in the latter cannot be readily explained given the current data set of defined source areas (Fig. 7; Wang et al., 2019a; Zhang et al., 2021c), and further work is required. Despite this limitation, the general stabilization of Nd isotopic compositions and zircon age signatures in the Neogene strata therein (Figs. 11E and 14) suggests the establishment of a near-modern Red River in the early Miocene.

Keynotes of Regional Landscape Change

The fluvial landscapes and drainage networks evolve over geologic time in response to a complex interplay of exogenic and endogenic factors. For large Asian rivers, in addition to the ongoing, internal drainage dynamics (Yang et al., 2015), the drainage basin sensitivity to endogenic forcing could have played a more competitive role, given that their headwaters come from an active convergent plate margin (e.g., Clark et al., 2004; Whipple et al., 2017; Yang et al., 2016). Thus, the fluvial landscape change of the region over the Cenozoic has been influenced by the evolution of the India-Asia collision and Asian monsoon systems (e.g., Brookfield, 1998; Clark et al., 2004; Zhang et al., 2019). A commonly assumed model for East Asia is the regional-scale topographic reversal from a west-tilting topography in the Paleogene to an east-tilting topography in the Neogene (e.g., Chen, 2000; Clift et al., 2006a; Wang, 2004; Zhang et al., 2021a). The idea was inspired by the observation of distinct orogenic evolution along the eastern and western margins of East Asia: In contrast to Cenozoic mountain building and plateau growth in the Himalayan-Tibetan orogen, the continental margin of South China underwent extension and collapse of preexisting high mountains that were once formed by the prolonged subduction of the Panthalassa Ocean (Chen et al., 2022; Suo et al., 2019; Wang et al., 2020c). In this model, the large river systems of East Asia were assumed to initially originate from the South China margin and internally drain inland areas (e.g., paleo-Yangtze River; Wang et al., 2018c) before radiating from the Himalayan-Tibetan region and discharging into the margin of the East and South China Seas.

Our provenance reevaluation of the Yangtze, Pearl, and Red Rivers and their sinks in the East and South China Seas favors an early Miocene initiation of near-modern drainage configurations

(Fig. 15). The interpreted Neogene stabilization of the fluvial landscape appears to fit the topographic reversal model of Wang (2004). However, fluvial landforms have not been present everywhere, and there remains a gap between fluvial and regional-scale landscapes. First, extensive areas of low relief are perched high in mountain ranges of the southeast Tibetan Plateau and dissected by deep gorges. Most of these surfaces have experienced little denudation ($< \sim 0.05$ mm/yr) since the Cenozoic, contrasting with the rapid incision in river courses (Fig. 2; e.g., Clark et al., 2005; Tian et al., 2014; Yuan et al., 2022; Zhang et al., 2015). Second, large rivers do not necessarily require elevation reduction of the coastal orogen of South China to find their outlets into the East and South China Seas. This is seen in the Pearl River Basin, where the main stream (Xi River) does not cut through the coastal mountains (Fig. 1). Third, early periods of terrane collision in the Tibetan Plateau region prior to the Cenozoic would likely have created a complex landscape with deep valleys and high mountains (Spicer et al., 2021; Tapponnier et al., 2001). Also, early Cenozoic exhumation and surface uplift were recorded in, for example, the early–middle Eocene Gonjo Basin (Xiong et al., 2020) and the Oligocene Jianchuan Basin (Cao et al., 2019; Shen et al., 2016; see Fig. 2). These observations argue against a low-elevation topography for the Paleogene Tibetan region and the Neogene South China margin as envisaged by the topographic reversal model (Wang, 2004). Still, the Paleogene landscape evolution of East Asia remains to be elucidated in detail, especially regarding the Oligocene, when large-scale drainage expansion likely occurred in different large river basins (Fig. 15).

The interpreted early Miocene initiation of the studied large rivers does not preclude the possibility of landscape change in the Neogene. In the headwater region, rapid exhumation episodes of middle–late Miocene or younger ages have been extensively reported near river courses (Fig. 2; e.g., Clark et al., 2005; Ouimet et al., 2010; Tian et al., 2015). Their near-synchronicity was proposed to signify uplift-induced river incision and the establishment of large rivers (e.g., Clark et al., 2005; Nie et al., 2018). However, it could be alternatively explained by local perturbations from tectonism and climate. Several Neogene thermochronometric ages, although somewhat biased by sampling strategy, coincide with the faulting activity, the most prominent of which can be found in the Xianshuihe fault along the eastern plateau margin (Fig. 3; Tao et al., 2020). The horizontal movements produced by the motion of faults were capable of reorganizing drainage networks (e.g., Dadu River; Zhang et al., 2015). However, they are interpreted to

have exerted a relatively limited influence on the whole-scale fluvial landscape, such that the provenance signals archived in the margin of the East and South China Seas did not significantly change over the Miocene. Instead, the main river courses in the headwater region were maintained during the process of rapid surface uplift (Yuan et al., 2022; Zheng et al., 2013): The progressive entrenchment of river gorges dissecting isolated low-relief surfaces left the drainage capture of one river by its neighbor hard to achieve. Climatic perturbation of river incision also existed but did not necessarily lead to changes in drainage networks. This control was especially evident in middle Miocene time. During the Middle Miocene Climatic Optimum (ca. 17–14 Ma), the warm climate and enhanced East Asian summer monsoon precipitation provided favorable conditions for generating rapid incision of large rivers (Holbourn et al., 2021; Nie et al., 2018). Correspondingly, the East China Sea Shelf Basin, Pearl River Mouth Basin, and Yinggehai Basin along the margin of the East and South China Seas consistently recorded an overall increase in sedimentation rate from the early to middle Miocene (Fig. S11; Clift, 2006; van Hoang et al., 2010b).

FUTURE PERSPECTIVES

In an ancient sedimentary system, the provenance signatures of sediments have been subject to various natural processes before and after deposition and tend to vary in space and time (Romans et al., 2016). The sampling strategy for specific provenance research normally involves a trade-off between several factors, including the spatio-temporal scale of the source-to-sink system, sample availability, and cost (Caracciolo, 2020; von Eynatten and Dunkl, 2012; Ibañez-Mejía et al., 2018). Thus, one prerequisite for the treatment and interpretation of provenance data is the evaluation of sample representativeness. In the case of larger Asian river systems, it is foreseeable that the number of provenance studies will continue to increase, and the complexity and heterogeneity of provenance signatures from different localities and strata will be further unveiled. For emerging analytical methods (e.g., detrital muscovite and feldspar $^{40}\text{Ar}/^{39}\text{Ar}$ geochronology; van Hoang et al., 2010a; Sun et al., 2021), it takes much work to achieve a desirable sample coverage from source to sink that meets the needs of sample representativeness and multisample comparison. For the currently available large data sets, e.g., detrital zircon U-Pb geochronology (Fig. 1), the issue of sampling bias should also not be ignored, especially in ocean sinks, where relatively low borehole coverage and sampling resolution and the effects

of sediment mixing and homogenization are common (Cao et al., 2021a; Caracciolo, 2020). Otherwise, attempts to compare provenance signatures across different basins would likely yield unreliable results. For example, many published samples from the Yinggehai Basin, which were often used to trace the evolution of the Red River (e.g., Chen et al., 2022; Guo et al., 2021; Wis-sink et al., 2016), were collected near the Hainan Island margin rather than in the depocenter and were strongly biased by sediment supply from small rivers of Hainan Island (Fig. 11D; Fig. S5). Our provenance investigation on the northern Pearl River Mouth Basin also indicated that even selection of samples closer to the river mouth does not necessarily guarantee a direct source-to-sink relationship to the large river, and a careful check of spatial variability is required to disentangle the provenance signal of interest from “noise.” Moreover, as shown in our MDS plots, a large difference in provenance signatures exists within the same sedimentary unit, and it is recommended to identify the potential intersample variability before interpreting the averaged signal of grouped samples (Zimmermann et al., 2015).

Inferring the sediment-routing system of a large paleoriver is one of the most difficult problems in provenance analysis (Allen, 2017; Brewer et al., 2020; Caracciolo, 2020). Comparing the similarity of provenance signatures between source and sink, as is usually done, is only capable of recognizing dominant contributions from a relatively limited number of source terranes, which cannot convey the complex drainage networks in natural systems (Cao et al., 2018). A promising solution is the “top-down” sediment mixture model, which uses the provenance signatures of source end members to model the best-fit combinations to sink mixtures (Sharman and Johnstone, 2017; Sundell and Saylor, 2017). With this approach, it can be determined whether a potential source terrane contributes sediment, and if so, its relative contribution can be estimated. Still, the potential source end members within a large river basin should be defined as detailed as possible to characterize the heterogeneity and complexity of provenance signatures and to provide more in-depth information on sediment-dispersal routes. To meet this requirement, defining source end members based on the discriminative signatures of modern sediments of major tributaries is a feasible alternative to that based on the catchment-scale tectonic plates (e.g., Cao et al., 2018; Sun et al., 2021; Wang et al., 2019a; Zhang et al., 2021c). Although the mixture model does not necessarily require prior information about source contributions, the modeled results may suffer from uncertainties induced by the small

sample size of particular data sets and poor characterization of source areas (Sharman and Johnstone, 2017; Sundell and Saylor, 2017) and remain to be examined for geologic plausibility. Given the current status of provenance data sets from the East and South China Seas and East Asian rivers (Fig. 1), zircon U-Pb geochronology and K-feldspar Pb isotopes play a dominant role over the traditional whole-rock-based proxies. Despite the growing use of the sediment mixture model for zircon age data sets of large Asian rivers (e.g., Cao et al., 2018; Clift et al., 2020; Zhang et al., 2021b), a larger sample coverage is required to further define potential source terranes at an adequate scale, especially within the Yangtze and Red River basins (Figs. 6 and 9). Feldspar is a promising alternative to zircon for tracing the first-cycle sediment source (Barham et al., 2021; Tyrrell et al., 2006). However, the Pb isotopic compositions of modern sediments of the studied large rivers show a high probability of overlap (Figs. 7A and 7B), and their relationship with bedrock geology remains poorly constrained.

To exploit the full potential of sediment provenance analysis in drainage reconstruction, the obtained good results from single-grain analyses deserve to be firmly linked to the whole rock from a mass balance perspective, which plays a central role in the concept of quantitative provenance analysis (Weltje and von Eynatten, 2004). This attempt is not easy to achieve. First, the mineral fertility of parent rocks is critical to calculating the production flux of detrital grains but is often unknown or shows large spatial diversity (Chew et al., 2020; Moecher and Samson, 2006). Nevertheless, for detrital zircon provenance, the volume content of zircon in the bulk rock can be roughly evaluated by the whole-rock zirconium content, assuming that zirconium is exclusively hosted in zircon (Dickinson, 2008). Second, compared to common heavy minerals that are transported as bed load, the dissolved and suspended loads are generally harder to quantify. Third, in ancient source-to-sink systems, the locations of potential sources are mostly unknown, and the effects of inversion tectonics and sedimentary recycling add further uncertainties (Andersen et al., 2022; Barham et al., 2021; Voigt et al., 2008). Despite these issues, the BQART model has the potential to serve as a framework for extrapolating the empirical relationships of sediment budgets built on modern rivers to the ancient source-to-sink systems (Brewer et al., 2020; Nyberg et al., 2021). This model quantifies the scaling relationship between sediment load and a series of factors such as catchment erodibility, drainage area, and maximum relief (Syvitski and Milliman, 2007). Depending on the available data sets

and target questions, some of these parameters can be measured, estimated, or modeled, while the others are kept as variables (Eide et al., 2018; Zhang et al., 2018b).

CONCLUDING REMARKS

Large Asian rivers are the backbone of sediment source-to-sink systems, linking the geologic histories of the high-altitude Tibetan Plateau and the marginal seas of the West Pacific Ocean. The long-standing controversies and uncertainties surrounding their drainage initiation and evolution emphasize the need for an alternative perspective from their sediment sinks in the East and South China Seas. To probe the evolution of three large rivers in China (the Yangtze, Pearl, and Red Rivers), we compiled and reexamined the provenance signatures of Cenozoic basins stretching from the East China Sea margin to the northwestern South China Sea margin, and we reconstructed the sediment source-to-sink relationship between the large rivers and ocean sinks.

Detrital zircon geochronology of modern sediments within individual river basins exhibits large intersample variability that has not been fully appreciated in previous definitions of potential source terranes. In addition, not all samples from the East and South China Seas should be used to trace the evolution of large rivers, and a careful evaluation of sampling bias is required. Those from areas far away from the river mouth and those from synrift strata could be, to a varying degree, influenced by sources from small rivers or basinal highs. Given the current limitations of compiled provenance data sets, detrital zircon geochronology and whole-rock Nd isotopes are shown to perform better than detrital K-feldspar Pb isotopes in distinguishing different source terranes and revealing changing patterns over time.

The integrated provenance results, albeit with persisting intersample variability, suggest a general provenance stabilization in the Neogene strata of the East and South China Seas, as reflected by the inheritance of detrital zircon U-Pb age spectral patterns and the small fluctuation in Nd isotopic values. Therefore, we interpret the establishment of near-modern drainage configurations and fluvial landscapes in the early Miocene of East Asia. Before the Miocene, the paleo-Pearl River was likely distributed as small rivers in the southeast China margin. The early histories of the Yangtze River and Red River remain poorly constrained due to the low sample coverage in Paleogene strata and tectonic perturbations within individual offshore basins. Nevertheless, a reevaluation of provenance signatures in sparse Paleogene strata from the southeast-

ern Tibetan Plateau margin does not support the commonly accepted model of a preexisting larger drainage area for the paleo-Red River.

ACKNOWLEDGMENTS

This work was supported by the National Natural Science Foundation of China (grants 42106073, 42076066, 41976073, and 92055203), Key Special Project for Introduced Talents Team of Southern Marine Science and Engineering Guangdong Laboratory (Guangdong) (grant GML2019ZD0102), Open Fund of the State Key Laboratory of Marine Geology (Tongji University) (grant MGK202107), and the Fundamental Research Funds for the Central Universities, China University of Geosciences (Wuhan) (grant 162301192662). D.J.J. van Hinsbergen acknowledges funding from the Netherlands Organization for Scientific Research, Vici grant 865.17.001. We acknowledge the support from China National Offshore Oil Corporation, which provided critical borehole samples and background information through years of collaborative research. L. Cao thanks Hongrui Zhang for help in generating maps, and also thanks Jie He, Shengli Li, Ce Wang, Wei Wang, Jingyu Zhang, Zengjie Zhang, and many others, who kindly shared their data sets. Constructive and careful reviews by two anonymous referees and editorial handling by Mihai Ducea and Eric Roberts are gratefully appreciated. Joel Saylor and Eduardo Garzanti are also thanked for commenting on a previous version of this paper.

REFERENCES CITED

- Allen, P.A., 2017, *Sediment Routing Systems: The Fate of Sediment from Source to Sink*: Cambridge, UK, University Printing House, 407 p., <https://doi.org/10.1017/9781316135754>.
- Anczkiewicz, R., Thirlwall, M., Alard, O., Rogers, N.W., and Clark, C., 2012, Diffusional homogenization of light REE in garnet from the Day Nui Con Voi Massif in N-Vietnam: Implications for Sm-Nd geochronology and timing of metamorphism in the Red River shear zone: *Chemical Geology*, v. 318–319, p. 16–30, <https://doi.org/10.1016/j.chemgeo.2012.04.024>.
- Andersen, T., van Niekerk, H., and Elburg, M.A., 2022, Detrital zircon in an active sedimentary recycling system: Challenging the ‘source-to-sink’ approach to zircon-based provenance analysis: *Sedimentology*, v. 69, p. 2436–2462, <https://doi.org/10.1111/sed.12996>.
- Ashworth, P.J., and Lewin, J., 2012, How do big rivers come to be different?: *Earth-Science Reviews*, v. 114, p. 84–107, <https://doi.org/10.1016/j.earscirev.2012.05.003>.
- Barbour, G.B., 1936, *Physiographic history of the Yangtze: The Geographical Journal*, v. 87, p. 17–32, <https://doi.org/10.2307/1786198>.
- Barham, M., Kirkland, C.L., Hovikoski, J., Alsen, P., Hollis, J., Tyrrell, S., and Tosca, N., 2021, Reduce or recycle? Revealing source to sink links through integrated zircon-feldspar provenance fingerprinting: *Sedimentology*, v. 68, p. 531–556, <https://doi.org/10.1111/sed.12790>.
- Bhattacharya, J.P., Copeland, P., Lawton, T.F., and Holbrook, J., 2016, Estimation of source area, river paleo-discharge, paleoslope, and sediment budgets of linked deep-time depositional systems and implications for hydrocarbon potential: *Earth-Science Reviews*, v. 153, p. 77–110, <https://doi.org/10.1016/j.earscirev.2015.10.013>.
- Bodet, F., and Schärer, U., 2001, Pb isotope systematics and time-integrated Th/U of SE-Asian continental crust recorded by single K-feldspar grains in large rivers: *Chemical Geology*, v. 177, p. 265–285, [https://doi.org/10.1016/S0009-2541\(00\)00413-7](https://doi.org/10.1016/S0009-2541(00)00413-7).
- Botsyun, S., Sepulchre, P., Donnadieu, Y., Risi, C., Licht, A., and Caves Rugenstein, J.K., 2019, Revised paleo-altimetry data show low Tibetan Plateau elevation during

- the Eocene: Science, v. 363, <https://doi.org/10.1126/science.aqj1436>.
- Brewer, C.J., Hampson, G.J., Whittaker, A.C., Roberts, G.G., and Watkins, S.E., 2020, Comparison of methods to estimate sediment flux in ancient sediment routing systems: Earth-Science Reviews, v. 207, <https://doi.org/10.1016/j.earscirev.2020.103217>.
- Briais, A., Patriat, P., and Tapponnier, P., 1993, Updated interpretation of magnetic anomalies and seafloor spreading stages in the South China Sea: Implications for the Tertiary tectonics of Southeast Asia: Journal of Geophysical Research, v. 98, p. 6299–6328, <https://doi.org/10.1029/92JB02280>.
- Brookfield, M.E., 1998, The evolution of the great river systems of southern Asia during the Cenozoic India-Asia collision: Rivers draining southwards: Geomorphology, v. 22, p. 285–312, [https://doi.org/10.1016/S0169-555X\(97\)00082-2](https://doi.org/10.1016/S0169-555X(97)00082-2).
- Cao, K., Wang, G.C., Leloup, P.H., Mahéo, G., Xu, Y.D., van der Beek, P.A., Replumaz, A., and Zhang, K.X., 2019, Oligocene–early Miocene topographic relief generation of southeastern Tibet triggered by thrusting: Tectonics, v. 38, p. 374–391, <https://doi.org/10.1029/2017TC004832>.
- Cao, K., Leloup, P.H., Wang, G., Liu, W., Mahéo, G., Shen, T., Xu, Y., Sorrel, P., and Zhang, K., 2021, Thrusting, exhumation, and basin fill on the western margin of the South China block during the India-Asia collision: Geological Society of America Bulletin, v. 133, p. 74–90, <https://doi.org/10.1130/B35349.1>.
- Cao, L., Jiang, T., Wang, Z., Zhang, Y., and Sun, H., 2015, Provenance of Upper Miocene sediments in the Yinggehai and Qiongdongnan Basins, northwestern South China Sea: Evidence from REE, heavy minerals and zircon U-Pb ages: Marine Geology, v. 361, p. 136–146, <https://doi.org/10.1016/j.margeo.2015.01.007>.
- Cao, L., Shao, L., Qiao, P., Chen, S., and Wu, M., 2017, Geochemical evolution of Oligocene–middle Miocene sediments in the deep-water area of the Pearl River Mouth Basin, northern South China Sea: Marine and Petroleum Geology, v. 80, p. 358–368, <https://doi.org/10.1016/j.marpetgeo.2016.12.010>.
- Cao, L., Shao, L., Qiao, P., Zhao, Z., and van Hinsbergen, D.J.J., 2018, Early Miocene birth of modern Pearl River recorded low-relief, high-elevation surface formation of SE Tibetan Plateau: Earth and Planetary Science Letters, v. 496, p. 120–131, <https://doi.org/10.1016/j.epsl.2018.05.039>.
- Cao, L., Jiang, T., and He, J., 2021a, Fingerprinting sand from Asian rivers to the deep central South China Sea since the late Miocene: Geological Society of America Bulletin, v. 133, p. 1964–1978, <https://doi.org/10.1130/B35845.1>.
- Cao, L., Shao, L., Qiao, P., Cui, Y., Zhang, G., and Zhang, X., 2021b, Formation and paleogeographic evolution of the Palawan continental terrane along the southeast Asian margin revealed by detrital fingerprints: Geological Society of America Bulletin, v. 133, p. 1167–1193, <https://doi.org/10.1130/B35707.1>.
- Caracciolo, L., 2020, Sediment generation and sediment routing systems from a quantitative provenance analysis perspective: Review, application and future development: Earth-Science Reviews, v. 209, <https://doi.org/10.1016/j.earscirev.2020.103226>.
- Chen, P., 2000, Paleoenvironmental changes during the Cretaceous in eastern China, in Okada, H., and Mater, N.J., eds., Cretaceous Environments of Asia: Amsterdam, Netherlands, Elsevier, Developments in Palaeontology and Stratigraphy 17, p. 81–90, [https://doi.org/10.1016/S0920-5446\(00\)80025-4](https://doi.org/10.1016/S0920-5446(00)80025-4).
- Chen, W.H., et al., 2021, Stratigraphy and provenance of the Paleogene syn-rift sediments in central-southern Palawan: Paleogeographic significance for the South China margin: Tectonics, v. 40, <https://doi.org/10.1029/2021TC006753>.
- Chen, W.S., 2016, An Introduction to the Geology of Taiwan: Taipei City, Taiwan, Geological Society of Taiwan, 204 p.
- Chen, W.-S., Chung, S.-L., Chou, H.-Y., Zui, Z., Shao, W.-Y., and Lee, Y.-H., 2017a, A reinterpretation of the metamorphic Yuli belt: Evidence for a middle-late Miocene accretionary prism in eastern Taiwan: Tectonics, v. 36, p. 188–206, <https://doi.org/10.1002/2016TC004383>.
- Chen, Y., et al., 2017b, Detrital zircon U-Pb geochronological and sedimentological study of the Simao Basin, Yunnan: Implications for the early Cenozoic evolution of the Red River: Earth and Planetary Science Letters, v. 476, p. 22–33, <https://doi.org/10.1016/j.epsl.2017.07.025>.
- Chen, Y., Meng, J., Liu, H., Wang, C., Tang, M., Liu, T., and Zhao, Y., 2022, Detrital zircons record the evolution of the Cathaysian Coastal Mountains along the South China margin: Basin Research, v. 34, no. 2, p. 688–701, <https://doi.org/10.1111/bre.12636>.
- Chew, D., O'Sullivan, G., Caracciolo, L., Mark, C., and Tyrrell, S., 2020, Sourcing the sand: Accessory mineral fertility, analytical and other biases in detrital U-Pb provenance analysis: Earth-Science Reviews, v. 202, <https://doi.org/10.1016/j.earscirev.2020.103093>.
- Chung, L.-H., Lee, Y.-H., Tsai, W.-L., Shea, K.-S., Teng, L.S., Lo, W., and Tan, X.-B., 2018, Refining stratigraphic ages of Northern Hsuehshan Range in northern Taiwan by detrital zircon U-Pb dating: Terrestrial, Atmospheric, and Oceanic Sciences (Journal), v. 29, p. 291–300, <https://doi.org/10.3319/TAO.2017.10.19.01>.
- Clark, M.K., and Royden, L.H., 2000, Topographic ooze: Building the eastern margin of Tibet by lower crustal flow: Geology, v. 28, p. 703–706, [https://doi.org/10.1130/0091-7613\(2000\)28<703:TOBTEM>2.0.CO;2](https://doi.org/10.1130/0091-7613(2000)28<703:TOBTEM>2.0.CO;2).
- Clark, M.K., Schoenbohm, L.M., Royden, L.H., Whipple, K.X., Burchfiel, B.C., Zhang, X., Tang, W., Wang, E., and Chen, L., 2004, Surface uplift, tectonics, and erosion of eastern Tibet from large-scale drainage patterns: Tectonics, v. 23, TC1006, <https://doi.org/10.1029/2002TC001402>.
- Clark, M.K., House, M., Royden, L., Whipple, K., Burchfiel, B., Zhang, X., and Tang, W., 2005, Late Cenozoic uplift of southeastern Tibet: Geology, v. 33, p. 525–528, <https://doi.org/10.1130/G21265.1>.
- Clift, P., Lee, J.I., Clark, M.K., and Blusztajn, J., 2002, Erosional response of South China to arc rifting and monsoonal strengthening: A record from the South China Sea: Marine Geology, v. 184, p. 207–226, [https://doi.org/10.1016/S0025-3227\(01\)00301-2](https://doi.org/10.1016/S0025-3227(01)00301-2).
- Clift, P.D., 2006, Controls on the erosion of Cenozoic Asia and the flux of clastic sediment to the ocean: Earth and Planetary Science Letters, v. 241, p. 571–580, <https://doi.org/10.1016/j.epsl.2005.11.028>.
- Clift, P.D., Blusztajn, J., and Nguyen, A.D., 2006a, Large-scale drainage capture and surface uplift in eastern Tibet–SW China before 24 Ma inferred from sediments of the Hanoi Basin, Vietnam: Geophysical Research Letters, v. 33, L19403, <https://doi.org/10.1029/2006GL027772>.
- Clift, P.D., Carter, A., Campbell, I.H., Pringle, M.S., Van Lap, N., Allen, C.M., Hodges, K.V., and Tan, M.T., 2006b, Thermochronology of mineral grains in the Red and Mekong Rivers, Vietnam: Provenance and exhumation implications for Southeast Asia: Geochemistry, Geophysics, Geosystems, v. 7, Q10005, <https://doi.org/10.1029/2006GC001336>.
- Clift, P.D., van Hoang, L., Hinton, R., Ellam, R.M., Hannigan, R., Tan, M.T., Blusztajn, J., and Duc, N.A., 2008, Evolving East Asian river systems reconstructed by trace element and Pb and Nd isotope variations in modern and ancient Red River–Song Hong sediments: Geochemistry, Geophysics, Geosystems, v. 9, Q04039, <https://doi.org/10.1029/2007GC001867>.
- Clift, P.D., Carter, A., Wysocka, A., Hoang, L.V., Zheng, H.B., and Neubeck, N., 2020, A late Eocene–Oligocene through-flowing river between the upper Yangtze and South China Sea: Geochemistry, Geophysics, Geosystems, v. 21, <https://doi.org/10.1029/2020GC009046>.
- Cohen, K.M., Finney, S.C., Gibbard, P.L., and Fan, J.-X., 2013, The ICS International Chronostratigraphic Chart: Episodes, v. 36, p. 199–204, <https://doi.org/10.18814/epiiugs/2013/v36i3/002>.
- Condie, K.C., Arndt, N., Davaille, A., and Puetz, S.J., 2017, Zircon age peaks: Production or preservation of continental crust?: Geosphere, v. 13, p. 227–234, <https://doi.org/10.1130/GES01361.1>.
- Craddock, W.H., Kirby, E., Harkins, N.W., Zhang, H., Shi, X., and Liu, J., 2010, Rapid fluvial incision along the Yellow River during headward basin integration: Nature Geoscience, v. 3, p. 209–213, <https://doi.org/10.1038/ngeo777>.
- Cui, Y., Shao, L., Li, Z.-X., Zhu, W., Qiao, P., and Zhang, X., 2021, A Mesozoic Andean-type active continental margin along coastal South China: New geological records from the basement of the northern South China Sea: Gondwana Research, v. 99, p. 36–52, <https://doi.org/10.1016/j.gr.2021.06.021>.
- Deng, B., Chew, D., Jiang, L., Mark, C., Cogné, N., Wang, Z., and Liu, S., 2018, Heavy mineral analysis and detrital U-Pb ages of the intracontinental paleo-Yangtze basin: Implications for a transcontinental source-to-sink system during Late Cretaceous time: Geological Society of America Bulletin, v. 130, p. 2087–2109, <https://doi.org/10.1130/B32037.1>.
- Deng, J., Wang, Q., Li, G., and Santosh, M., 2014, Cenozoic tectono-magmatic and metallogenic processes in the Sanjiang region, southwestern China: Earth-Science Reviews, v. 138, p. 268–299, <https://doi.org/10.1016/j.earscirev.2014.05.015>.
- Deng, K., Yang, S., Li, C., Su, N., Bi, L., Chang, Y.-P., and Chang, S.-C., 2017, Detrital zircon geochronology of river sands from Taiwan: Implications for sedimentary provenance of Taiwan and its source link with the east China mainland: Earth-Science Reviews, v. 164, p. 31–47, <https://doi.org/10.1016/j.earscirev.2016.10.015>.
- Dickinson, W.R., 2008, Impact of differential zircon fertility of granitoid basement rocks in North America on age populations of detrital zircons and implications for granite petrogenesis: Earth and Planetary Science Letters, v. 275, p. 80–92, <https://doi.org/10.1016/j.epsl.2008.08.003>.
- Ding, Y., and Chan, J.C.L., 2005, The East Asian summer monsoon: An overview: Meteorology and Atmospheric Physics, v. 89, p. 117–142, <https://doi.org/10.1007/s00703-005-0125-z>.
- Eide, C.H., Muller, R., and Helland-Hansen, W., 2018, Using climate to relate water discharge and area in modern and ancient catchments: Sedimentology, v. 65, p. 1378–1389, <https://doi.org/10.1111/sed.12426>.
- England, P., and Molnar, P., 1990, Surface uplift, uplift of rocks, and exhumation of rocks: Geology, v. 18, p. 1173–1177, [https://doi.org/10.1130/0091-7613\(1990\)018<1173:SUUORA>2.3.CO;2](https://doi.org/10.1130/0091-7613(1990)018<1173:SUUORA>2.3.CO;2).
- Fan, D., and Li, C., 2008, Timing of the Yangtze initiation draining the Tibetan Plateau throughout to the East China Sea: A review: Frontiers of Earth Science in China, v. 2, p. 302–313, <https://doi.org/10.1007/s11707-008-0018-9>.
- Fedo, C.M., Sircombe, K.N., and Rainbird, R.H., 2003, Detrital zircon analysis of the sedimentary record: Reviews in Mineralogy and Geochemistry, v. 53, p. 277–303, <https://doi.org/10.2113/0530277>.
- Feng, J., Yao, H., Chen, L., and Wang, W., 2022, Massive lithospheric delamination in southeastern Tibet facilitating continental extrusion: National Science Review, v. 9, no. 4, <https://doi.org/10.1093/nsr/nwab174>.
- Feng, Y., Song, C., He, P., Meng, Q., Wang, Q., Wang, X., and Chen, W., 2021, Detrital zircon U-Pb geochronology of the Jianchuan Basin, southeastern Tibetan Plateau, and its implications for tectonic and paleodrainage evolution: Terra Nova, v. 33, p. 560–572, <https://doi.org/10.1111/ter.12548>.
- Fu, C., Li, S., Li, S., and Xu, J., 2021a, Spatial and temporal variability of sediment infilling and episodic rifting in the North Pearl River Mouth Basin, South China Sea: Journal of Asian Earth Sciences, v. 211, <https://doi.org/10.1016/j.jseas.2021.104702>.
- Fu, X., Zhu, W., Geng, J., Yang, S., Zhong, K., Huang, X., Zhang, L., and Xu, X., 2021b, The present-day Yangtze River was established in the late Miocene: Evidence from detrital zircon ages: Journal of Asian Earth Sciences, v. 205, <https://doi.org/10.1016/j.jseas.2020.104600>.
- Fyhn, M.B.W., et al., 2019, Detrital zircon ages and heavy mineral composition along the Gulf of Tonkin—Implication for sand provenance in the Yinggehai–Song Hong and Qiongdongnan Basins: Marine and Petroleum Geology, v. 101, p. 162–179, <https://doi.org/10.1016/j.marpetgeo.2018.11.051>.
- Garçon, M., Chauvel, C., France-Lanord, C., Limonta, M., and Garzanti, E., 2014, Which minerals control the Nd-Hf-Sr-Pb isotopic compositions of river sediments?: Chemical Geology, v. 364, p. 42–55, <https://doi.org/10.1016/j.chemgeo.2013.11.018>.

- Garzanti, E., Barbarano, M., Andò, S., Lenzi, M., Deng, K., and Yang, S., 2021, Provenance of Neogene sandstones in western Taiwan traced with garnet geochemistry and zircon geochronology: *Basin Research*, v. 33, p. 2069–2088, <https://doi.org/10.1111/bre.12548>.
- Gawthorpe, R.L., and Leeder, M.R., 2000, Tectono-sedimentary evolution of active extensional basins: *Basin Research*, v. 12, p. 195–218, <https://doi.org/10.1111/j.1365-2117.2000.00121.x>.
- Gehrels, G.R., 2014, Detrital zircon U-Pb geochronology applied to tectonics: *Annual Review of Earth and Planetary Sciences*, v. 42, p. 127–149, <https://doi.org/10.1146/annurev-earth-050212-124012>.
- Geological Survey of Canada, 1995, General Geologic Map of the World (scale 1:35,000,000): <https://mrdata.usgs.gov/geology/world/> (accessed November 2021).
- Gibling, M.R., 2017, River history and longevity through geological time: An update, in Hubbard, S.M., Durkin, P.R., Leckie, D.A., and Simpson, C.J., eds., 11th International Conference on Fluvial Sedimentology: Calgary, Canada, University of Calgary, p. 61.
- Gourbet, L., et al., 2017, Reappraisal of the Jianchuan Cenozoic basin stratigraphy and its implications on the SE Tibetan Plateau evolution: *Tectonophysics*, v. 700–701, p. 162–179, <https://doi.org/10.1016/j.tecto.2017.02.007>.
- Guo, R., et al., 2021, Cenozoic evolution of the Yangtze River: Constraints from detrital zircon U-Pb ages: *Palaeogeography, Palaeoclimatology, Palaeoecology*, v. 579, <https://doi.org/10.1016/j.palaeo.2021.110586>.
- Gupta, A., Slaymaker, O., and Junk, W.J., 2020, Geological history of large river systems, in Gupta, A., Slaymaker, O., and Junk, W.J., eds., *Introducing Large Rivers*: New York, John Wiley & Sons, p. 119–145, <https://doi.org/10.1002/9781118451410.ch7>.
- Hallet, B., and Molnar, P., 2001, Distorted drainage basins as markers of crustal strain east of the Himalaya: *Journal of Geophysical Research*, v. 106, p. 13,697–13,709, <https://doi.org/10.1029/2000JB900335>.
- Hamilton, P.J., O’Nions, R.K., Bridgwater, D., and Nutman, A., 1983, Sm-Nd studies of Archaean metasediments and metavolcanics from West Greenland and their implications for the Earth’s early history: *Earth and Planetary Science Letters*, v. 62, p. 263–272, [https://doi.org/10.1016/0012-821X\(83\)90089-4](https://doi.org/10.1016/0012-821X(83)90089-4).
- Han, Y., Wang, L., Yang, D., Zeng, Q., Bai, H., Guo, S., and Yang, X., 2017, Southern provenance supply of Zhuhai Formation and its significance on oil and gas accumulation in Baiyun Sag, Pearl River Mouth Basin: *Natural Gas Geoscience*, v. 28, p. 1537–1545, <https://doi.org/10.11764/j.issn.1672-1926.2017.07.011> [in Chinese with English abstract].
- Haughton, P.D.W., Todd, S.P., and Morton, A.C., 1991, Sedimentary provenance studies, in Morton, A.C., Todd, S.P., and Haughton, P.D.W., eds., *Developments in Sedimentary Provenance Studies*: Geological Society, London, Special Publication 57, p. 1–11, <https://doi.org/10.1144/GSL.SP.1991.057.01.01>.
- He, J., Garzanti, E., Cao, L., and Wang, H., 2020a, The zircon story of the Pearl River (China) from Cretaceous to present: *Earth-Science Reviews*, v. 201, <https://doi.org/10.1016/j.earscirev.2019.103078>.
- He, M., Zheng, H., and Clift, P.D., 2013, Zircon U-Pb geochronology and Hf isotope data from the Yangtze River sands: Implications for major magmatic events and crustal evolution in central China: *Chemical Geology*, v. 360–361, p. 186–203, <https://doi.org/10.1016/j.chemgeo.2013.10.020>.
- He, M., Zheng, H., Bookhagen, B., and Clift, P.D., 2014, Controls on erosion intensity in the Yangtze River basin tracked by U-Pb detrital zircon dating: *Earth-Science Reviews*, v. 136, p. 121–140, <https://doi.org/10.1016/j.earscirev.2014.05.014>.
- He, M., Zheng, H., Clift, P.D., Bian, Z., Yang, Q., Zhang, B., and Xia, L., 2021, Paleogene sedimentary records of the paleo-Jinshajiang (upper Yangtze) in the Jianchuan Basin, Yunnan, SW China: *Geochemistry, Geophysics, Geosystems*, v. 22, <https://doi.org/10.1029/2020GC009500>.
- He, X., Tan, S., Zhou, J., Liu, Z., Zhao, Z., Yang, S., and Zhang, Y., 2020b, Identifying the leucogranites in the Ailaoshan–Red River shear zone: Constraints on the timing of the southeastward expansion of the Tibetan Plateau: *Geoscience Frontiers*, v. 11, p. 765–781, <https://doi.org/10.1016/j.gsf.2019.07.008>.
- Hennig, J., Breiffeld, H.T., Gough, A., Hall, R., Long, T.V., Kim, V.M., and Quang, S.D., 2018, U-Pb zircon ages and provenance of Upper Cenozoic sediments from the Da Lat zone, SE Vietnam: Implications for an intra-Miocene unconformity and paleo-drainage of the proto-Mekong River: *Journal of Sedimentary Research*, v. 88, p. 495–515, <https://doi.org/10.2110/jsr.2018.26>.
- Hoang, L.V., Wu, F., Clift, P.D., Wysocka, A., and Swierczewska, A., 2009, Evaluating the evolution of the Red River system based on in situ U-Pb dating and Hf isotope analysis of zircons: *Geochemistry, Geophysics, Geosystems*, v. 10, Q11008, <https://doi.org/10.1029/2009GC002819>.
- Hoang, L.V., Clift, P.D., Mark, D., Zheng, H., and Tan, M.T., 2010a, Ar–Ar muscovite dating as a constraint on sediment provenance and erosion processes in the Red and Yangtze River systems, SE Asia: *Earth and Planetary Science Letters*, v. 295, p. 379–389, <https://doi.org/10.1016/j.epsl.2010.04.012>.
- Hoang, L.V., Clift, P.D., Schwab, A.M., Huuse, M., Nguyen, D.A., and Sun, Z., 2010b, Large-scale erosional response of SE Asia to monsoon evolution reconstructed from sedimentary records of the Song Hong–Yinggehai and Qiongdongnan Basins, South China Sea, in Clift, P.D., Tada, R., and Zheng, H., eds., *Monsoon Evolution and Tectonics–Climate Linkage in Asia*: Geological Society, London, Special Publication 342, p. 219–244, <https://doi.org/10.1144/SP342.13>.
- Hoke, G.D., Liu-Zeng, J., Hren, M.T., Wissink, G.K., and Garzanti, E., 2014, Stable isotopes reveal high southeast Tibetan Plateau margin since the Paleogene: *Earth and Planetary Science Letters*, v. 394, p. 270–278, <https://doi.org/10.1016/j.epsl.2014.03.007>.
- Holbourn, A., Kuhnt, W., Clemens, S.C., and Heslop, D., 2021, A ~12 myr Miocene record of East Asian monsoon variability from the South China Sea: *Paleoceanography and Paleoclimatology*, v. 36, <https://doi.org/10.1029/2021PA004267>.
- Hou, Y., Zhu, W., Qiao, P., Huang, C.-Y., Cui, Y., and Meng, X., 2021, Sediment source and environment evolution in Taiwan Island during the Eocene–Miocene: *Acta Oceanologica Sinica*, v. 40, p. 114–122, <https://doi.org/10.1007/s13131-021-1756-8>.
- Hou, Y., Shao, L., Cui, Y., Allen, M.B., Zhu, W., Qiao, P., Huang, C.-Y., Yao, Y., and Goh, T.-L., 2022, Sediment features and provenance analysis of the late Mesozoic–early Cenozoic strata of the Ryukyu Islands: Implications for paleogeography of East China Sea: *Marine and Petroleum Geology*, v. 145, <https://doi.org/10.1016/j.marpetgeo.2022.105840>.
- Huang, C.-Y., Yen, Y., Zhao, Q., and Lin, C.-T., 2012, Cenozoic stratigraphy of Taiwan: Window into rifting, stratigraphy and paleoceanography of South China Sea: *Chinese Science Bulletin*, v. 57, p. 3130–3149, <https://doi.org/10.1007/s11434-012-5349-y>.
- Huang, C.-Y., Shao, L., Wang, M.-H., Xue, W.-G., Qiao, P.-J., Cui, Y.-C., and Hou, Y.-L., 2018, Benthic foraminiferal fauna and sediment provenance of Eocene syn-rift sequences in Taiwan: Implication for onset of Asian epi-continental marginal seas off China coast: *Marine Geophysical Researches*, v. 40, p. 111–127, <https://doi.org/10.1007/s11001-018-9366-3>.
- Huang, X., Song, J., Yue, W., Wang, Z., Mei, X., Li, Y., Li, F., Lian, E., and Yang, S., 2020, Detrital zircon U-Pb ages in the East China Seas: Implications for provenance analysis and sediment budgeting: *Minerals (Basel)*, v. 10, 398, <https://doi.org/10.3390/min10050398>.
- Ibañez-Mejía, M., Pullen, A., Pepper, M., Urbani, F., Ghoshal, G., and Ibañez-Mejía, J.C., 2018, Use and abuse of detrital zircon U-Pb geochronology—A case from the Río Orinoco delta, eastern Venezuela: *Geology*, v. 46, p. 1019–1022, <https://doi.org/10.1130/G45596.1>.
- Jia, J., Zheng, H., Huang, X., Wu, F., Yang, S., Wang, K., and He, M., 2010, Detrital zircon U-Pb ages of late Cenozoic sediments from the Yangtze delta: Implication for the evolution of the Yangtze River: *Chinese Science Bulletin*, v. 55, p. 1520–1528, <https://doi.org/10.1007/s11434-010-3091-x>.
- Jiang, T., Cao, L., Xie, X., Wang, Z., Li, X., Zhang, Y., Zhang, D., and Sun, H., 2015, Insights from heavy minerals and zircon U-Pb ages into the middle Miocene–Pliocene provenance evolution of the Yinggehai Basin, northwestern South China Sea: *Sedimentary Geology*, v. 327, p. 32–42, <https://doi.org/10.1016/j.sedgeo.2015.07.011>.
- Jiao, R., Yang, R., and Yuan, X., 2021, Incision history of the Three Gorges, Yangtze River, constrained from inversion of river profiles and low-temperature thermochronological data: *Journal of Geophysical Research–Earth Surface*, v. 126, <https://doi.org/10.1029/2020JF005767>.
- Kong, P., Granger, D., Wu, F., Caffee, M., Wang, Y., Zhao, X., and Zheng, Y., 2009, Cosmogenic nuclide burial ages and provenance of the Xigeda paleo-lake: Implications for evolution of the middle Yangtze River: *Earth and Planetary Science Letters*, v. 278, p. 131–141, <https://doi.org/10.1016/j.epsl.2008.12.003>.
- Kong, P., Zheng, Y., and Fu, B., 2011, Cosmogenic nuclide burial ages and provenance of late Cenozoic deposits in the Sichuan Basin: Implications for early Quaternary glaciations in east Tibet: *Quaternary Geochronology*, v. 6, p. 304–312, <https://doi.org/10.1016/j.quageo.2011.03.006>.
- Lan, C.-Y., Chung, S.-L., Shen, J.J.-S., Lo, C.-H., Wang, P.-L., Hoa, T.T., Thanh, H.H., and Mertzman, S.A., 2000, Geochemical and Sr-Nd isotopic characteristics of granitic rocks from northern Vietnam: *Journal of Asian Earth Sciences*, v. 18, p. 267–280, [https://doi.org/10.1016/S1367-9120\(99\)00063-2](https://doi.org/10.1016/S1367-9120(99)00063-2).
- Lan, Q., Yan, Y., Huang, C.-Y., Clift, P.D., Li, X., Chen, W., Zhang, X., and Yu, M., 2014, Tectonics, topography, and river system transition in east Tibet: Insights from the sedimentary record in Taiwan: *Geochemistry, Geophysics, Geosystems*, v. 15, p. 3658–3674, <https://doi.org/10.1002/2014GC005310>.
- Lan, Q., Yan, Y., Huang, C.-Y., Santosh, M., Shan, Y.-H., Chen, W., Yu, M., and Qian, K., 2016, Topographic architecture and drainage reorganization in southeast China: Zircon U-Pb chronology and Hf isotope evidence from Taiwan: *Gondwana Research*, v. 36, p. 376–389, <https://doi.org/10.1016/j.gr.2015.07.008>.
- Lang, K.A., and Huntington, K.W., 2014, Antecedence of the Yarlung-Siang-Brahmaputra River, eastern Himalaya: *Earth and Planetary Science Letters*, v. 397, p. 145–158, <https://doi.org/10.1016/j.epsl.2014.04.026>.
- Larsen, H.C., et al., 2018, Rapid transition from continental breakup to igneous oceanic crust in the South China Sea: *Nature Geoscience*, v. 11, p. 782–789, <https://doi.org/10.1038/s41561-018-0198-1>.
- Lei, C., Clift, P.D., Ren, J., Ogg, J., and Tong, C., 2019, A rapid shift in the sediment routing system of Lower–Upper Oligocene strata in the Qiongdongnan Basin (Xisha Trough), northwest South China Sea: *Marine and Petroleum Geology*, v. 104, p. 249–258, <https://doi.org/10.1016/j.marpetgeo.2019.03.012>.
- Leloup, P.H., Arnaud, N., Lacassin, R., Kienast, J.R., Harrison, T.M., Trong, T.T., Replumaz, A., and Tapponnier, P., 2001, New constraints on the structure, thermochronology, and timing of the Ailao Shan–Red River shear zone, SE Asia: *Journal of Geophysical Research–Solid Earth*, v. 106, p. 6683–6732, <https://doi.org/10.1029/2000JB900322>.
- Li, C.F., et al., 2015a, Expedition 349 summary, in Li, C.-F., Lin, J., Kulhanek, D.K., and the Expedition 349 Scientists, eds., *Proceedings of the International Ocean Discovery Program, Volume 349: South China Sea Tectonics*: College Station, Texas, International Ocean Discovery Program, p. 1–43, <https://doi.org/10.14379/iodp.proc.349.101.2015>.
- Li, D., Dong, B., Jiang, X., and Xing, J., 2016a, Geochemical evidence for provenance and tectonic background from the Paleogene sedimentary rocks of the East China Sea Shelf Basin: *Geological Journal*, v. 51, p. 209–228, <https://doi.org/10.1002/gj.2825>.
- Li, Q., Wu, G., Zhang, L., Shu, Y., and Shao, L., 2016b, Paleogene marine deposition records of rifting and breakup of the South China Sea: An overview: *Science China–Earth Sciences*, v. 60, p. 2128–2140, <https://doi.org/10.1007/s11430-016-0163-x>.
- Li, S., Currie, B.S., Rowley, D.B., and Ingalls, M., 2015b, Cenozoic paleolatimetry of the SE margin of the

- Tibetan Plateau: Constraints on the tectonic evolution of the region: *Earth and Planetary Science Letters*, v. 432, p. 415–424, <https://doi.org/10.1016/j.epsl.2015.09.044>.
- Li, S., Advokaat, E.L., van Hinsbergen, D.J.J., Koymans, M., Deng, C., and Zhu, R., 2017, Paleomagnetic constraints on the Mesozoic–Cenozoic paleolatitudinal and rotational history of Indochina and South China: Review and updated kinematic reconstruction: *Earth-Science Reviews*, v. 171, p. 58–77, <https://doi.org/10.1016/j.earscirev.2017.05.007>.
- Li, S., et al., 2020, Oligocene deformation of the Chuandian terrane in the SE margin of the Tibetan Plateau related to the extrusion of Indochina: *Tectonics*, v. 39, <https://doi.org/10.1029/2019TC005974>.
- Li, X.H., Wei, G.J., Shao, L., Liu, Y., Liang, X.R., Han, Z.M., Sun, M., and Wang, P.X., 2003, Geochemical and Nd isotopic variations in sediments of the South China Sea: A response to Cenozoic tectonism in SE Asia: *Earth and Planetary Science Letters*, v. 211, p. 207–220, [https://doi.org/10.1016/S0012-821X\(03\)00229-2](https://doi.org/10.1016/S0012-821X(03)00229-2).
- Li, Z.-X., and Li, X.-H., 2007, Formation of the 1300-km-wide intracontinental orogen and postorogenic magmatic province in Mesozoic South China: A flat-slab subduction model: *Geology*, v. 35, p. 179–182, <https://doi.org/10.1130/G23193A.1>.
- Linnemann, U., et al., 2018, New U-Pb dates show a Paleogene origin for the modern Asian biodiversity hot spots: *Geology*, v. 46, p. 3–6, <https://doi.org/10.1130/G39693.1>.
- Liu, C., Cliff, P.D., Carter, A., Böning, P., Hu, Z., Sun, Z., and Pahnke, K., 2017, Controls on modern erosion and the development of the Pearl River drainage in the late Paleogene: *Marine Geology*, v. 394, p. 52–68, <https://doi.org/10.1016/j.margeo.2017.07.011>.
- Liu, X., Xu, Q., and Ding, L., 2016, Differential surface uplift: Cenozoic paleoelevation history of the Tibetan Plateau: *Science China—Earth Sciences*, v. 59, p. 2105–2120, <https://doi.org/10.1007/s11430-015-5486-y>.
- Liu-Zeng, J., et al., 2018, Multiple episodes of fast exhumation since Cretaceous in southeast Tibet, revealed by low-temperature thermochronology: *Earth and Planetary Science Letters*, v. 490, p. 62–76, <https://doi.org/10.1016/j.epsl.2018.03.011>.
- McCulloch, M.T., and Wasserburg, G.J., 1978, Sm-Nd and Rb-Sr chronology of continental crust formation: *Science*, v. 200, p. 1003–1011, <https://doi.org/10.1126/science.200.4345.1003>.
- McLennan, S.M., Hemming, S., McDaniel, D.K., and Hanson, G.N., 1993, Geochemical approaches to sedimentation, provenance, and tectonics, in Johnsson, M.J., and Basu, A., eds., *Processes Controlling the Composition of Clastic Sediments*: Geological Society of America Special Paper 284, p. 21–40, <https://doi.org/10.1130/SPE284-p21>.
- Métivier, F., Gaudemer, Y., Tapponnier, P., and Klein, M., 1999, Mass accumulation rates in Asia during the Cenozoic: *Geophysical Journal International*, v. 137, p. 280–318, <https://doi.org/10.1046/j.1365-246X.1999.00802.x>.
- Miall, A.D., 2006, How do we identify big rivers? And how big is big?: *Sedimentary Geology*, v. 186, p. 39–50, <https://doi.org/10.1016/j.sedgeo.2005.10.001>.
- Milliman, J.D., and Farnsworth, K.L., 2011, *River Discharge to the Coastal Ocean: A Global Synthesis*: New York, Cambridge University Press, 384 p., <https://doi.org/10.1017/CBO9780511781247>.
- Moecher, D.P., and Samson, S.D., 2006, Differential zircon fertility of source terranes and natural bias in the detrital zircon record: Implications for sedimentary provenance analysis: *Earth and Planetary Science Letters*, v. 247, p. 252–266, <https://doi.org/10.1016/j.epsl.2006.04.035>.
- Morley, C.K., 2016, Major unconformities/termination of extension events and associated surfaces in the South China Seas: Review and implications for tectonic development: *Journal of Asian Earth Sciences*, v. 120, p. 62–86, <https://doi.org/10.1016/j.jseaes.2016.01.013>.
- Nemchin, A.A., and Cawood, P.A., 2005, Discordance of the U-Pb system in detrital zircons: Implication for provenance studies of sedimentary rocks: *Sedimentary Geology*, v. 182, p. 143–162, <https://doi.org/10.1016/j.sedgeo.2005.07.011>.
- Nie, J., et al., 2018, Rapid incision of the Mekong River in the middle Miocene linked to monsoonal precipitation: *Nature Geoscience*, v. 11, p. 944–948, <https://doi.org/10.1038/s41561-018-0244-z>.
- Nyberg, B., Helland-Hansen, W., Gawthorpe, R., Tillmans, F., and Sandbakken, P., 2021, Assessing first-order BQART estimates for ancient source-to-sink mass budget calculations: *Basin Research*, v. 33, p. 2435–2452, <https://doi.org/10.1111/bre.12563>.
- Ou, X., Replumaz, A., and van der Beek, P., 2021, Contrasting exhumation histories and relief development within the Three Rivers region (southeast Tibet): *Solid Earth Discussions*, v. 12, p. 563–580, <https://doi.org/10.5194/se-12-563-2021>.
- Ouimet, W., Whipple, K., Royden, L., Reiners, P., Hodges, K., and Pringle, M., 2010, Regional incision of the eastern margin of the Tibetan Plateau: *Lithosphere*, v. 2, p. 50–63, <https://doi.org/10.1130/L57.1>.
- Pang, X., Chen, C., Zhu, M., He, M., Shen, J., Lian, S., Wu, X., and Shao, L., 2009, Baiyun movement: A significant tectonic event on Oligocene/Miocene boundary in the northern South China Sea and its regional implications: *Journal of Earth Science*, v. 20, p. 49–56, <https://doi.org/10.1007/s12583-009-0005-4>.
- Puetz, S.J., Spencer, C.J., and Ganade, C.E., 2021, Analyses from a validated global U-Pb detrital zircon database: Enhanced methods for filtering discordant U-Pb zircon analyses and optimizing crystallization age estimates: *Earth-Science Reviews*, v. 220, <https://doi.org/10.1016/j.earscirev.2021.103745>.
- Reiners, P.W., and Brandon, M.T., 2006, Using thermochronology to understand orogenic erosion: *Annual Review of Earth and Planetary Sciences*, v. 34, p. 419–466, <https://doi.org/10.1146/annurev.earth.34.031405.125202>.
- Replumaz, A., et al., 2020, Tectonic control on rapid late Miocene–Quaternary incision of the Mekong River knickzone, southeast Tibetan Plateau: *Tectonics*, v. 39, <https://doi.org/10.1029/2019TC005782>.
- Richardson, N.J., Densmore, A.L., Seward, D., Wipf, M., and Li, Y., 2010, Did incision of the Three Gorges begin in the Eocene?: *Geology*, v. 38, p. 551–554, <https://doi.org/10.1130/G30527.1>.
- Romans, B.W., Castelltort, S., Covault, J.A., Fildani, A., and Walsh, J.P., 2016, Environmental signal propagation in sedimentary systems across timescales: *Earth-Science Reviews*, v. 153, p. 7–29, <https://doi.org/10.1016/j.earscirev.2015.07.012>.
- Rowley, D.B., and Garzone, C.N., 2007, Stable isotope-based paleoaltimetry: *Annual Review of Earth and Planetary Sciences*, v. 35, p. 463–508, <https://doi.org/10.1146/annurev.earth.35.031306.140155>.
- Royden, L.H., Burchfiel, B.C., and van der Hilst, R.D., 2008, The geological evolution of the Tibetan Plateau: *Science*, v. 321, p. 1054–1058, <https://doi.org/10.1126/science.1155371>.
- Saylor, J.E., and Sundell, K.E., 2016, Quantifying comparison of large detrital geochronology data sets: *Geosphere*, v. 12, p. 203–220, <https://doi.org/10.1130/GES01237.1>.
- Schärer, U., Zhang, L., and Tapponnier, P., 1994, Duration of strike-slip movements in large shear zones: The Red River belt, China: *Earth and Planetary Science Letters*, v. 126, p. 379–397, [https://doi.org/10.1016/0012-821X\(94\)90119-8](https://doi.org/10.1016/0012-821X(94)90119-8).
- Shao, L., Li, X., Wang, P., Jian, Z., Wei, G., Pang, X., and Liu, Y., 2004, Sedimentary record of the tectonic evolution of the South China Sea since the Oligocene—Evidence from deep sea sediments of ODP Site 1148: *Advance in Earth Sciences (Diqui Kexue Jinzhan)*, v. 19, p. 539–544, <https://doi.org/10.11867/j.issn.1001-8166.2004.04.0539> [in Chinese with English abstract].
- Shao, L., Qiao, P., Zhao, M., Li, Q., Wu, M., Pang, X., and Zhang, H., 2016a, Depositional characteristics of the northern South China Sea in response to the evolution of the Pearl River, in Cliff, P.D., Harff, J., Wu, J., and Qui, Y., eds., *River-Dominated Shelf Sediments of East Asian Seas*: Geological Society, London, Special Publication 429, p. 31–44, <https://doi.org/10.1144/SP429.2>.
- Shao, L., Cao, L., Pang, X., Jiang, T., Qiao, P., and Zhao, M., 2016b, Detrital zircon provenance of the Paleogene syn-rift sediments in the northern South China Sea: *Geochemistry, Geophysics, Geosystems*, v. 17, p. 255–269, <https://doi.org/10.1002/2015GC006113>.
- Shao, L., Cui, Y., Statterger, K., Zhu, W., Qiao, P., and Zhao, Z., 2019, Drainage control of Eocene to Miocene sedimentary records in the southeastern margin of Eurasian plate: *Geological Society of America Bulletin*, v. 131, p. 461–478, <https://doi.org/10.1130/B32053.1>.
- Sharman, G.R., and Johnstone, S.A., 2017, Sediment unmixing using detrital geochronology: *Earth and Planetary Science Letters*, v. 477, p. 183–194, <https://doi.org/10.1016/j.epsl.2017.07.044>.
- Shen, X., Tian, Y., Li, D., Qin, S., Vermeesch, P., and Schwanethal, J., 2016, Oligocene–early Miocene river incision near the first bend of the Yangtze River: Insights from apatite (U-Th-Sm)/He thermochronology: *Tectonophysics*, v. 687, p. 223–231, <https://doi.org/10.1016/j.tecto.2016.08.006>.
- Spicer, R.A., Su, T., Valdes, P.J., Farnsworth, A., Wu, F.-X., Shi, G., Spicer, T.E.V., and Zhou, Z., 2021, Why ‘the uplift of the Tibetan Plateau’ is a myth: *National Science Review*, v. 8, <https://doi.org/10.1093/nsr/nwaa091>.
- Stacey, J.S., and Kramers, J.D., 1975, Approximation of terrestrial lead isotope evolution by a two-stage model: *Earth and Planetary Science Letters*, v. 26, p. 207–221, [https://doi.org/10.1016/0012-821X\(75\)90088-6](https://doi.org/10.1016/0012-821X(75)90088-6).
- Su, T., et al., 2019, Uplift, climate and biotic changes at the Eocene–Oligocene transition in south-eastern Tibet: *National Science Review*, v. 6, p. 495–504, <https://doi.org/10.1093/nsr/nwy062>.
- Sun, X., Li, C., Kuiper, K.F., Wang, J., Tian, Y., Vermeesch, P., Zhang, Z., Zhao, J., and Wijbrans, J.R., 2018, Geochronology of detrital muscovite and zircon constrains the sediment provenance changes in the Yangtze River during the late Cenozoic: *Basin Research*, v. 30, p. 636–649, <https://doi.org/10.1111/bre.12268>.
- Sun, X., Tian, Y., Kuiper, K.F., Li, C., Zhang, Z., and Wijbrans, J.R., 2021, No Yangtze River prior to the late Miocene: Evidence from detrital muscovite and K-feldspar ⁴⁰Ar/³⁹Ar geochronology: *Geophysical Research Letters*, v. 48, <https://doi.org/10.1029/2020GL089903>.
- Sun, Z., Zhai, S., Xiu, C., Liu, X., Zong, T., Luo, W., Liu, X., Chen, K., and Li, N., 2014, Geochemical characteristics and their significances of rare-earth elements in deep-water well core at the Lingnan low uplift area of the Qiongdongnan Basin: *Acta Oceanologica Sinica*, v. 33, p. 81–95, <https://doi.org/10.1007/s13131-014-0578-3>.
- Sundell, K., and Saylor, J.E., 2017, Unmixing detrital geochronology age distributions: *Geochemistry, Geophysics, Geosystems*, v. 18, p. 2872–2886, <https://doi.org/10.1002/2016GC006774>.
- Suo, Y., et al., 2019, Eastward tectonic migration and transition of the Jurassic–Cretaceous Andean-type continental margin along southeast China: *Earth-Science Reviews*, v. 196, <https://doi.org/10.1016/j.earscirev.2019.102884>.
- Syvitski, J.P.M., and Milliman, J.D., 2007, Geology, geography, and humans battle for dominance over the delivery of fluvial sediment to the coastal ocean: *The Journal of Geology*, v. 115, p. 1–19, <https://doi.org/10.1086/509246>.
- Tao, Y., Zhang, H., Ge, Y., Pang, J., Yu, J., Zhang, J., Zhao, X., and Ma, Z., 2020, Cenozoic exhumation and fault activities across eastern Tibet: Constraints from low-temperature thermochronological data: *Chinese Journal of Geophysics*, v. 63, p. 4154–4167, <https://doi.org/10.6038/cjg202000300> [in Chinese with English abstract].
- Tapponnier, P., Zhiqin, X., Roger, F., Meyer, B., Arnaud, N., Wittlinger, G., and Jingsui, Y., 2001, Oblique stepwise rise and growth of the Tibet Plateau: *Science*, v. 294, p. 1671–1677, <https://doi.org/10.1126/science.105978>.
- Tian, Y., Kohn, B.P., Gleadow, A.J.W., and Hu, S., 2014, A thermochronological perspective on the morphotectonic evolution of the southeastern Tibetan Plateau: *Journal of Geophysical Research—Solid Earth*, v. 119, p. 676–698, <https://doi.org/10.1002/2013JB010429>.
- Tian, Y., Kohn, B.P., Hu, S., and Gleadow, A.J.W., 2015, Synchronous fluvial response to surface uplift in the eastern Tibetan Plateau: Implications for crustal dynamics: *Geophysical Research Letters*, v. 42, p. 29–35, <https://doi.org/10.1002/2014GL062383>.

- Tyrrell, S., Haughton, P.D.W., Daly, J.S., Kokfelt, T.F., and Gagnevin, D., 2006, The use of the common Pb isotope composition of detrital K-feldspar grains as a provenance tool and its application to Upper Carboniferous paleodrainage, northern England: *Journal of Sedimentary Research*, v. 76, p. 324–345, <https://doi.org/10.2110/jsr.2006.023>.
- Tyrrell, S., Haughton, P.D.W., and Daly, J.S., 2007, Drainage reorganization during breakup of Pangea revealed by in-situ Pb isotopic analysis of detrital K-feldspar: *Geology*, v. 35, p. 971–974, <https://doi.org/10.1130/G4123A.1>.
- Vandenbergh, J., Cordier, S., and Bridgland, D.R., 2010, Extrinsic and intrinsic forcing of fluvial development: Understanding natural and anthropogenic influences: *Proceedings of the Geologists' Association*, v. 121, p. 107–112, <https://doi.org/10.1016/j.pgeola.2010.05.002>.
- Vermeesch, P., 2012, On the visualisation of detrital age distributions: *Chemical Geology*, v. 312–313, p. 190–194, <https://doi.org/10.1016/j.chemgeo.2012.04.021>.
- Vermeesch, P., 2013, Multi-sample comparison of detrital age distributions: *Chemical Geology*, v. 341, p. 140–146, <https://doi.org/10.1016/j.chemgeo.2013.01.010>.
- Vermeesch, P., 2018, Dissimilarity measures in detrital geochronology: *Earth-Science Reviews*, v. 178, p. 310–321, <https://doi.org/10.1016/j.earscirev.2017.11.027>.
- Vermeesch, P., and Garzanti, E., 2015, Making geological sense of 'Big Data' in sedimentary provenance analysis: *Chemical Geology*, v. 409, p. 20–27, <https://doi.org/10.1016/j.chemgeo.2015.05.004>.
- Vezzoli, G., Garzanti, E., Limonta, M., Andò, S., and Yang, S., 2016, Erosion patterns in the Changjiang (Yangtze River) catchment revealed by bulk-sample versus single-mineral provenance budgets: *Geomorphology*, v. 261, p. 177–192, <https://doi.org/10.1016/j.geomorph.2016.02.031>.
- Voigt, T., Reicherter, K., von Eynatten, H., Littke, R., Voigt, S., and Kley, J., 2008, Sedimentation during basin inversion, *in* Littke, R., Beyer, U., Gajewski, D., and Nelskamp, S., eds., *Dynamics of Complex Intracontinental Basins: The Central European Basin System*: Berlin, Springer, p. 211–228, <https://oceanrep.geomar.de/id/eprint/7136/>.
- von Eynatten, H., and Dunkl, I., 2012, Assessing the sediment factory: The role of single grain analysis: *Earth-Science Reviews*, v. 115, p. 97–120, <https://doi.org/10.1016/j.earscirev.2012.08.001>.
- Wang, A., Li, X., Luo, X., Santosh, M., Cui, Y., Li, Q., Lai, D., Wan, J., and Zhang, X., 2020a, Crustal growth as revealed by integrated U-Pb and Lu-Hf isotope analyses of detrital zircons from the Ganjiang River, southeastern China: *Geological Magazine*, v. 157, p. 666–676, <https://doi.org/10.1017/S001675681900116X>.
- Wang, C., et al., 2014a, Provenance of Upper Miocene to Quaternary sediments in the Yinggehai–Song Hong Basin, South China Sea: Evidence from detrital zircon U-Pb ages: *Marine Geology*, v. 355, p. 202–217, <https://doi.org/10.1016/j.margeo.2014.06.004>.
- Wang, C., et al., 2016a, Zircon U-Pb geochronology and heavy mineral composition constraints on the provenance of the middle Miocene deep-water reservoir sedimentary rocks in the Yinggehai–Song Hong Basin, South China Sea: *Marine and Petroleum Geology*, v. 77, p. 819–834, <https://doi.org/10.1016/j.marpetgeo.2016.05.009>.
- Wang, C., Liang, X., Foster, D.A., Tong, C., Liu, P., Liang, X., and Zhang, L., 2018a, Linking source and sink: Detrital zircon provenance record of drainage systems in Vietnam and the Yinggehai–Song Hong Basin, South China Sea: *Geological Society of America Bulletin*, v. 131, p. 191–204, <https://doi.org/10.1130/B32007.1>.
- Wang, C., Wen, S., Liang, X., Shi, H., and Liang, X., 2018b, Detrital zircon provenance record of the Oligocene Zhuhai Formation in the Pearl River Mouth Basin, northern South China Sea: *Marine and Petroleum Geology*, v. 98, p. 448–461, <https://doi.org/10.1016/j.marpetgeo.2018.08.032>.
- Wang, C., Liang, X., Foster, D.A., Liang, X., Zhang, L., and Su, M., 2019a, Provenance and drainage evolution of the Red River revealed by Pb isotopic analysis of detrital K-feldspar: *Geophysical Research Letters*, v. 46, p. 6415–6424, <https://doi.org/10.1029/2019GL083000>.
- Wang, C., Zeng, L., Lei, Y., Su, M., and Liang, X., 2020b, Tracking the detrital zircon provenance of early Miocene sediments in the continental shelf of the northwestern South China Sea: *Minerals (Basel)*, v. 10, 752, <https://doi.org/10.3390/min10090752>.
- Wang, C.-Y., Flesch, L.M., Silver, P.G., Chang, L.-J., and Chan, W.W., 2008, Evidence for mechanically coupled lithosphere in central Asia and resulting implications: *Geology*, v. 36, p. 363–366, <https://doi.org/10.1130/G24450A.1>.
- Wang, P., 2004, Cenozoic deformation and the history of sea-land interactions in Asia, *in* Clift, P., Kuhnt, W., Wang, P., and Hayes, D., eds., *Continent-Ocean Interactions Within East Asian Marginal Seas: American Geophysical Union Geophysical Monograph 149*, p. 1–22, <https://doi.org/10.1029/149GM01>.
- Wang, P., and Li, Q., eds., 2009, *The South China Sea: Paleooceanography and Sedimentology*: Dordrecht, Netherlands, Springer, *Developments in Paleoenvironmental Research* 13, 506 p., <https://doi.org/10.1007/978-1-4020-9745-4>.
- Wang, P., Li, Q., and Li, C.-F., 2014b, *Geology of the China Seas*: Amsterdam, Netherlands, Elsevier, *Developments in Marine Geology* 6, 687 p.
- Wang, P., Zheng, H., Chen, L., Chen, J., Xu, Y., Wei, X., and Yao, X., 2014c, Exhumation of the Huangling anticline in the Three Gorges region: Cenozoic sedimentary record from the western Jiangnan Basin, China: *Basin Research*, v. 26, p. 505–522, <https://doi.org/10.1111/bre.12047>.
- Wang, P., Zheng, H., Liu, S., and Hoke, G., 2018c, Late Cretaceous drainage reorganization of the Middle Yangtze River: *Lithosphere*, v. 10, p. 392–405, <https://doi.org/10.1130/L695.1>.
- Wang, W., Ye, J., Bidgoli, T., Yang, X., Shi, H., and Shu, Y., 2017, Using detrital zircon geochronology to constrain Paleogene provenance and its relationship to rifting in the Zhu 1 Depression, Pearl River Mouth Basin, South China Sea: *Geochemistry, Geophysics, Geosystems*, v. 18, p. 3976–3999, <https://doi.org/10.1002/2017GC007110>.
- Wang, W., Bidgoli, T., Yang, X., and Ye, J., 2018d, Source-to-sink links between East Asia and Taiwan from detrital zircon geochronology of the Oligocene Huangang Formation in the East China Sea Shelf Basin: *Geochemistry, Geophysics, Geosystems*, v. 19, p. 3673–3688, <https://doi.org/10.1029/2018GC007576>.
- Wang, W., Yang, X., Bidgoli, T.S., and Ye, J., 2019b, Detrital zircon geochronology reveals source-to-sink relationships in the Pearl River Mouth Basin, China: *Sedimentary Geology*, v. 388, p. 81–98, <https://doi.org/10.1016/j.sedgeo.2019.04.004>.
- Wang, Y., Zhang, B., Schoenbohm, L.M., Zhang, J., Zhou, R., Hou, J., and Ai, S., 2016b, Late Cenozoic tectonic evolution of the Ailao Shan–Red River fault (SE Tibet): Implications for kinematic change during plateau growth: *Tectonics*, v. 35, p. 1969–1988, <https://doi.org/10.1002/2016TC004229>.
- Wang, Y., Wang, Y., Li, S., Seagren, E., Zhang, Y., Zhang, P., and Qian, X., 2020c, Exhumation and landscape evolution in eastern South China since the Cretaceous: New insights from fission-track thermochronology: *Journal of Asian Earth Sciences*, v. 191, <https://doi.org/10.1016/j.jseas.2020.104239>.
- Wei, H.-H., Wang, E., Wu, G.-L., and Meng, K., 2016, No sedimentary records indicating southerly flow of the paleo-Upper Yangtze River from the First Bend in southeastern Tibet: *Gondwana Research*, v. 32, p. 93–104, <https://doi.org/10.1016/j.gr.2015.02.006>.
- Weltje, G.J., and von Eynatten, H., 2004, Quantitative provenance analysis of sediments: Review and outlook: *Sedimentary Geology*, v. 171, p. 1–11, <https://doi.org/10.1016/j.sedgeo.2004.05.007>.
- Whipple, K.X., DiBiase, R.A., Ouimet, W.B., and Forte, A.M., 2017, Preservation or piracy: Diagnosing low-relief, high-elevation surface formation mechanisms: *REPLY: Geology*, v. 45, p. e422, <https://doi.org/10.1130/G39252Y.1>.
- Willett, S.D., McCoy, S.W., Perron, J.T., Goren, L., and Chen, C.Y., 2014, Dynamic reorganization of river basins: *Science*, v. 343, <https://doi.org/10.1126/science.1248765>.
- Wissink, G.K., Hoke, G.D., Garzione, C.N., and Liu-Zeng, J., 2016, Temporal and spatial patterns of sediment routing across the southeast margin of the Tibetan Plateau: Insights from detrital zircon: *Tectonics*, v. 35, p. 2538–2563, <https://doi.org/10.1002/2016TC004252>.
- Wissink, G.K., Wilkinson, B.H., and Hoke, G.D., 2018, Pairwise sample comparisons and multidimensional scaling of detrital zircon ages with examples from the North American platform, basin, and passive margin settings: *Lithosphere*, v. 10, p. 478–491, <https://doi.org/10.1130/L700.1>.
- Wu, L., Mei, L., Liu, Y., Luo, J., Min, C., Lu, S., Li, M., and Guo, L., 2017, Multiple provenance of rift sediments in the composite basin-mountain system: Constraints from detrital zircon U-Pb geochronology and heavy minerals of the early Eocene Jiangnan Basin, central China: *Sedimentary Geology*, v. 349, p. 46–61, <https://doi.org/10.1016/j.sedgeo.2016.12.003>.
- Wysocka, A., and Świerczewska, A., 2010, Lithofacies and depositional environments of Miocene deposits from tectonically-controlled basins (Red River fault zone, northern Vietnam): *Journal of Asian Earth Sciences*, v. 39, p. 109–124, <https://doi.org/10.1016/j.jseas.2010.02.013>.
- Xiao, G., et al., 2020, Early Pleistocene integration of the Yellow River I: Detrital-zircon evidence from the North China Plain: *Palaeogeography, Palaeoclimatology, Palaeoecology*, v. 546, <https://doi.org/10.1016/j.palaeo.2020.109691>.
- Xie, Y., Li, X., Fan, C., Tan, J., Liu, K., Lu, Y., Hu, W., Li, H., and Wu, J., 2016, The axial channel provenance system and natural gas accumulation of the Upper Miocene Huangliu Formation in Qiongdongnan Basin, South China Sea: *Petroleum Exploration and Development*, v. 43, p. 570–578, [https://doi.org/10.1016/S1876-3804\(16\)30067-2](https://doi.org/10.1016/S1876-3804(16)30067-2).
- Xiong, Z., et al., 2020, The early Eocene rise of the Gonjo Basin, SE Tibet: From low desert to high forest: *Earth and Planetary Science Letters*, v. 543, <https://doi.org/10.1016/j.epsl.2020.116312>.
- Xu, Y., 2017, Comment on "Detrital zircon geochronology of river sands from Taiwan: Implications for sedimentary provenance of Taiwan and its source link with the east China mainland": *Earth-Science Reviews*, v. 168, p. 232–234, <https://doi.org/10.1016/j.earscirev.2017.03.008>.
- Yan, Y., Xia, B., Lin, G., Carter, A., Hu, X.Q., Cui, X.J., Liu, B.M., Yan, P., and Song, Z.J., 2007, Geochemical and Nd isotope composition of detrital sediments on the north margin of the South China Sea: Provenance and tectonic implications: *Sedimentology*, v. 54, p. 1–17, <https://doi.org/10.1111/j.1365-3091.2006.00816.x>.
- Yan, Y., Carter, A., Xia, B., Ge, L., Blichau, S., and Hu, X., 2009, A fission-track and (U-Th)/He thermochronometric study of the northern margin of the South China Sea: An example of a complex passive margin: *Tectonophysics*, v. 474, p. 584–594, <https://doi.org/10.1016/j.tecto.2009.04.030>.
- Yan, Y., Carter, A., Palk, C., Blichau, S., and Hu, X.Q., 2011, Understanding sedimentation in the Song Hong–Yinggehai Basin, South China Sea: *Geochemistry, Geophysics, Geosystems*, v. 12, Q06014, <https://doi.org/10.1029/2011GC003533>.
- Yan, Y., Carter, A., Huang, C.-Y., Chan, L.-S., Hu, X.-Q., and Lan, Q., 2012, Constraints on Cenozoic regional drainage evolution of SW China from the provenance of the Jianchuan Basin: *Geochemistry, Geophysics, Geosystems*, v. 13, Q03001, <https://doi.org/10.1029/2011GC003803>.
- Yan, Y., Yao, D., Tian, Z.-X., Huang, C.-Y., Dilek, Y., Clift, P.D., and Li, Z.-A., 2018, Tectonic topography changes in Cenozoic East Asia: A landscape erosion-sediment archive in the South China Sea: *Geochemistry, Geophysics, Geosystems*, v. 19, p. 1731–1750, <https://doi.org/10.1029/2017GC007356>.
- Yang, C., Shen, C., Zattin, M., Yu, W., Shi, S., and Mei, L., 2019, Provenances of Cenozoic sediments in the Jiangnan Basin and implications for the formation of the Three Gorges: *International Geology Review*, v. 61, p. 1980–1999, <https://doi.org/10.1080/00206814.2019.1576066>.

- Yang, C., Shen, C., Zattin, M., and Yu, W., 2021, Formation of the Yangtze Three Gorges: Insights from detrital apatite fission-track dating of sediments from the Jiangnan Basin: *Terra Nova*, v. 33, p. 511–520, <https://doi.org/10.1111/ter.12543>.
- Yang, R., Willett, S.D., and Goren, L., 2015, In situ low-relief landscape formation as a result of river network disruption: *Nature*, v. 520, p. 526–529, <https://doi.org/10.1038/nature14354>.
- Yang, R., Fellin, M.G., Herman, F., Willet, S.D., Wang, W., and Maden, C., 2016, Spatial and temporal pattern of erosion in the Three Rivers region, southeastern Tibet: *Earth and Planetary Science Letters*, v. 433, p. 10–20, <https://doi.org/10.1016/j.epsl.2015.10.032>.
- Yang, S., Li, C., and Yokoyama, K., 2006a, Elemental compositions and monazite age patterns of core sediments in the Changjiang Delta: Implications for sediment provenance and development history of the Changjiang River: *Earth and Planetary Science Letters*, v. 245, p. 762–776, <https://doi.org/10.1016/j.epsl.2006.03.042>.
- Yang, S., Zhang, F., and Wang, Z., 2012, Grain size distribution and age population of detrital zircons from the Changjiang (Yangtze) River system, China: *Chemical Geology*, v. 296–297, p. 26–38, <https://doi.org/10.1016/j.chemgeo.2011.12.016>.
- Yang, X., Li, A., Qin, Y., Wu, S., Wu, Z., and Zhang, J., 2006b, U-Pb dating of zircons from Cenozoic sandstone: Constraint on the geodynamic setting of East China Sea Shelf Basin: *Marine Geology and Quaternary Geology (Haiyang Dizhi Yu Disiji Dizhi)*, v. 26, p. 75–85, <https://doi.org/10.16562/j.cnki.0256-1492.2006.03.011>.
- Yin, A., 2010, Cenozoic tectonic evolution of Asia: A preliminary synthesis: *Tectonophysics*, v. 488, p. 293–325, <https://doi.org/10.1016/j.tecto.2009.06.002>.
- Yin, A., and Harrison, T.M., 2000, Geologic evolution of the Himalayan-Tibetan orogen: *Annual Review of Earth and Planetary Sciences*, v. 28, p. 211–280, <https://doi.org/10.1146/annurev.earth.28.1.211>.
- Yuan, W., Xu, X., and Zhou, X., 2014, The new geochronology results of the Pinghu Formation in Xihu Depression: Evidence from the SHRIMP zircon U-Pb ages of the volcanic rocks: *Geological Journal of China Universities (Gaoxiao Dizhi Xuebao)*, v. 20, p. 407–414, <https://doi.org/10.16108/j.issn1006-7493.2014.03.023>, [in Chinese with English abstract].
- Yuan, X.P., Huppert, K.L., Braun, J., Shen, X., Liu-Zeng, J., Guertl, L., Wolf, S.G., Zhang, J.F., and Jolivet, M., 2022, Propagating uplift controls on high-elevation, low-relief landscape formation in the southeast Tibetan Plateau: *Geology*, v. 50, p. 60–65, <https://doi.org/10.1130/G49022.1>.
- Zhang, G., Shao, L., Qiao, P., Cao, L., Pang, X., Zhao, Z., Xiang, X., and Cui, Y., 2020a, Cretaceous–Palaeogene sedimentary evolution of the South China Sea region: A preliminary synthesis: *Geological Journal*, v. 55, p. 2662–2683, <https://doi.org/10.1002/gj.3533>.
- Zhang, H., Shao, L., Zhang, G.C., Cui, Y.C., Zhao, Z.G., and Hou, Y.L., 2020b, The response of Cenozoic sedimentary evolution coupled with the formation of the South China Sea: *Geological Journal*, v. 55, p. 6989–7010, <https://doi.org/10.1002/gj.3856>.
- Zhang, H., Cui, Y., Qiao, P., Zhao, M., and Xiang, X., 2021a, Pearl River evolution and its implication to the East Asian continental landscape reversion: *Acta Geologica Sinica*, v. 95, p. 66–76, <https://doi.org/10.1111/1755-6724.14641>.
- Zhang, J., Li, S., and Suo, Y., 2016, Formation, tectonic evolution and dynamics of the East China Sea Shelf Basin: *Geological Journal*, v. 51, p. 162–175, <https://doi.org/10.1002/gj.2808>.
- Zhang, J., et al., 2018a, Source to sink transport in the Oligocene Huagang Formation of the Xihu Depression, East China Sea Shelf Basin: *Marine and Petroleum Geology*, v. 98, p. 733–745, <https://doi.org/10.1016/j.marpetgeo.2018.09.014>.
- Zhang, J., Covault, J., Pyrcz, M., Sharman, G., Carvajal, C., and Milliken, K., 2018b, Quantifying sediment supply to continental margins: Application to the Paleogene Wilcox Group, Gulf of Mexico: *American Association of Petroleum Geologists Bulletin*, v. 102, p. 1685–1702, <https://doi.org/10.1306/01081817308>.
- Zhang, J., Pas, D., Krijgsman, W., Wei, W., Du, X., Zhang, C., Liu, J., and Lu, Y., 2020c, Astronomical forcing of the Paleogene coal-bearing hydrocarbon source rocks of the East China Sea Shelf Basin: *Sedimentary Geology*, v. 406, <https://doi.org/10.1016/j.sedgeo.2020.105715>.
- Zhang, J., Krijgsman, W., Lu, Y., Liu, J., Li, X., Du, X., Wei, W., and Lin, H., 2021b, Detrital zircon ages reveal Yangtze provenance since the early Oligocene in the East China Sea Shelf Basin: *Palaeogeography, Palaeoclimatology, Palaeoecology*, v. 577, <https://doi.org/10.1016/j.palaeo.2021.110548>.
- Zhang, K., et al., 2010, Paleogene–Neogene stratigraphic realm and sedimentary sequence of the Qinghai-Tibet Plateau and their response to uplift of the plateau: *Science China–Earth Sciences*, v. 53, p. 1271–1294, <https://doi.org/10.1007/s11430-010-4048-2>.
- Zhang, P., et al., 2019, Palaeodrainage evolution of the large rivers of East Asia, and Himalayan-Tibet tectonics: *Earth-Science Reviews*, v. 192, p. 601–630, <https://doi.org/10.1016/j.earscirev.2019.02.003>.
- Zhang, Y.-Z., et al., 2015, Timing and rate of exhumation along the Litang fault system: Implication for fault reorganization in southeast Tibet: *Tectonics*, v. 34, p. 1219–1243, <https://doi.org/10.1002/2014TC003671>.
- Zhang, Z., Tyrrell, S., Li, C., Daly, J.S., Sun, X., and Li, Q., 2014, Pb isotope compositions of detrital K-feldspar grains in the upper-middle Yangtze River system: Implications for sediment provenance and drainage evolution: *Geochemistry, Geophysics, Geosystems*, v. 15, p. 2765–2779, <https://doi.org/10.1002/2014GC005391>.
- Zhang, Z., Daly, J.S., Li, C., Tyrrell, S., Sun, X., and Yan, Y., 2017, Sedimentary provenance constraints on drainage evolution models for SE Tibet: Evidence from detrital K-feldspar: *Geophysical Research Letters*, v. 44, p. 4064–4073, <https://doi.org/10.1002/2017GL073185>.
- Zhang, Z., Daly, J.S., Li, C., Tyrrell, S., Badenszki, E., Sun, X., Tian, Y., and Yan, Y., 2020d, Southeastern Tibetan Plateau serves as the dominant sand contributor to the Yangtze River: Evidence from Pb isotopic compositions of detrital K-feldspar: *Terra Nova*, v. 33, p. 195–207, <https://doi.org/10.1111/ter.12505>.
- Zhang, Z., Daly, J.S., Yan, Y., Lei, C., Badenszki, E., Sun, X., and Tian, Y., 2021c, No connection between the Yangtze and Red Rivers since the late Eocene: *Marine and Petroleum Geology*, v. 129, <https://doi.org/10.1016/j.marpetgeo.2021.105115>.
- Zhang, Z., et al., 2021d, Formation of the Three Gorges (Yangtze River) no earlier than 10 Ma: *Earth-Science Reviews*, v. 216, <https://doi.org/10.1016/j.earscirev.2021.103601>.
- Zhao, M., 2015, The Evolution of the Pearl River and its Sedimentary Record in the Northern South China Sea [Ph.D. thesis]: Shanghai, China, Tongji University, 124 p.
- Zhao, M., Shao, L., and Qiao, P., 2015a, Characteristics of detrital zircon U-Pb geochronology of the Pearl River sands and its implication on provenances: *Journal of Tongji University [Natural Science]*, v. 43, p. 89–97, <https://doi.org/10.11908/j.issn.0253-374x.2015.06.018> [in Chinese with English abstract].
- Zhao, M., Shao, L., Liang, J., and Li, Q., 2015b, No Red River capture since the late Oligocene: Geochemical evidence from the northwestern South China Sea: *Deep-Sea Research II—Topical Studies in Oceanography*, v. 122, p. 185–194, <https://doi.org/10.1016/j.dsr2.2015.02.029>.
- Zhao, X., et al., 2021, Existence of a continental-scale river system in eastern Tibet during the Late Cretaceous–early Palaeogene: *Nature Communications*, v. 12, 7231, <https://doi.org/10.1038/s41467-021-27587-9>.
- Zheng, H., 2015, Birth of the Yangtze River: Age and tectonic-geomorphic implications: *National Science Review*, v. 2, p. 438–453, <https://doi.org/10.1093/nsr/nw063>.
- Zheng, H., Clift, P.D., Wang, P., Tada, R., Jia, J., Hee, M., and Jourdan, F., 2013, Pre-Miocene birth of the Yangtze River: Proceedings of the National Academy of Sciences of the United States of America, v. 110, p. 7556–7561, <https://doi.org/10.1073/pnas.1216241110>.
- Zheng, H., Clift, P.D., He, M., Bian, Z., Liu, G., Liu, X., Xia, L., Yang, Q., and Jourdan, F., 2021, Formation of the First Bend in the late Eocene gave birth to the modern Yangtze River, China: *Geology*, v. 49, p. 35–39, <https://doi.org/10.1130/G48149.1>.
- Zhu, W., Zhong, K., Fu, X., Chen, C., Zhang, M., and Gao, S., 2019, The formation and evolution of the East China Sea Shelf Basin: A new view: *Earth-Science Reviews*, v. 190, p. 89–111, <https://doi.org/10.1016/j.earscirev.2018.12.009>.
- Zimmermann, U., Andersen, T., Madland, M.V., and Larsen, I.S., 2015, The role of U-Pb ages of detrital zircons in sedimentology—An alarming case study for the impact of sampling for provenance interpretation: *Sedimentary Geology*, v. 320, p. 38–50, <https://doi.org/10.1016/j.sedgeo.2015.02.006>.

SCIENCE EDITOR: MIHAI DUCEA
ASSOCIATE EDITOR: ERIC ROBERTS

MANUSCRIPT RECEIVED 23 APRIL 2022
REVISED MANUSCRIPT RECEIVED 27 JULY 2022
MANUSCRIPT ACCEPTED 18 NOVEMBER 2022

Printed in the USA